New and Successful Technique for the Management of Parry-Romberg Syndrome's Soft Tissue Atrophy

Viviana Gómez Ortega, MD[*] and Daniel Sastoque, MD[†]

Abstract: Parry-Romberg syndrome (PRS) is an infrequent, acquired disorder characterized by progressive hemiatrophy of the skin and soft tissue of the face and, in some patients, results in atrophy of muscles, cartilage, and the underlying bony structures.

The disease process exhibits varying speeds of development, with onset occurring in early infancy or adolescence. Clinicians have classically reserved treatment until the end of the process. Various treatment modalities have been attempted with differing results. Described treatments include free tissue transfer (omentum, rectus, latissimus, serratus, diep, scapula, and parascapular), pedicled flaps, autologous tissue (dermis-fat, bone and cartilage, and fat), and biomaterials (silicone, polyethylene, and Alloderm).

In this article, the authors present a patient of Parry-Romberg syndrome in a young boy who had undergone a free flap previously, which failed to fill the atrophy of the right hemifacial soft tissues. The authors used Integra, which is a bilayer porous matrix of cross-linked bovine tendon collagen and glycosaminoglycan, and a semipermeable polysiloxane (silicone layer) and fat grafts enriched with Harvest PRP, to produce volume and symmetric contour on the affected side. The patient had a follow up of 2 years with excellent esthetic and functional results.

Objective: The authors present a technique of volume replacement in patients with hemifacial atrophy because of Parry-Romberg syndrome, which has never been reported before in the international literature.

Study: Microsurgical reconstruction is considered the gold standard to restore facial symmetry. Given a free flap morbidity and risk of complications, some patients opt for less extensive procedures. The authors present the case of a 12-year-old boy with a history of Parry-Romberg syndrome with resultant right hemifacial atrophy. Consistent with the usual pattern of atrophy, the onset of the patient's disease began at the age of 5 years.

Methods: The senior authors used a combination of a stacked Integra cheek implant and fat grafts enriched with Harvest PRP to produce volume and symmetric contour on the affected side. The patient was discharged home the next day after the surgical procedure from the recovery room, without complications.

Results: The patient was followed for 2 years. He has had no complications and maintains an excellent symmetric result. The patient is highly satisfied with his result and has not required any further surgery. Preoperative and postoperative photos at year of follow up are presented.

Discussion: Less invasive treatment options exist for hemifacial atrophy from Parry-Romberg syndrome.

Key Words: Atrophy, enriched platelet plasma, Integra, management, Parry-Romberg syndrome, soft tissues

Parry-Romberg syndrome (PRS), also known as Romberg disease, is a rare, acquired craniofacial disorder characterized by a slow progressive hemiatrophy, variably affecting the skin and subcutaneous tissue and, in some patients, muscles, cartilage, and underlying bony structures. First described by Parry in 1825 and Romberg in 1846, it was later named as progressive hemifacial atrophy (PHA) by Eulenberg in 1871.[1–4]

Through its slow progress, the disease commonly affects dermatomes of 1 or multiple branches of the trigeminal nerve. The onset of the disease begins between the ages of 5 and 15 years. The progression of the atrophy lasts a decade. Patients with PRS experience a progressive shrinking and deformation of 1 side of the face followed by unilateral facial atrophy, ipsilateral enophthalmos, and deviation of the mouth and nose toward the affected side. Skin discoloration, cicatricial alopecia, and intraoral involvement with tongue hemiatrophy may associate as well. Bilateral atrophies were observed yet not common.[5–8] It is typically restricted to one half of the face but occasionally involves the arm, trunk, and leg.

The etiology of the disease is not well understood. Some possible causes were proposed, including trauma, infection, cranial vascular malformation, immune-mediated processes, disturbance of fat metabolism, and sympathetic dysfunction. It appears to be more common in the female gender.

Patients of Parry-Romberg syndrome are classified as mild, moderate, or severe in relation to atrophy of the skin, subcutaneous tissue, and bone involvement in territories of the trigeminal nerve as follows:

Mild: Atrophy of the skin and subcutaneous tissues is observable in the territory of just 1 of the sensory branches of the trigeminal nerve; bone involvement is not observable. Moderate: Atrophy of the skin and subcutaneous tissues is observable in the territory of 2 of the sensory branches of the trigeminal nerve, without the involvement of the osseous orbital region or maxillary and mandibular growth.

Severe: Atrophy of the skin and subcutaneous tissues is observable in all 3 of the sensory branches of the trigeminal nerve or bone involvement.

Treatment for the atrophy is recommended after the quiescence of disease progression. Multiple surgical procedures have been used to improve the facial volume and contours of patients with this disease, including alloplastic, silicone, or collagen implants; lipofilling; and pedicled or free-flap transplants.

The most appropriate treatment modality for these patients can be determined based upon the observations noted during their clinical examination.[9] Regardless of the specific modality chosen, treatment involves augmentation of the atrophied region and restoration of facial symmetry to provide great psychologic and emotional benefits to the patient. The use of autologous fat grafts, alone or in combination with other surgical methods, offers a practical treatment of the condition. Alternatively, the injection of biomaterials, such as alloplastic materials, silicone, or collagen, also provides practical solutions. Other treatment methods include pedicled or free flap grafts.

From the [*]Plastic and Reconstructive Surgery Department of the Hospital Simón Bolivar and La Fundación Santa Fé de Bogotá and Hospital de la Policia; and [†]Plastic and Reconstructive Surgery Department of the Hospital Simón Bolivar, Bogota, Columbia.

Received January 15, 2015.
Accepted for publication June 28, 2015.

Address correspondence and reprint requests to Viviana Gómez Ortega, MD, Hospital Simón Bolivar, Fundación Santa Fé de Bogotá, Hospital de la Policia, Cra 7[a] No 121-33, Bogotá, Colombia;
E-mail: vivigor7@gmail.com

The authors report no conflicts of interests.

Copyright © 2015 by Mutaz B. Habal, MD

ISSN: 1049-2275
DOI: 10.1097/SCS.0000000000002023

Various treatment modalities have been attempted with differing results. Described treatments include free tissue transfer (omentum,[10] rectus,[11] latissimus,[12] serratus,[13] diep,[14] scapula,[15] and parascapular[16]), pedicled flaps,[17] autologous tissue (dermis-fat,[18] bone and cartilage, and fat[19]), and biomaterials (silicone,[20] polyethylene,[21] and Alloderm[22]).

PATIENT AND METHODS

A 12-year-old boy presented with a history of PRS, characterized by right facial atrophy of the subcutaneous tissues that began when he was 5 years old. The objective of clinical examination indicated moderate to severe soft tissue deficits affecting the zygomatic, buccal, mental, cheek, and orbital regions of his right face without significant alteration of the skin pigmentation. The patient was treated in other institution until he was 9 years old. When he was 8 years old he underwent a latissimus dorsi free flap surgery to treat his right facial atrophy. The free flap was originally presented as the best solution for soft tissue augmentation in this patient. The free flap was performed but after some time it suffered a retraction placing itself in the right preauricular región, the assymetry of the face persisted after this procedure as it is shown in the Fig. 1A-G. We decided to perform another surgical procedure in which we used Integra as a filler to improve his face contour (Fig. 2A) and fat grafts enriched with Harvest PRP to produce volume and symmetric contour on the affected side (Fig. 2B). The patient?s bone involvement was mild whereas the atrophy of the skin and subcutaneous tissues was presented in all 3 of the sensory branches of the trigeminal nerve (Fig. 3).

Operative Technique

With the patient under general anesthesia, we used a combined unilateral facelift approach (right preauricular incision), to access the face. We dissected the tissues until we reached the supra superficial muscular aponeurotic system (SMAS) plane. Once there, we dissected the soft tissues until we reached the right oral commissure preserving the facial nerve and its branches. When the surgical area was exposed we identified the free flap, which was located in the preauricular area and we relocated it over the right mandibular border to fill the depressed area in that zone (Fig. 4). A fixation suture was used to hold the free flap in the right mandibular border (Fig. 5). We used Integra to fill the depressed area in the zygomatic, buccal, mental, cheek, and orbital regions (Fig. 6A-B). Integra provided the needed framework for the blood vessels and dermal skin cells to regrow. In the same surgical time we completed some atrophied areas with fat grafts and platelet-enriched plasma using Harvest PRP. The plasma sample was taken during the anesthetic induction (Fig. 7). The blood sample was taken to the Harvest PRP device where it was centrifugated to separate the autologous platelet concentrate from the other cells.

Fat was harvested from the abdomen, flank, medial thigh, and buttock. Fat was harvested using manual suction to a 10 mL syringe with a 3 mm blunt cannula. After the supernatant was removed, fat was transferred into syringes and immediately injected into the affected regions of the face. Multiple access sites for injection and a "fanning-out" technique were used to transfer small aliquots of fat into various depths of the soft tissue and hypoplastic regions. The buffy coat layer was transferred to the syringe and was injected in the areas where the fat grafts were injected.

After the surgical procedure the patient was taken to the recovery room where he spent 1 night. The following day he was discharged from the hospital. He did not have any complications (Fig. 8).

A year later of the surgical procedure, a soft tissue sample was taken for histopathological examination; during this surgical time it was observed 100% intake of the Integra by the patient' soft tissues (Fig. 9). The biopsy reported that the collagen fibers were aligned. The pathologist did not find a solid strange material, which shows the Integra integrated to the soft tissues without losing its filler quality. A computer tomography was taken and the symmetry was maintained as shown in the Fig. 10.

The patient was followed up for a period of 2 years. The results are successfully adequate. The patient and his parents are happy with the esthetic and functional results.

FIGURE 1. A, Frontal view of the patient. It shows the free flap located in the right preauricular region with persisted atrophy of the right hemifacial region. B, Basal view of the patient. It shows the deviation to the compromised side. C, Oblique left view of the patient. D, Oblique right view of the patient. E, Left view of the patient. F, Right view of the patient. G, Frontal view of the patient showing his occlusion. It shows a mild deviation to the right of the middle dental line. This picture also shows a right deviation of the nose.

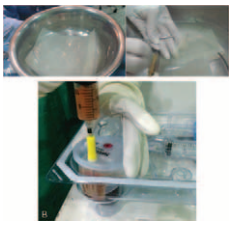

FIGURE 2. A, Integra which is a bilayer matrix used for wound dressing composed of a porous matrix of cross-linked bovine tendon collagen and glycosaminoglycan and a semipermeable polysiloxane (silicone layer). The photo shows when we removed the silicone layer of the Integra, to use the collagen matrix only as the filler. B, Harvest autologous platelet concentrate.

FIGURE 3. The patient's bone involvement was mild.

RESULTS

The patient was followed for 2 years. He has had no complications as: infection, seroma, capsule formation, exposure, migration, and long term scar formation and maintains an excellent symmetric

FIGURE 4. Location of the free flap, which was in the right preauricular area.

FIGURE 5. A fixation suture was used to hold the free flap in the right mandibular border.

© 2015 Mutaz B. Habal, MD

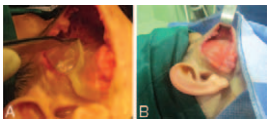

FIGURE 6. A, Integra in place filling the depressed areas. B, Integra was used to fill the depressed areas in the zygomatic, buccal, mental, cheek, and orbital regions.

FIGURE 7. The photo shows when the plasma sample was taken.

result. The patient is highly satisfied with his result and has not required any further surgery. Preoperative and postoperative photos during the follow-up are presented (Figs. 11-12).

DISCUSSION

Parry-Romberg syndrome results in progressive hemifacial atrophy and may be highly variable. For soft tissue reconstruction, severity of the disease plays a significant role in determining how to restore facial symmetry through volume augmentation of the atrophied side. Patients with mild to moderate deformity are typically treated with serial fat grafting procedures. Fat grafting is preferred over injection of silicone and other synthetic injectables because of higher rates of infection, seroma, capsule formation, exposure, migration, and long-term scar formation. For skeletally mature patients with severe deformity, dermal fat graft, or an adipofacial free flap (such as an inframammary extended circumflex scapular (IMECS) flap) are accepted alternatives. Although excellent results may be obtained with an IMECS flap, this is a major procedure and subsequent revisions or debulking procedures are typically necessary.

Because we know that "fat take" is significantly less in diseased Romberg tissue compared with normal tissues (41% versus 80%)[23]; we performed a different surgical management to decrease the number of surgeries in this patient. For Romberg patients, it is unknown whether this poorer fat take was because of suboptimal blood supply in the recipient bed or because of something else intrinsic to Romberg diseased tissue. This higher resorption of fat leads to the need for multiple fat injection procedures and the need for overfill to achieve the necessary augmentation.

Our article offers improvements in fat grafting techniques, in an attempt to achieve more predictable augmentation results, with the use of key biological cells obtained by Harvest PRP, which have showed to improve the fat take in Romberg patients.

FIGURE 8. The photo shows the patient during the immediate postoperative period in the recovery room.

FIGURE 9. The photo shows 100% intake of the Integra by the patients' soft tissues.

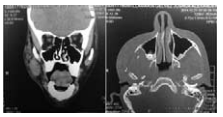

FIGURE 10. CT coronal and axial view of the symmetry achieved after 2 years of follow up.

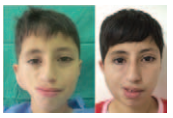

FIGURE 11. Frontal view of preoperative and postoperative photos during the follow up.

Platelet-rich plasma (PRP) is used in several clinical disciplines and is considered to ameliorate tissue regeneration because of the presence of essential cytokines and growth factors (GFs).

Marx et al[24] defined PRP as a portion of the plasma fraction of autologous blood, having a platelet concentration above baseline values. Platelet-rich plasma is made by centrifugation of whole blood (drawn from a peripheral vein and stored in an acid citrate dextrose solution A (ACD-A) anticoagulant), which separates the various components of blood by their specific weight and increases the concentration of platelets. At the same time, platelet-poor plasma (PPP) is formed as a by-product, which is transformed into fibrin glue (FG) by activation. In thrombocytes, cytokines and GFs are stored in α-granules in their incomplete form. In physiological conditions, through activation of platelets, these cytokines and GFs are transformed into their bioactive status and actively secreted within 10 minutes after clotting, with >95% of the presynthesized GFs released within 1 hour.[24] This process can be reproduced in clinical settings through activation of PRP by using an activator, for example, thrombin, resulting in the formation of platelet gel (PG). This gel acts as a drug-delivery system because it comprises a high concentration of platelets and their active cytokines and GFs, which stimulate physiological processes as local tissue repair and regrowth.

As to Integra, there is limited documentation of its utility in the pediatric plastic surgery population. Integra is a bilaminar dermal regeneration template, the top layer being a silicone sheet mimicking the protective epidermis. The matrix is composed of a proprietary mixture of bovine collagen and glycosaminoglycans, from shark chondroitin-6-sulfate. This regenerative template, or matrix, serves as a framework for GFs and cells during the 2 to 3 weeks it takes to become vascularized and remodeled into native tissue.

In all children regardless of age, the focus is as much on aesthetic as functional outcome. Integra is a unique acellular dermal regeneration template that acts as a scaffold for tissue regeneration, integration, and the eventual development of durable soft tissue filler.

The importance of this article is that there are no reports in the international literature in which the Integra matrix has been used as a filler in a craniomaxillofacial malformation. There are 2 posters in which Alloderm was used to provide volume in adults with an esthetic purpose, but this is the first time an acellular matrix is used to reconstruct an atrophied face in a child with Parry-Romberg syndrome. During the 2 years of follow up we have observed an adequate evolution of the patient without the need of another

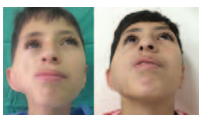

FIGURE 12. Basal view of preoperative and postoperative photos during the follow up.

© 2015 Mutaz B. Habal, MD

surgical procedure and we have observed that the adequate results have maintained in time.

This is a case report; more studies are needed to confirm our results. A great advantage of our proposed surgical management is that the donor site is avoided, a vital reason when talking about a child. In this patient, that was not true because the patient arrived to our clinic when he had already undergone a free flap, which failed to achieve its purpose.

A disadvantage of our proposed surgical management is the cost of the Integra and in a less amount the HarvestPRP. But once again, when we plan to treat a child the cost should not be an important factor when it implies less surgical times and less morbidities with excellent results that persist in time.

REFERENCES

1. Parry CH. Collections from the Unpublished Medical Writings of the Late Caleb Hillier Parry. London, UK: Underwoods; 1825:478–480
2. Romberg HM. Klinische Ergebnisse. *Krankheiten des nervensystems (IV: Trophoneurosen)* [in German]. Berlin, Germany: Forrtner; 1846:75–81
3. Eulenberg A. *Hemiatrophia facialis progressiva* [in German]. *Lehrbuch der Functionellen Nervenkrankheiten auf Physiologischer Basis*. Berlin, Germany: Verlag von August Hirschwald; 1871:712–726
4. El-Kehdy J, Abbas O, Rubeiz N. A review of Parry-Romberg syndrome. *J Am Acad Dermatol* 2012;67:769–784
5. Slack GC, Tabit CJ, Allam KA, et al. Parry-Romberg reconstruction: optimal timing for hard and soft tissue procedures. *J Craniofac Surg* 2012;23:1969–1973
6. Rogers BO. Progressive facial hemiatrophy: Romberg's disease, a review of 772 cases. *Proc 3d Int Cong Plast Surg Excerpta Medica ICS* 1964;66:681–689
7. Stone J. Parry-Romberg syndrome: a global survey of 205 patients using the internet. *Neurology* 2003;61:674–676
8. Tollefson MM, Witman PM. En coup de sabre morphea and Parry-Romberg syndrome: a retrospective review of 54 patients. *J Am Acad Dermatol* 2007;56:257–263
9. Guerrerosantos J, Guerrerosantos F, Orozco J. Classification and treatment of facial tissue atrophy in Parry-Romberg disease. *Aesth Plast Surg* 2007;31:424–434
10. Losken A, Carlson GW, Culbertson JH, et al. Omental free flap reconstruction in complex head and neck deformities. *Head Neck* 2002;24:326–331
11. Inigo F, Jimenez-Murat Y, Arroyo O, et al. Restoration of facial contour in Romberg's disease and hemifacial microsomia: experience with 118 cases. *Microsurgery* 2000;20:167–172
12. Cho BC, Lee JH, Ramasastry SS, et al. Free latissimus dorsi muscle transfer using an endoscopic technique. *Ann Plast Surg* 1997;38:586–593
13. Angel MF, Bridges RM, Levine PA, et al. The serratus anterior free tissue transfer for craniofacial reconstruction. *J Craniofac Surg* 1992;3:207–212
14. Koshima I, Inagawa K, Urushibara K, et al. Deep inferior epigastric perforator dermal-fat or adiposal flap for correction of craniofacial contour deformities. *Plast Reconstr Surg* 2000;106:10–15
15. Upton J, Albin RE, Mulliken JB, et al. The use of scapular and parascapular flaps for cheek reconstruction. *Plast Reconstr Surg* 1992;90:959–971
16. Rigotti G, Cristofoli C, Marchi A, et al. Treatment of Romberg's disease with parascapular free flap and polyethylene porous implants. *Facial Plast Surg* 1999;15:317–325
17. Sabapathy SR, Venkatramani H, Bharathi R. Romberg's disease: modified Washio flap for facial contour reconstruction. *Plast Reconstr Surg* 2001;108:705–708
18. Williams HB, Crepeau RJ. Free dermal fat flaps to the face. *Ann Plast Surg* 1979;3:1–12
19. Guerrerosantos J. Long-term outcome of autologous fat transplantation in aesthetic facial recontouring: sixteen years of experience with 1936 cases. *Clin Plast Surg* 2000;27:515–543
20. Rees TD, Ashley FL, Delgado JP. Silicone fluid injections for facial atrophy. A ten-year study. *Plast Reconstr Surg* 1973;52:118–127
21. Ozturk S, Acarturk TO, Yapici K, et al. Treatment of 'en coup de sabre' deformity with porous polyethylene implant. *J Craniofac Surg* 2006;17:696–701
22. Robitschek J, Wang D, Hall D. Treatment of linear scleroderma "en coup de sabre" with AlloDerm tissue matrix. *Otolaryngol Head Neck Surg* 2008;138:540–541
23. Slack G, Tabit C, Allam K, et al. Parry-Romberg reconstruction beneficial results despite poorer fat take. *Ann Plast Surg* 2014;73:307–310
24. Marx R, Carlson E, Eichstaedt R, et al. Platelet-rich plasma: growth factor enhancement for bone grafts. *Oral Surg Oral Med Oral Pathol Oral Radiol Endod* 1998:638–646

OPEN

Acute Hemorrhagic Apoplectic Pituitary Adenoma: Endoscopic Management, Surgical Outcomes, and Complications

Rucai Zhan, MD, PhD,[*†] *Yanxin Zhao, MD, PhD,*[‡] *Timothy M. Wiebe, MD,*[§] *and Xingang Li, MD, PhD*[*]

Objective: To assess safety and effectiveness of endoscopic transsphenoidal surgery (ETS) for acute hemorrhagic apoplectic pituitary adenoma.

Methods: Eighty nine patients with hemorrhagic apoplectic pituitary tumor undergoing endoscopic transsphenoidal surgery were included into a retrospective chart of this study. Charts were reviewed for patient age, sex, presentation, lesion size, surgical procedure, extent of resection, clinical outcome, and surgical complications.

Results: Seventy eight (87.7%) patients achieved total resection, 9 (10.1%) had subtotal resection, and 2 (2.2%) patients had partial resection; no patient experienced insufficient resection. After surgery, 65 (90.3%) of 72 patients who had visual acuity deterioration preoperatively normalized and improved significantly; the rate for remission of visual field was 87.7%. All other acute symptoms,

From the *Department of Neurosurgery, Qilu Hospital of Shandong University, Brain Science Research Institute, Shandong University; †Department of Neurosurgery, The Third People's Hospital of Jinan, Jinan, Shandong, China; ‡Department of Neurology, Jinan Central Hospital Affiliated to Shandong University, Jinan, Shandong, China; and §Private Practice, Bakersfield, CA.

Received May 18, 2014.
Accepted for publication June 28, 2015.

Address correspondence and reprint requests to Xingang Li, MD, PhD, 107 Wenhua Xilu Rd, Jinan, Shandong 250012, China; E-mail: lixg@sdu.edu.cn

Dr R.Z. and Dr Y.Z. contributed equally to this paper and shared first authorship.

Financial support: National Natural Science Foundation of China (NNSFC) (No. 81172404) Special Foundation for Taishan Scholars (No. ts20110814).

The authors report no conflicts of interest.

This is an open access article distributed under the terms of the Creative Commons Attribution-NonCommercial-NoDerivatives 4.0 License, where it is permissible to download and share the work provided it is properly cited. The work cannot be changed in any way or used commercially.
Copyright © 2015 by Mutaz B. Habal, MD

ISSN: 1049-2275
DOI: 10.1097/SCS.0000000000002026

such as severe headache, nausea, vomiting, alteration of mental status, and loss of consciousness, vanished postoperatively. Twenty eight (90.4%) of 31 patients with active secreting adenoma had hormonal remission based on endocrinological evaluation. Three (3.4%) patients incurred CSF leakage which was managed with lumbar drainage. Nine (10.1%) patients incurred transient DI postoperatively, and 2 (2.2%) of them developed permanent DI. Seven (7.9%) patients developed hypopituitarism which was treated with replacement therapy of hormone. One (1.1%) experienced craniotomy for intracranial hemorrhage and died from severe surgical complications postoperatively. There were no patients of meningitis or carotid artery injury.

Conclusion: Early detection and emergent endoscopic transsphenoidal surgery provided a safe and effective surgical option for hemorrhagic apoplectic pituitary tumor with a low morbidity and mortality.

Key Words: Acute, complications, endoscope transsphenoidal surgery, hemorrhage, outcomes, pituitary adenoma, pituitary apoplexy

Pituitary tumor apoplexy, especially acute hemorrhagic apoplexy, is infrequent and life-threatening medical condition that requires emergent neurosurgical intervention, which may lead to catastrophic consequence, such as permanent blindness, coma, and even death if misdiagnosed and untreated.[1,2] An appropriate and effective approach is crucial to manage the lesion with better outcomes. The original introduction into resection for the pituitary region of endoscopic transsphenoidal surgery (ETS) can be backed to the last half of the 20th century;[3] now ETS has obtained significant popularity for the management of pituitary lesions.[4,5] Is ETS also an option to treat hemorrhagic apoplectic pituitary adenoma that carries significant morbidity and mortality if untreated, especially for patients with altered consciousness, and visual loss? There was little information in the literature[6] which exists applying ETS for management of hemorrhagic apoplectic pituitary adenoma in a high-volume series. In this study, we presented a series of 89 patients who were diagnosed hemorrhagic apoplectic pituitary adenoma and underwent an emergent operation through ETS for resection of the lesion with favorable results in a period of 10 years, which may answer the above question.

METHODS

Experimental Design

A retrospective chart analysis was performed to identify 89 patients who presented acute symptoms due to hemorrhagic pituitary adenoma and underwent a TTEA for resection of the lesion at Qilu Hospital of Shandong University between July 2004 and June 2014. Records of those patients were evaluated for patient age, sex, presentation, tumor size, extent of resection, clinical outcomes, and surgical complications. Patients without any acute symptom who preoperatively, however, informed apoplexy intraoperatively were excluded from this study, because those patients were asymptomatic and treated as general pituitary adenoma. The protocol for this study was reviewed and approved by the Ethics Committee of Qilu Hospital of Shandong University (No. KYLL-2013-010).

Endoscopic Technique

Patients were diagnosed as having acute symptoms of headache and visual loss, signs of hemorrhage on imaging examinations, and subsequent course, such as informed findings intraoperative. All the patients were performed emergent EETA for resection of hemorrhagic pituitary adenoma in 24 hours of initial symptoms. The detailed endoscopic procedure was described in our previous report.[7] In most patients, the dural of the sellar floor was bluish violet and under high tension. Cruciate durotomy followed with drainage of dark red bloody fluid from sella turcica. Tumor with old blood clot was removed with curettage and/or suction, and a 30° endoscope was used to inspect the sellar region for residual tumor—which was removed. Skull base was reconstructed by the multilayered technique.

Postoperative Management

Intravenous infusion of a third-generation cephalosporin was continued for 3–7 days. Fluid intake and urine output were monitored. Hormones were replaced as necessary. MR imaging was performed within 1–3 days and at 3 months after surgery to evaluate the extent of tumor resection. Extent of resection was classified into 4 categories: total resection, subtotal resection, partial resection, and insufficient resection.[8] Nasal packing was generally removed endoscopically 1–3 days after surgery. Patients were instructed to avoid any activity that can raise intracranial pressure such as Valsalva maneuvers or nose blowing. Lumbar drainage was applied for patients who developed CSF leakage postoperatively. Early postoperative diabetes insipidus (DI) was treated with subcutaneous injection of Hypophysin for 3 days. Persistent DI was treated with daily administration of Minirin. We do not use controlled released vasopressin tannate because its effects may be difficult to control, and because it is an inconvenient method of treatment for patients.

Illustrative Case

This 43-year-old female patient presented with severe headache and acute deterioration of visual acuity and field. Visual acuity was 0.1/0.3 bilaterally, with bitemporal hemianopia. Admission T1-weighted MR imaging demonstrated hemorrhage in a pituitary tumor and obvious compression of the optic chiasm (Fig. 1A-B). The patient was treated with emergent endoscopic transsphenoidal surgery within 24 hours of initial presentations. Intraoperative endoscopic views showed dural of the sellar floor was bluish violet and under high tension (Fig. 1C- D). After surgery, her headache disappeared and visual acuity obviously improved to 0.5/0.8 bilaterally, with resolution of hemipanopia. On follow-up at 6 months postoperatively, MR imaging demonstrated no recurrence or residual adenoma (Fig. 1E-F).

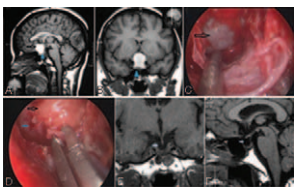

FIGURE 1. A, B, Findings of MR imaging examination preoperatively. MR imaging for 43-year-old female patient presenting with severe headache and acute deterioration of visual acuity and field. Initial sagittal (A) and coronal (B) T1-weighted MR imaging demonstrated hemorrhage (black arrowhead) in a pituitary tumor and marked compression of the optic chiasm (white arrowhead). Blue triangles point to the adenoma (A, B). C, D, Intraoperative endoscopic views. The patient was treated with emergent endoscopic transsphenoidal surgery within 24 hours of initial presentations. Intraoperative endoscopic views showed dural of the sellar floor was bluish violet and under high tension (black arrowhead), (C) tumor (black arrowhead) and hemorrhage (blue arrowhead) underneath of the dural (D). E, F, Following-up MR imagings. On follow-up at 6 months postoperatively, sagittal (E) and coronal (F) T1-weighted MR imaging demonstrated no recurrence or residual of the adenoma. (Blue arrowhead) Optic chiasm (red fine arrowhead, E) and pituitary stalk (red bold arrowhead, F) also were showed clear.

© 2015 Mutaz B. Habal, MD

RESULTS

Cohort consisted of 37 (41.6%) male and 52 (58.4%) female patients aged 14–73 years (mean 41.8 years). Follow-up ranged from 6 to 125 months (mean 51 months). The most frequent clinical presentation was onset of severe headache, 86 (96.6%) patients experienced headache in this series, followed by nausea and vomiting (93.3%), and then deterioration of visual acuity and visual field with rates of 80.9% and 73.0%, respectively. As results of the preoperative radiological study, 46 (51.7%) showed suprasellar extension, 15 had cavernous sinus invasion, 20 showed suprasellar and cavernous sinus extension, and only 8 patients were intrasellar. Thirty one (34.8%) of the 89 adenomas were active secreting, most of which were PRL-secreting adenoma, accounting for 19.1% of 89 patients (Table 1).

Seventy eight (87.7%) patients achieved total resection, 7 (7.9%) had subtotal resection, and 2 (2.2%) patients had partial resection; no patient experienced insufficient resection. After surgery, 57 (90.5%) of 63 patients who had visual acuity deterioration preoperatively obtained visual acuity improvement and normalization, and the rate for visual field improvement was 87.5%. Other symptoms, such as severe headache, mental status alteration, and loss of consciousness, had recovery with 100% of the rates. Endocrinological remission encountered in 28 (90.4%) of 31 patients with active secreting adenoma. Three (3.4%) patients incurred CSF leakage which was managed with lumbar drainage. Nine (10.1%) patients incurred transient DI postoperatively, and 2 (2.2%) of them developed persistent DI. Seven (7.9%) patients developed hypopituitarism which was treated with replacement therapy of hormone. One (1.1%) experienced craniotomy for intracranial hemorrhage and died from severe surgical complications postoperatively. There were no patients of meningitis or carotid artery injury (Table 2).

TABLE 1. Summary of Clinical Characteristics in 89 Patients

	No	Rate
Sex		
Male	37	41.6%
Female	52	58.4%
Age group		
<20	3	3.4%
20–29	12	13.5%
30–39	34	38.2%
40–49	21	23.6%
50–59	9	10.1%
60–69	6	6.7%
>70	4	4.5%
Presentations		
Headache	86	96.6%
Nausea and vomiting	83	93.3%
Visual acuity deterioration	72	80.9%
Visual field deterioration	65	73.0%
Alteration of mental status	5	5.6%
Loss of consciousness	2	2.2%
Extent of adenoma		
Intrasellar	8	9.0%
Suprasellar extension	46	51.7%
Cavernous sinus extension	15	16.8%
Suprasellar and cavernous sinus extension	20	22.5%

TABLE 2. Surgical Outcomes and Complications

	No	Rate
Extent of resection		
Total resection	78	87.7%
Subtotal resection	9	10.1%
Partial resection	2	2.2%
Pathologic type		
Active secreting	31	34.8%
PRL	17	19.1%
GH	7	7.9%
ACTH	4	4.5%
TSH	3	3.4%
Inactive secreting	58	65.2%
Initial symptom		
Headache		
Normalized	86/86	100%
Nausea and vomiting		
Normalized	83/83	100%
Visual acuity deterioration		
Normalized	40/72	55.6%
Improved	25/72	34.7%
No changed	7/72	9.7%
Visual field deterioration		
Normalized	43/65	66.2%
Improved	14/65	21.5%
No changed	8/65	12.3%
Alteration of mental status		
Normalized	5/5	100%
Loss of consciousness		
Normalized	2/2	100%
Endocrinologic recovery		
Normalized	10/31	32.3%
Improved	18/31	58.1%
No changed	3/31	9.6%
Surgical complication		
CSF leakage	3	3.4%
Hypopituitarism	7	7.9%
Transient DI	9	10.1%
Persistent DI	2	2.2%
Intracerebral hemorrhage	1	1.1%
Meningitis	0	0%
Carotid artery injury	0	0%
Death	1	1.1%

DISCUSSION

Apoplectic pituitary adenoma consists of approximately 10% of pituitary adenoma,[9] and is associated with severe morbidity and potential fatality.[10] The pathophysiological mechanism of the lesion is not being explained clearly, although pregnancy, trauma, surgery, dynamic endocrine testing, and stress can be precipitating factors.[11–15] Apoplectic pituitary adenoma was classified into hemorrhagic and infarcted.[16] Hemorrhagic apoplectic pituitary adenoma may consist of majority of these fatal clinical syndromes,[17,18] and may present a series of acute symptoms including onset of severe headache, sudden decreased vision, nausea and vomiting, altered consciousness,[19,20] and infrequently cranial nerve palsy.[21] Most pituitary tumor apoplexy occurs in pituitary adenoma, although ectopic pituitary apoplexy has been described in the cavernous sinus[21] and the clivus.[22] The management of hemorrhagic pituitary adenoma usually involves medical treatment and emergent transsphenoidal resection of lesion, early detection and effective decompression of the optic chiasm and optic nerve may be crucial to prevent mortality.[23–25]

© 2015 Mutaz B. Habal, MD

Surgical Results

Hemorrhagic apoplectic pituitary adenoma can occur in any age group; the majority of this population was middle-aged patients who aged 30–49 years, which accounted for 61.8% of 89 patients and was consistent with prior reports.[25] The most frequent complaint was onset of severe headache, 86 (96.6%) patients presented above symptom in this series, followed by nausea and vomiting with rate of 93.3%, headache and nausea were associated with rapid compression of sellar and parasellar structures due to expansion of hemorrhagic pituitary adenoma,[26,27] and headache may also have resulted from meningeal irritation.[1] Optic chiasm and optic nerve compression from hemorrhagic pituitary adenoma also result in sudden deterioration of visual acuity and visual field,[28,29] with rates of 80.9% and 73.0%, respectively, in our series. Alerted mental status was uncommon, which occurred in 5 (5.6%) patients in the current study, but more likely to indicate damage to hypothalamus and emergent surgical management.[30] Apoplectic hemorrhage of pituitary adenoma most typically encountered in macroadenoma, with predominance of inactive secreting adenoma.[31] The rates of macroadenoma and inactive secreting adenoma were 91% and 65.2% in the present study in agreement with prior reports.[25,31,32] Of active secreting adenomas accounted for 34.8% of the pituitary adenomas with hemorrhagic apoplexy, the majority was prolactin (PRL) secreting adenomas with a rate of 19.1%, which is correlated with the high prevalence of PRL-adenoma.[33,34] The rate of biochemical remission for active secreting adenoma was 90.4% in our series.

During follow-up period of mean 51 months, 87.7% patients obtained total resection (Table 2), which is comparable with prior reports of endoscopic transsphenoidal surgery.[23,35] The rate of resection may be associated with appropriate approach, surgeon's experience, morphological and biological characteristics of tumor, such as volume, location, and adherence. In our opinion, good lighting and panoramic view provided by the endoscope allows a neurosurgeon to obtain a better surgical condition, which together with meticulous and precise manipulation permits the neurosurgeon to resect lesion more extensively with less injury. During the operation, the use of angled endoscopes allows the surgeon to remove the tumor around corners of surgical field. Moreover, hemorrhage from pituitary adenoma apoplexy may be helpful to resection with lower risk of impairment to parasellar neurovasculature.[16,36] Acute deterioration of visual acuity and visual field may be associated with rapid compression of chiasm and optic nerve due to sudden extension of the adenoma caused by intratumoral hemorrhage. Cardoso et al[37] indicated in a review that the level of visual recovery depended mainly on early and effective transsphenoidal decompression rather than on the severity of initial visual loss. All the patients underwent emergent endoscopic transsphenoidal decompression of optic chiasm or nerve in 24 hours of onset of initial symptoms. Preoperative deterioration visual acuity and visual field were normalized or improved significantly with 90.5% and 87.5% of rates respectively, which supported previous reports.[23,38] As our experience, timely and effective endoscopic transsphenoidal decompression facilitated improvement of visual symptoms.

Morbidity Related to Surgery

Despite techniques of skull base reconstruction,[39–41] CSF leak remains a considerable associated complication of ETS. Three (3.4%) patients in this series experienced postsurgical CSF leak which was managed successfully with lumbar drainage, which is comparable to previously reported rates of CSF leak from ETS for the sellar and parasellar region.[42,43] Factors that may lead to CSF leak include surgical manipulation, surgeon's experience, tumor's location, volume, and relationship to surrounding neurovascular structures. The most important factor that leads to postoperative CSF leakage might be repair technique of the skull base, although feature of the tumor and surgeon's preference may affect surgical result. In our institute, we routinely used reconstruction of skull base on the basis of the multilayered technique with or without PNSF resulting in an excellent result, which showed that hemorrhage from pituitary tumor apoplexy did not affect reconstruction of the skull base or increase occurrence of CSF leakage. Furthermore, the unparalleled panoramic endoscopic view in ETS enables detection of tiny fistulas which can be repaired with skull base reconstruction.

Transient DI also is a common complaint related to endoscopic approach. It is possible that surgical manipulation to the sellar in the context of preexisting compromise of the blood supply to the magnocellular neurons of the hypothalamus from apoplexy manifested as a reversible disturbance of arginine vasopressin (AVP) transport to the posterior pituitary gland. In this study, transient DI was 10.1% which was consistent with most reported results.[44,45] However, the presence of permanent DI (2.2%) is lower than most reported rates,[46,47] and indicates that most surgical injury is reversible. Pituitary dysfunction may be associated with compression or destruction of the posterior labe of pituitary gland from hemorrhagic apoplexy. Chowdhury et al observed in a series of 152 patients that 71% of the patients with apoplexy encountered postsurgical DI.[48] Also, 16% incidence of transient DI in patients of pituitary apoplexy was reported in a series of Randeva et al.[49] The above observations may indicate that incurrence of DI was associated with pituitary apoplexy; therefore, timely decompression was crucial for saving endocrinological function of pituitary gland. Besides interruption of the blood supply to pituitary gland due to hemorrhage, injury or edema of pituitary stalk is an important reason that results in postoperative DI.[48,50] Nemergut et al[51] found that postoperative DI, both transient and permanent, may be associated with intraoperative leak resulting from aggressive manipulation; however, our results did not support the above conclusion. Meticulous manipulation to avoid track injury of pituitary stalk may decrease the risk of postoperative endocrinological complication. All the patients encountering hypopituitarism postoperatively were managed by replacement of hormone with better outcomes.

Intracranial hemorrhage after endoscopic resection of acute hemorrhagic pituitary tumor is uncommon and lethal, which often occurs in 12 hours after surgery, and also often encounters in the patients who experienced subtotal removal of macroadenoma. Patel and colleagues[52] reported a patient of delayed postoperative pituitary hemorrhagic apoplexy treated by emergent reexploration. In our series, 1 (1.1%) patient incurred postoperative intracranial hematoma and died following transcranial approach. Any acute complication from hemorrhagic apoplectic pituitary tumor can lead to death; cares should be taken to prevent perioperative hemorrhage.

CONCLUSION

In the current series, we obtained excellent surgical outcomes and comparable lower complications after ETS for management of hemorrhagic apoplectic pituitary adenoma. Acute hemorrhage from apoplectic pituitary tumor is an emergent and life-threatening condition that may require surgical intervention to prevent progression and morbidity. On the contrary, ETS provided a safe and effective surgical option for acute hemorrhagic apoplexy of pituitary adenoma. Early detection and timely emergent endoscopic transsphenoidal surgery resulted in a favorable surgical outcome with low rate of surgical complications.

© 2015 Mutaz B. Habal, MD

REFERENCES

1. Bills DC, Meyer FB, Laws ER Jr, et al. A retrospective analysis of pituitary apoplexy. *Neurosurgery* 1993;33:602–609
2. Bonicki W, Kasperlik-Zaluska A, Koszewski W, et al. Pituitary apoplexy: endocrine, surgical and oncological emergency. Incidence, clinical course and treatment with reference to 799 cases of pituitary adenomas. *Acta Neurochir* 1993;120:118–122
3. Apuzzo ML, Heifetz MD, Weiss MH, et al. Neurosurgical endoscopy using the side-viewing telescope. *J Neurosurg* 1977;46:398–400
4. Powell M, Gnanalinghan KK. Endoscopic trans-sphenoidal pituitary surgery: is it here to stay? *Br J Neurosurg* 2007;21:315–317
5. Jho HD, Carrau RL. Endoscopic endonasal transsphenoidal surgery: experience with 50 patients. *J Neurosurg* 1997;87:44–51
6. Hasegawa Y, Yano S, Sakurama T, et al. Endoscopic surgical treatment for pituitary apoplexy in three elderly patients over the age of 80. *Acta Neurochir* 2011;Suppl. 111:429–433
7. Zhan R, Chen S, Xu S, et al. Postoperative low-flow cerebrospinal fluid leak of endoscopic endonasal transsphenoidal surgery for pituitary adenoma: wait and see, or lumbar drain? *J Craniofac Surg* 2015;26:1261–1264
8. Frank G, Pasquini E. Endoscopic endonasal cavernous sinus surgery, with special reference to pituitary adenomas. *Front Horm Res* 2006;34:64–82
9. Turgut M, Ozsunar Y, Başak S, et al. Pituitary apoplexy: an overview of 186 cases published during the last century. *Acta Neurochir (Wien)* 2010;152:749–761
10. Johnston PC, Hamrahian AH, Weil RJ, et al. Pituitary tumor apoplexy. *J Clin Neurosci* 2015;22:939–944
11. Okuda O, Umezawa H, Miyaoka M. Pituitary apoplexy caused by endocrine stimulation tests: a case report. *Surg Neurol* 1994;42:19–22
12. Fyrmpas G, Constantinidis J, Foroglou N, et al. Pituitary apoplexy following endoscopic sinus surgery. *J Laryngol Otol* 2010;124:677–679
13. Proust F, Hannequin D, Bellow F, et al. Stress-induced pituitary apoplexy in 2 phases. *Neurochirurgie* 1995;41:372–376
14. Sun T, Liu L, Sunnassee A, et al. Sudden death in custody due to pituitary apoplexy during long restriction in a sitting position: a case report and review of the literature. *J Forensic Leg Med* 2013;20:812–815
15. de Heide LJM, van Tol KM, Doorenbos B. Pituitary apoplexy presenting during pregnancy. *The Netherlands J Med* 2004;62:393–396
16. Chang CV, Felicio AC, Toscanini AC. Pituitary tumor apoplexy. *Arq Neuropsiquiatr* 2009;67:328–333
17. Elias WJ, Laws ER Jr. Transsphenoidal approaches to lesions of the sella. In: Schmidek A, Sweet WH, eds. *Operative Neurosurgical Techniques.* Philadelphia, PA: W. B. Saunders; 2000. 373–384
18. Lazaro CM, Guo WY, Sami M, et al. Haemorrhagic pituitary tumours. *Neuroradiology* 1994;36:111–114
19. Sibal L, Ball SG, Connolly V, et al. Pituitary apoplexy: a review of clinical presentation, management and outcome in 45 cases. *Pituitary* 2004;7:157–163
20. Dubuisson AS, Beckers A, Stevenaert A. Classical pituitary tumour apoplexy: clinical features, management and outcomes in a series of 24 patients. *Clin Neurol Neurosurg* 2007;109:63–70
21. Zoli M, Mazzatenta D, Pasquini E, et al. Cavernous sinus apoplexy presenting isolated sixth cranial nerve palsy: case report. *Pituitary* 2012;15(Suppl 1):S37–40
22. Mudd PA, Hohensee S, Lillehei KO, et al. Ectopic pituitary adenoma of the clivus presenting with apoplexy: case report and review of the literature. *Clin Neuropathol* 2012;31:24–30
23. Zhang X, Zhang W, Fu LA, et al. Hemorrhagic pituitary macroadenoma: characteristics, endoscopic endonasal transsphenoidal surgery, and outcomes. *Ann Surg Oncol* 2011;18:246–252
24. Ayuk J, McGregor EJ, Mitchell RD, et al. Acute management of pituitary apoplexy-surgery or conservative management? *Clin Endocrinol* 2004;61:747–752
25. Randeva HS, Schoebel J, Byrne J, et al. Classical pituitary apoplexy: clinical features, management and outcome. *Clin Endocrinol* 1999;51:181–188
26. da Motta LA, de Mello PA, de Lacerda CM, et al. Pituitary apoplexy: clinical course, endocrine evaluations and treatment analysis. *J Neurosurg Sci* 1999;43:25–36
27. Rolih CA, Ober KP. Pituitary apoplexy. *Endocrinol Metab Clin North Am* 1993;22:291–302
28. Semple PL, Webb MK, de Villiers JC, et al. Pituitary apoplexy. *Neurosurgery* 2005;56:65–73
29. Sibal L, Ball S, Connolly V, et al. Pituitary apoplexy: a review of clinical presentation, management and outcome in 45 cases. *Pituitary* 2004;7:157–163
30. Rajasekaran S, Vanderpump M, Baldeweg S, et al. UK guidelines for the management of pituitary apoplexy. *Clin Endocrinol (Oxf)* 2011;74: 9–20
31. Arita K, Tominaga A, Sugiyama K, et al. Natural course of incidentally found nonfunctioning pituitary adenoma, with special reference to pituitary apoplexy during follow-up examination. *J Neurosurg* 2006;104:884–891
32. Hewidy MS. An urgent trans-sphenoidal approach for surgical treatment of pituitary apoplexy: is it life saving? *Egypt J Neurol Surg* 2009;24: 45–53
33. Dessimoz C, Browaeys P, Maeder P, et al. Transformation of a microprolactinoma into a mixed growth hormone and prolactin-secreting pituitary adenoma. *Front in Endocrinol* 2012;12:1–5
34. Arafah BM, Nasrallah MP. Pituitary tumors: pathophysiology, clinical manifestations and management. *Endocrine-Related Cancer* 2001;8:287–305
35. Gondim JA, Schops M, de Almeida JP, et al. Endoscopic endonasal transsphenoidal surgery: surgical results of 228 pituitary adenomas treated in a pituitary center. *Pituitary* 2010;13:68–77
36. Onesti ST, Wisniewski T, Post KD. Clinical versus subclinical pituitary apoplexy: presentation, surgical management, and outcome in 21 patients. *Neurosurgery* 1990;26:980–986
37. Cardoso ER, Peterson EW. Pituitary apoplexy: a review. *Neurosurgery* 1984;14:363–373
38. Zhang X, Fei Z, Zhang W, et al. Emergency transsphenoidal surgery for hemorrhagic pituitary adenomas. *Surg Oncol* 2007;16:115–120
39. Eloy JA, Shukla PA, Choudhry OJ, et al. Assessment of frontal lobe sagging after endoscopic endonasal transcribriform resection of anterior skull base tumors: is rigid structural reconstruction of the cranial base defect necessary? *Laryngoscope* 2012;122:2652–2657
40. Greenfield JP, Anand VK, Kacker A, et al. Endoscopic endonasal transsphenoidal transcribriform transfovea ethmoidalis approach to the anterior cranial fossa and skull base. *Neurosurgery* 2010;66:883–892
41. Hadad G, Bassagasteguy L, Carrau RL. A novel reconstructive technique after endoscopic expanded endonasal approaches: vascular pedicle nasoseptal flap. *Laryngoscope* 2006;116:1882–1886
42. Berker M, Aghayev K, Yücel T, et al. Management of cerebrospinal fluid leak during endoscopic pituitary surgery. *Auris Nasus Larynx* 2013;40:373–378
43. Bokhari AR, Davies MA, Diamond T. Endoscopic transsphenoidal pituitary surgery: a single surgeon experience and the learning curve. *Br J Neurosurg* 2013;27:44–49
44. Senior BA, Ebert CS, Bednarski KK, et al. Minimally invasive pituitary surgery. *Laryngoscope* 2008;118:1842–1855
45. Sigounas DG, Sharpless JL, Cheng DM, et al. Predictors and incidence of central diabetes insipidus after endoscopic pituitary surgery. *Neurosurgery* 2008;62:71–78
46. Koutourousiou M, Gardner PA, Fernandez-Miranda JC, et al. Snyderman. Endoscopic endonasal surgery for giant pituitary adenomas: advantages and limitations. *J Neurosurg* 2013;118:621–631
47. Schreckinger M, Walker B, Knepper J, et al. Post-operative diabetes insipidus after endoscopic transsphenoidal surgery. *Pituitary* 2013;16:445–451
48. Chowdhury T, Prabhakar H, Bithal PK, et al. Immediate postoperative complications in transsphenoidal pituitary surgery: a prospective study. *Saudi J Anaesth* 2014;8:335–341
49. Randeva HS, Schoebel J, Byrne J, et al. Classical pituitary apoplexy: clinical features, management and outcome. *Clin Endocrinol (Oxf)* 1999;51:181–188
50. Xiao G, Yuan X, Yuan J, et al. Pituitary stalk management during the microsurgery of craniopharyngiomas. *Exp Ther Med* 2014;7: 1055–1064

© 2015 Mutaz B. Habal, MD

51. Nemergut EC, Zuo Z, Jane JA Jr et al. Predictors of diabetes insipidus after transsphenoidal surgery: a review of 881 patients. *J Neurosurg* 2005;103:448–454
52. Patel SK, Christiano LD, Eloy JA, et al. Delayed postoperative pituitary apoplexy after endoscopic transsphenoidal resection of a giant pituitary macroadenoma. *J Clin Neurosci* 2012;19:1296–1298

Electromyographic Evaluation of Temporalis Muscle Following Temporalis Tendon Transfer (Facial Reanimation) Surgery

Orhan Ozturan, MD, Berke Ozucer, MD,* and Azize Esra Gursoy, MD†*

Abstract: Facial paralysis is a significant functional and aesthetic handicap. Many techniques have been defined for facial reanimation. The aim of the study was to evaluate postoperative electromyographical (EMG) activity of temporalis muscle to assess the potential neural impairments related to the surgical procedure.

Methodology: Four patients with facial paralysis were operated with the temporalis muscle tendon transfer technique. Simultaneous surface electromyographic (sEMG) activity at first postoperative year from the bilateral temporalis and masseter muscles was obtained at mandibular rest position and then during maximal clenching.

Results: Patients were followed for a minimum period of 18 months. Surface electromyographic evaluations during passive state revealed similar values for the operated and contralateral side. Measurements during active "clench-smiling" of the jaw revealed similar amplitudes for both muscles of the operated side in all cases except case #2. Case #2 revealed lower values for both measurements of temporalis and masseter muscles of the operated side compared with the contralateral side. Dissonant results of case #2 can be the consequence of impaired temporalis muscle activity because of the tension on the muscle as a consequence of overcorrection.

Conclusion: Temporalis muscle transfer to the perioral region does not hinder contractility of the muscle as long as the facial deformity is not overcorrected.

Key Words: Facial paralysis, facial reanimation, temporalis tendon transfer, electromyography

From the *Department of Otorhinolaryngology and Head and Neck Surgery, Bezmialem Vakif University; and †Department of Neurology, Bezmialem Vakif University, Fatih, Istanbul, Turkey.
Received October 8, 2014.
Accepted for publication June 28, 2015.
Address correspondence and reprint requests to Berke Ozucer, MD, Department of Otorhinolaryngology, Medical Faculty, Bezmialem Vakif University, Fatih, Istanbul, Turkey;
E-mail: berkeozucer@gmail.com
The authors report no conflicts of interest.
Copyright © 2015 by Mutaz B. Habal, MD
ISSN: 1049-2275
DOI: 10.1097/SCS.0000000000002027

Facial paralysis is considered a significant functional and aesthetic handicap. It severely impairs mastication, speech production, and eye protection, but above all it deprives one of the essential means of mental and affective expressions: mimesis and the smile. Many operative techniques have been defined for facial reanimation. Rubin, Baker, and Conley popularized use of the temporalis muscle turn-down flap in reanimation of the paralyzed lower face in the early 1970s.[1,2] The classic technique of temporalis muscle transfer described by Rubin and others has the disadvantages of donor site depression and midfacial widening. In addition, it depends on a nonanatomic contraction of the transposed muscle segment. McLaughlin[3] described the orthodromic transoral technique for transferring the coronoid process with the attached temporalis tendon to the corner of the mouth. This process avoids the fullness over the zygomatic arch area and the temporal donor site depression that is produced by the turned-down temporalis muscle flap. Dynamic temporal muscle tendon transfer was recently reintroduced and refined by Boahene et al.[4]

As with the other muscles of mastication, control of the temporal muscle comes from the third (mandibular) branch of the trigeminal nerve. Specifically, the muscle is innervated by the deep temporal nerves. Thorough dissection and freeing of the temporalis muscle required for complete releasing and transfer of the tendon with the coronoid process is needed during this procedure. Temporalis tendon transfer necessitates to stretching of the tendon along with the coronoid to the perioral region. It is necessary to mobilize the temporalis muscle by performing releasing dissections over and below the muscle and tendon. Temporalis muscle innervation has the potential to be injured because of exposure, release, and transfer of the temporalis muscle tendon.

Surface electromyography (sEMG) has been reliably used to evaluate the functional status and innervation of the facial musculature after surgery. The aim of this study was to evaluate postoperative electromyographical (EMG) activity of temporalis muscle in comparison with the unoperated contralateral side.

PATIENTS AND METHODS

Four patients who had facial paralysis >2 years were operated with the temporalis muscle tendon transfer technique as reported by Boahene et al.[4]

Surgical Technique

Through the melolabial crease, an approximately 2-cm incision was made. Through this incision, dissection was bluntly performed in the buccal space, and deep retractors were placed to retain the buccal fat. By palpation and by manually opening and closing the jaw, the anterior edge of the ascending mandibular ramus was identified. Using an angled clamp, the mandibular notch was identified, and the coronoid process was exposed. Dissection was performed bluntly to expose the anterior edge of the ascending mandibular ramus. Using electrocautery, the periosteum was incised, and soft tissues enclosing the temporalis tendon were elevated from the medial and lateral aspects of the coronoid process and ascending ramus. The coronoid process was cut of using osteom and drill-burr at the level of incisura mandibula and kept attached with the temporal tendon. Temporalis tendon was isolated as medial as possible and down to the buccinator muscle to obtain adequate tendon length. The temporalis tendon was transposed through the buccal space and was secured to the orbicularis oris and zygomaticus muscle insertion. The tendon was then sutured into place with 3-0 taper mattress sutures.[4] Incisions were meticulously

FIGURE 1. Case #1: preoperative and postoperative photos—A, passive; B, smile; and C, eye closure. Facial reanimation (temporalis muscle dynamic tendon transfer and golden weight applied to left eyelid) as well as septoplasty (septal subluxation to left can be observed on preoperative photos) and Paniello suture applied for correction of left nasal valve deformity.

sutured with absorbable sutures following cauterization of bleeding sites.

Surface Electromyographic Recording

Postoperative sEMG of the temporalis muscles was recorded individually during rest and maximal clenching. Values were compared with healthy contralateral side: all the study participants underwent an sEMG recording with a commercially available device—a 4-channel electromyograph (Keypoint-Dantec, Skovlunde, Denmark). The patients were comfortably seated in a chair inside a room with a controlled temperature (22°C). After the skin was cleaned with 95% alcohol, the recording was performed by the use of silver/silver chloride bipolar surface electrodes (diameter 10 mm, interelectrode distance 21 ± 1 mm). The electrodes were placed bilaterally on the patient's skin overlying the anterior temporalis, vertically along the anterior muscular margin, approximatively over the coronal suture. For the masseter, the electrodes were placed parallel to muscular fibers, with the upper pole of the electrode at the intersection between the tragus–labial commissure and the exocanthion–gonion lines, perpendicular to the skin surface. A plate ground electrode was secured to the forehead.

FIGURE 2. Case #2: preoperative and postoperative photos—A, passive; B, smile; and C, eye closure.

FIGURE 3. Case #3: preoperative and postoperative photos—A, passive; B, smile; and C, D, profile. Facial reanimation (temporalis muscle dynamic tendon transfer and golden weight applied to right eyelid) as well as wide open septorhinoplasty operation to ptotic nose with thick skin.

Simultaneous sEMG activity from the bilateral temporalis and masseter muscles was obtained at mandibular rest position and then during maximal clenching. The patient was asked to clench the teeth as hard as possible, 10 times for 5 seconds, with 10-second relaxation between each clench. The tests were explained and shown to the patients, who practiced before actual data acquisition. By using the derived EMG, the root mean square (RMS) value in microvolts was calculated, using a data analysis system. For evaluation, the mean value of 10 recordings at resting position and 10 consecutive clenching cycles was recorded.[5]

RESULTS

Three patients were male and one was female (Figs. 1–4Figs. 1-4). Mean age was 40 years. Patients were followed for a minimum period of 18 months (Table 1), mean duration of follow-up was 21.0 ± 2.4 months. Patients were subjected to sEMG assessment at first postoperative year. Surface electromyographic evaluations during passive state revealed similar values of RMS and amplitude for the operated and contralateral side. Measurements during active ''clench-smiling'' of the jaw revealed either equal or slightly higher amplitudes for both muscles of the operated side in all cases except case #2 (Table 1) (Fig. 2). Case #2 revealed lower values for both measurements of temporalis and masseter muscles of the operated side compared with the contralateral side.

Ratio of amplitudes of temporal and massater muscles were calculated individually for each case (Table 2). All temporal-to-massater ratios, except case #2, in both the operated and contralateral side were ≤ 1 (Table 2). This value was 1.52 and 1.22 for operated and contralateral sides of case #2, respectively.

DISCUSSION

Temporalis tendon transfer necessitates to stretching of the tendon along with the coronoid to the perioral region. It is necessary to mobilize the temporalis muscle by performing releasing dissections over and below the muscle and tendon. The exposure, release, and transfer of the temporalis muscle insertion may cause impairment of temporalis muscle innervation. All surgical techniques have some drawbacks and shortcomings.

Results revealed unhampered activity of the temporalis muscle on the operated side. Mobilization and transfer of the temporalis

FIGURE 4. Case #4: postoperative photos—A, passive; B, smile; and C, eye closure.

© 2015 Mutaz B. Habal, MD

TABLE 1. Comparison of Operated and Contralateral Side EMG values During Active "Clench-Smiling"

					Operated Side—Temporal Muscle		Contralateral Temporal Muscle		Operated Side—Massater Muscle		Contralateral Massater Muscle	
	Time Elapsed	Age	Sex	Operated Side	Amp.	RMS	Amp.	RMS	Amp.	RMS	Amp.	RMS
Case #1	24 mo	40	F	Left	430	189	394	177	430	190	409	185
Case #2	21 mo	36	M	Right	279	97	381	167	183	56	313	131
Case #3	21 mo	52	M	Right	398	171	354	149	421	177	429	184
Case #4	18 mo	30	M	Left	301	124	287	111	313	137	272	108

Amp., amplitude (microvolts); EMG, electromyographical; F, female; M, male; RMS, root mean squared.

TABLE 2. Comparison of Operated and Contralateral Temporal/Massater EMG Amplitude Ratios

	Operated Temporal/Massater	Contralateral Temporal/Massater
Case #1	1	0.96
Case #2	1.52	1.22
Case #3	0.95	0.83
Case #4	0.96	1.05

EMG, electromyographical.

muscle to the perioral region does not hinder contractility of the muscle as long as the facial deformity is not overcorrected.

In the presented photos of the operated patients (Figs. 1–4), case #2 presents with a slight overcorrection of temporal reanimation repair compared with other three cases (Fig. 2). Dissonant results of case #2 can be the consequence of impaired temporalis muscle activity because of the tension on the muscle. Therefore, we concluded overcorrection in these type of patients will limit the activity of temporalis muscle and adaptation to "clench-smiling."

CONCLUSION

Although dynamic muscle transfer may cause postoperative impairment of temporalis muscle activity, postoperative training for adaptation to "clench-smiling" and compensation of this impairment can yield satisfactory clinical and EMG results. Results revealed unhampered EMG activity of the temporalis muscle on the operated side. Mobilization and transfer of the temporalis muscle to the perioral region does not hinder contractility of the muscle as long as the facial deformity is not overcorrected. Overcorrection in these cases may limit the activity of temporalis muscle and adaptation to "clench-smiling."

REFERENCES

1. Rubin LR, ed. *Reanimation of the Paralyzed Face. Reanimation of the Paralyzed Face*. St Louis, MO: CV Mosby; 1977
2. Baker DC, Conley J. Regional muscle transposition for rehabilitation of the paralyzed face. *Clin Plast Surg* 1979;6:317–331
3. McLaughlin CR. Permanent facial paralysis: the role of surgical support. *Lancet* 1952;2:647–651
4. Boahene KD, Farrag TY, Ishii L, et al. Minimally invasive temporalis tendon transposition. *Arch Facial Plast Surg* 2011;13:8–13
5. Haughton JF, Little JW, Powers RK, et al. M/RMS: an EMG method for quantifying upper motoneuron and functional weakness. *Muscle Nerve* 1994;17:936–942

Characteristics of Maxillary Morphology in Unilateral Cleft Lip and Palate Patients Compared to Normal Subjects and Skeletal Class III Patients

Chanyuan Jiang, MD, Ningbei Yin, MD, Yilue Zheng, MD, and Tao Song, MD

Abstract: This study is to investigate the anatomical features of maxillae in unilateral cleft lip and palate (UCLP) patients with maxillary retrusion. Additionally, the dissimilarities of retruded maxillae between the UCLP patients and the skeletal class III patients were compared. Craniofacial measurements were carried out among 32 UCLP adult patients with maxillary retrusion (GC), 24 adult patients in class III (SNA $< 80^\circ$, ANB $< 0^\circ$) patients (GIII), and 32 normal controls (GN). The authors measured the width and length of the maxillae, as well as their relative positions to the coronal plane passing through basion. The independent sample group *t* test was performed, and $P < 0.05$ was regarded as statistically significant. In the GC group, the anterior and posterior maxillary length ($A_1P_{3M}\perp CP$ and P_{3M}-$P_{6M}\perp CP$) and overall maxillary length (A_1-$P_{6M}\perp CP$) at the dental level, the interdental widths of the maxillae, the maxillary volume (G_M), and the volume consisting of maxilla and maxillary sinus (G_T) significantly reduced compared with the GN group ($P < 0.05$). The distances from the points on the maxillae to the coronal plane ($A_1\perp CP$, $P_{3M}\perp CP$, and $P_{6M}\perp CP$) in

From the Center of Cleft Lip and Palate Treatment, Plastic Surgery Hospital, Chinese Academy of Medical Sciences and Peking Union Medical College, Beijing, China.

Received December 6, 2014.
Accepted for publication June 28, 2015.

Address correspondence and reprint requests to Tao Song, MD, Center for Cleft Lip and Palate Treatment, Plastic and Surgery Hospital, Chinese Academy of Medical Science, Peking Union Medical College, No 33, Ba-Da-Chu Rd, Shi Jing Shan District, Beijing 100144, China; E-mail: songtao2059@gmail.com

This work was supported by the Capital Medical Development Fund of China (Z141107002514095).
The authors report no conflicts of interest.

Copyright © 2015 by Mutaz B. Habal, MD

ISSN: 1049-2275
DOI: 10.1097/SCS.0000000000002028

the GC and GIII groups were smaller than those in the GN group ($P < 0.05$). In summary, for the UCLP patients, the decreased prominence of maxillary complex could be mainly caused by the shortened maxillary length; meanwhile, posterior position of the maxillary body may have some influence on the maxillary protrusion. While for the class III patients, maxillary retrusion was resulted from malposition and malmorphology on an equal basis.

Key Words: Cleft and palate, maxillary retrusion, skeletal class III

Orofacial clefts in newborns are the most common facial deformities. Intrinsic developmental deficiency, as well as functional and iatrogenic factors,[1–5] often result in inhibited maxillary growth. The hypogenetic maxillae can affect the alveolus, dentition, and associated soft-tissue structures.[6] Patients with significant disturbances of growth of the jaws, dental arch stenosis, malocclusions, and discrepancies in maxillomandibular skeletal alignment should have correction with orthodontics or orthognathic surgeries. Eventually, 25–60% of the patients with cleft lip and/or palate need maxillary advancement to correct the maxillary hypoplasia and improve aesthetic facial proportions.[7] The positive results of Lefort I osteotomy, the standard procedure for class III patients with maxillary retrusion, have been universally recognized. For most class III patients, advancing the integrated maxillary body could result in occlusal, esthetic, and functional improvement. However, in some patients who have unilateral cleft lip and palate (UCLP), leading the intact maxillae forward for anterior crossbite correction is likely to be at the expense of molar occlusion.

Are there any differences in the retruded maxillae between the class III patients with and without cleft? Information regarding maxillae is important to clinicians in orthodontics, prosthodontics, and orthognathics. With the advances in medical imaging and reconstruction techniques, three-dimensional (3D) computed tomography (CT) stereoscopic measurement has been used to study the craniomaxillofacial structure for decades.[8–10]

The purpose of this study was to investigate the anatomical features of maxillae in unilateral cleft lip and palate (UCLP) patients with maxillary retrusion. Additionally, the dissimilarities of retruded maxillae between the UCLP patients and the skeletal class III patients were compared.

PATIENTS AND METHODS

Research Patients

This study was approved by Plastic Surgery Hospital, Chinese Academy of Medical Sciences and Peking Union Medical College ethics committee and performed according to the principles of Declaration of Helsinki. Written consents were obtained from the participants or their custodians. From 2011 to 2014, 88 patients of Chinese origin were enrolled from our center. Patients were divided into 3 groups: the group of 32 complete UCLP patients with maxillary retrusion who received Millard cleft lip repairs and unilateral von Langenbeck palatoplasty during childhood (GC); the group of 24 class III patients with maxillary retrusion ($ANB < 0°$, $SNA < 80°$) but without any other craniofacial deformities (GIII); and the group of 32 normal adults with ideal occlusion (GN). Patients who had other deformities in the maxillofacial region or had a history of any orthodontic or orthognathic treatment were excluded.

Spiral CT Scanning

All patients were placed statically in the supine position with the facial midline coinciding with the long axis of the CT machine on the Frankfort horizontal plane perpendicular to the floor. The CT slice date was from the Light Speed CT scanner (Brilliance CT 64 Slice, Philips Medical Systems, Inc, USA) using a high-resolution bone algorithm with a slice thickness of 1.00 mm at 120.0 kV and 280 mA. The image covered the areas from the basis crania to the inferior border of the mandibular body and had a pixel matrix of 512×512.

TABLE 1. Landmarks Used in the Current Study

Landmarks	Definition
A	Most posterior point on contour of maxillary alveolar process
A_1	Most inferior and anterior point on alveolar crest of maxilla
ANS	Most anterior point of anterior nasalspine
B	Most posterior point on contour of mandibular alveolar process
Ba	Anterior midpoint of foramen magnum
M_{1M}	Middle point of cut edge of incisor
M_{2M}	Middle point of cut edge of literal incisor
M_3	Maxillary canine cusp
M_4	Buccal cusp of maxillary first premolar
M_5	Buccal cusp of maxillary second premolar
M_{6m}	Mesiobuccal cusp of maxillary first molar
M_{6d}	Distobuccal cusp of maxillary first molar
M_{7m}	Mesiobuccal cusp of maxillary second molar
M_{7d}	Distobuccal cusp of maxillary second molar
Mx	Lowermost point on zygomaticoalveolar ridge
OrL	Lowest point on edge of left orbital
PL	Uppermost point on left bony external auditory meatus
PR	Uppermost point on right bony external auditory meatus
PNS	Most posterior midpoint of posterior nasalspine
P_3	Midpoint of palatally gingival margin of maxillary canine
P_4	Midpoint of palatally gingival margin of maxillary first premolar
P_5	Midpoint of palatally gingival margin of maxillary second premolar
P_6	Midpoint of palatally gingival margin of maxillary first molar
P_7	Midpoint of palatally gingival margin of maxillary second molar
P_{3M}	Midpoint of the line between bilateral P_3 points
P_{6M}	Midpoint of the line between bilateral P_6 points
S	Center of sella turcica

P_*: represents P_3, P_4, P_5, P_6, P_7 points. M_*: represents M_{1M}, M_{2M}, M_3, M_4, M_5, M_{6m}, M_{6d}, M_{7m}, and M_{7d} points. M_*L: M_* of the left side in GN and GIII groups/M_* of the cleft side in GC group. M_*R: M_* of the right side in GN and GIII groups/M_* of the healthy side in GC group.

Three-Dimensional Craniometric Analysis

The axial images were reconstructed into a 3D video model using Mimics, software, version 16.0. All landmarks and measurements are defined in Tables 1-2.

Statistical Methods

All statistical analyses were conducted by IBM SPSS Statistics software, version 20.0. Descriptive statistics included means and standard deviations of the individual groups. The independent sample group t test was used to compare means of cleft side and healthy side in GC group, means of left and right sides in GN and GIII groups, as well as means of GC and GN, GC and GIII, GIII and GN. The levels of significance were set at $P < 0.05$.

RESULTS

Reliability

All cephalometric landmarks on 3D-CT were digitized twice by the same investigator to eliminate measurement errors. First and

© 2015 Mutaz B. Habal, MD

TABLE 2. Measurements Used in Current Study

Measurements	Definition
HP	Horizontal plane containing the Ba point and parallel to Frankfort plane constructed by OrL, PL, and PR points
SP	Sagittal plane containing the Ba and S points and perpendicular to the horizontal plane
CP	Coronal plane containing the Ba point and perpendicular to HP and SP
S-N	Length of the anterior cranial base from S to N points
S-Ba	Length of the posterior cranial base from S to Ba points
Ba-N	Length of the whole cranial base from Ba to N points
∠NSBa	Angel from N to S to Ba points
∠SNA	Angle from N to S to A points
∠SNB	Angle from N to S to B points
MH	Length of the anterior maxilla from N to ANS points
MW	Width of the maxilla between bilateral Mx points
PL	Length of the palate from ANS to PNS points
M_*W	Distance between bilateral M_* points
M_*L-SP	Distance from M_*L point to SP
M_*R-SP	Distance from M_*R point to SP
P_*W	Distance between bilateral P_* points
A_1-CP	Distance from A_1 point to CP
P_{3M}-CP	Distance from P_{3M} point to CP
P_{6M}-CP	Distance from P_{6M} point to CP
A_1-P_{3M}⊥CP	Distance from A_1 to P_{3M} points perpendicular to CP
P_{3M}-P_{6M}⊥CP	Distance from P_{3M} to P_{6M} points perpendicular to CP
A_1-P_{6M}⊥CP	Distance from A_1 to P_{6M} points perpendicular to CP
V_M	Volume of maxillary body
V_{S1}	Volume of right maxillary sinus in GN and GIII groups/volume of maxillary sinus on healthy side in GC group
V_{S2}	Volume of left maxillary sinus in GN and GIII groups/volume of maxillary sinus on cleft side in GC group
V_T	Total volume consisting of maxillary body and maxillary sinuses

second measurements were compared, and the paired *t* test was calculated. In our study, $P < 0.05$, indicating that all landmarks could be reproducibly identified.

Demography

The mean age of the GC group was 20.2 years (range 17–28 years), the GIII group was 22.3 years (range 17–27 years), and the GN was 21.7 years (range 19–26 years). There were no significant differences of age among these 3 groups ($P > 0.05$).

Teeth Missing

In the GC group, 6 patients missed the incisor on the cleft side, 22 patients missed the literal incisor on the cleft side, 9 patients missed the literal incisor on the healthy side, 7 patients missed the literal incisors on both sides, only 1 patient missed the second premolar on the cleft side. In the GIII group, 3 patients missed the second premolar on the left side, and 2 patients missed the second molar on the left side, 3 on the right. Patients in the GN group all had complete teeth.

Comparison Between 2 Sides in Each Group

Descriptive statistical data and results of the independent samples group *t* test between 2 sides in GC, GN, and GIII groups are shown in Table 3.

In GC group, the distances from incisor and literal incisor on the cleft side ($M1_{ML}$-SP, $M2_{ML}$-SP) were significantly longer than the healthy side ($P < 0.01$); M_3L-SP was significantly shorter than M_3R-SP ($P < 0.01$); while $M_{7m}L$-SP was significantly longer than $M_{7m}R$-SP ($P < 0.05$); though M_4L was shorter than M_4R, $M_{6m}L$, $M_{6d}L$, and $M_{7d}L$ were longer than $M_{6m}R$, $M_{6d}R$, and $M_{7d}R$, the differences were not significant. In GN group, there were no significant differences of distances from teeth points to SP on both sides. In GIII group, except that $M_{1M}L$-SP was obviously shorter than $M_{1M}R$ ($P < 0.01$), there were no significant differences of distances from other teeth points to SP on both sides.

Fitting Curve of Dental Arch

According to the three-dimensional coordinates of the points on the teeth, the fitting curves of dental arch in GC, GN, and GIII groups are given in Figure 1.

The width of the dental arch curve of the GC group was more constrictive than GN and GIII groups. The curve on the cleft side of the GC group rotated clockwise and the anterior part collapsed. The whole fitting curve of the GIII was the nearest to the CP plane.

Descriptive statistical data and results of the independent samples group *t* test among groups are shown in Table 4.

Comparison of GC and GN Groups

There were no obvious differences in the cranial base measurements between the GC and GN groups ($P > 0.05$) The distances of A_1⊥CP, P_{3M}⊥CP, and P_{6M}⊥CP were significantly shorter in the GC group than in the GN group ($P < 0.01$, $P < 0.01$, and $P < 0.05$, respectively). The anterior and posterior parts of the maxillary length (A_1-P_{3M}⊥CP and P_{3M}-P_{6M}⊥CP) and overall maxillary length (A_1-P_{6M}⊥CP) at the dental level were all significantly reduced in the GC group ($P < 0.01$). For patients in the GC group, the proportions of A_1-P_{3M}⊥CP, P_{3M}-P_{6M}⊥CP, and A_1-P_{6M}⊥CP in A_1⊥CP(A_1-P_{3M}⊥CP/A_1⊥CP, P_{3M}-P_{6M}⊥CP/A_1⊥CP, and A_1-P_{6M}⊥CP/A_1⊥CP) were significantly decreased ($P < 0.01$), but the proportions of P_{3M}⊥CP and P_{6M}⊥CP in A_1⊥CP (P_{3M}⊥CP/A_1⊥CP and P_{6M}⊥CP/A_1⊥CP) both increased compared with the GN group ($P < 0.01$). The interdental widths (M_3W, M_4W, M_5W, and M_6W) were obviously more constrictive in the GC group than in the GN group, and from the anterior part up to the first molar, the gap gradually narrowed ($P < 0.01$). The palatal widths (P_3W, P_4W, P_5W, and P_6W) indicated the same trend ($P < 0.01$). The widths between both bilateral second molar cusps ($M_{7m}W$, $M_{7d}W$) and P_7W in GC could be comparable to those in the GN group ($P > 0.05$). The maxillary volume (G_M) and the volume consisting of maxilla and maxillary sinuses (G_T) in the GC group were significantly smaller than those in the GN group ($P < 0.01$) (Fig. 2). The maxillary width (MW), palatal length (PL), and ∠SNA A were both significantly smaller in the GC group ($P < 0.05$, $P < 0.01$, and $P < 0.01$, respectively), while there was no difference in the anterior maxillary height (MH), ∠SNB, and volume of maxillary sinus (V_{S1} and V_{S2}) (Fig. 2) between the 2 groups ($P > 0.05$).

Comparison of GC and GIII Groups

There was no significant difference of the distance of A_1⊥CP between the 2 groups ($P > 0.05$), while the P_{3M}-CP and P_{6M}-CP in the GIII group were significantly shorter ($P < 0.01$, and $P < 0.05$, respectively). The anterior and overall maxillary length at the dental level (A_1-P_{3M}⊥CP and A_1-P_{6M}⊥CP) in the GC group was significantly smaller than that in the GIII group ($P < 0.01$, and $P < 0.05$, respectively). For patients in the GC group, A_1-P_{3M}⊥CP/A_1⊥CP and A_1-P_{6M}⊥CP/A_1⊥CP both significantly decreased ($P < 0.01$, and $P < 0.05$, respectively); meanwhile, P_{6M}⊥CP/A_1⊥CP increased compared with that in the GIII group ($P > 0.05$). The interdental widths such as M_3W, M_4W, M_5W, and M_6W were narrower in the GC group ($P < 0.01$), and anterior arch stenosis was more obvious compared with patients in the GIII group. The palatal widths in the GC group from canine to first molar were significantly smaller than in the GIII group ($P < 0.01$). The PL, ∠SNA, and ∠SNB

© 2015 Mutaz B. Habal, MD

TABLE 3. Comparison of Distances From Maxillary Teeth to Sagittal Plane

Table 3.1 Comparison of Measurements Between Cleft Side and Healthy Side of GC Group

	Cleft Side		Healthy Side		
GC	N	Mean ± SD	N	Mean ± SD	*P*
M1m-SP	26	7.44 ± 2.11	32	1.88 ± 1.18	0.000*
M2m-SP	3	9.39 ± 0.35	16	7.95 ± 3.65	0.001*
M3-SP	32	10.04 ± 3.65	32	12.81 ± 3.05	0.002*
M4-SP	32	15.79 ± 3.68	32	16.96 ± 3.98	0.228
M5-SP	32	20.10 ± 4.41	31	19.10 ± 4.50	0.376
M6m-SP	32	23.95 ± 3.10	32	22.74 ± 3.48	0.149
M6d-SP	32	25.70 ± 3.10	32	24.25 ± 2.98	0.061
M7m-SP	32	29.10 ± 2.89	32	27.44 ± 2.43	0.016*
M7d-SP	32	30.14 ± 2.81	32	28.95 ± 2.31	0.068

Table 3.2 Comparison of Measurements Between Left Side and Right Side of GN Group

	Left Side		Right Side		
GN	N	Mean ± SD	N	Mean ± SD	*P*
M_{1M}-SP	32	4.14 ± 1.96	32	4.76 ± 1.81	0.193
M2m-SP	32	11.31 ± 1.60	32	11.61 ± 2.28	0.545
M3-SP	32	16.41 ± 1.69	32	16.99 ± 2.56	0.292
M4-SP	32	20.59 ± 1.60	32	20.93 ± 2.05	0.459
M5-SP	32	22.95 ± 1.66	32	23.47 ± 1.87	0.246
M6m-SP	32	26.28 ± 1.81	32	26.62 ± 2.09	0.493
M6d-SP	32	26.18 ± 1.98	32	26.42 ± 1.47	0.581
M7m-SP	32	29.18 ± 1.32	32	29.89 ± 1.78	0.074
M7d-SP	32	29.51 ± 1.69	32	30.00 ± 1.59	0.239

Table 3.3 Comparison of Measurements Between Left Side and Right Side of GIII Group

	Left Side		Right Side		
GIII	N	Mean ± SD	N	Mean ± SD	*P*
M1m-SP	24	3.53 ± 1.18	24	5.00 ± 1.71	0.001*
M2m-SP	24	12.14 ± 1.69	22	11.85 ± 2.14	0.618
M3-SP	24	17.68 ± 2.57	24	18.23 ± 2.75	0.471
M4-SP	24	22.98 ± 2.24	24	22.93 ± 2.45	0.944
M5-SP	21	24.47 ± 2.66	21	24.51 ± 2.54	0.964
M6m-SP	24	27.72 ± 3.16	24	26.19 ± 2.09	0.077
M6d-SP	24	29.14 ± 3.59	24	28.02 ± 2.09	0.193
M7m-SP	22	30.52 ± 4.17	21	31.78 ± 2.04	0.214
M7d-SP	22	32.03 ± 2.79	21	31.39 ± 1.82	0.376

Distance: mm. Independent samples *t* test, significance at $P < 0.05$. *P**: statistically significant.

were both significantly smaller in the GC group ($P < 0.01$), while there was no obvious difference in MW, MH, V_M, V_{S1}, V_{S2}, and V_T (Fig. 2) between the 2 groups ($P > 0.05$).

Comparison of GIII and GN Groups

In the GIII group, length of anterior cranial base (S-N), length of overall cranial base (Ba-N), and ∠BaSN were significantly reduced compared with the other 2 groups ($P < 0.05$). The distances of $A_1\perp$CP, $P_{3M}\perp$CP, and $P_{6M}\perp$CP were obviously smaller in the GIII group than in the GN group ($P < 0.01$). In addition, P_{3M}-$P_{6M}\perp$CP and A_1-$P_{6M}\perp$CP were significantly reduced ($P < 0.01$). There was no difference of $P_{3M}\perp$CP/$A_1\perp$CP, $P_{6M}\perp$CP/$A_1\perp$CP, A_1-$P_{3M}\perp$CP/$A_1\perp$CP, P_{3M}-$P_{6M}\perp$CP/$A_1\perp$CP, and A_1-$P_{6M}\perp$CP /$A_1\perp$CP between GIII and GN groups ($P > 0.05$). With the exception that M_4W and M_5W were wider and P_3W was narrower in the GIII group ($P < 0.01$, $P < 0.05$, and $P < 0.05$, respectively), there were no obvious differences in dental and palatal widths between the 2 groups ($P > .05$). The MW and ∠SNA were both significantly smaller ($P < 0.01$), and∠SNB was larger in the GIII group ($P < 0.01$). There was no difference in MH, PL, V_M, V_{S1}, V_{S2}, and V_T (Fig. 2) between the 2 groups ($P > 0.05$).

The patients in the GC group were divided into 3 subgroups according to the normal value (mean ± SD) of $P_{6M}\perp$CP (58.84 ± 4.61 mm): $P_{6M}\perp$CP of 6 individuals were less than 54.84 mm, 24 individuals had in the normal range, and for 2 individuals, they were more than 63.45 mm. Approximately 75% of UCLP patients needing orthognathic surgery were likely to have regular posterior maxillary position.

© 2015 Mutaz B. Habal, MD

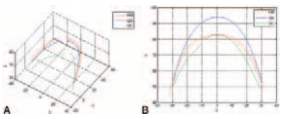

FIGURE 1. The fitting curves of maxillary dental arch in GC, GIII, and GN groups. Distance: mm.

DISCUSSION

Three-dimensional CT reconstruction methods have existed for more than 20 years.[8,11] One of the main applications of 3D-CT in orthodontics and maxillofacial surgery is as measurement method and shape descriptor. Some studies testified to the quantitative accuracy of the method.[12,13] By means of the 3D-CT techniques, the investigators can clearly recognize the malmophology and malposition of the maxillary complex.

In our study, we found no abnormal growth in cranial base structures between patients in the GC and GN groups, and this finding agrees with the published literature.[14–16] While Abuhijleh reported that the posterior cranial base and total cranial base of the UCLP patients were significantly shorter at all skeletal periods,[17] and it was in agreement with another study of the UCLP patients in mixed dentition.[18] In the GIII group, S-N, Ba-N, and ∠BaSN were significantly decreased, which could result from hypodevelopment of the craniofacial structures. The factors causing the retruded maxillae could also inhibit the anterior–posterior growth of other skeletal units. Thus, in our study, because of the reduced ∠BaSN and S-N in the GIII group, using ∠SNA to assess the degree of maxillary prominence could conduce error. While $A_1 \perp CP$, the distance from the most protruded point to the coronal plane passing through basion, may be an important parameter to evaluate maxillary retrusion. There was no significant difference in $A_1 \perp CP$ between the GIII and GC groups, meaning that in the 2 groups, the maxillary prominence decreased in the same degree.

For patients in the GC group, the trend of the dental arch construction from the back to the front increased, and on the cleft side, the anterior part of the dental arch was closer, while the posterior part was further to the SP plane than the healthy side, the dental arch

TABLE 4. Comparison of Measuremens in GC, GIII, and GN Groups

	GC		GN		GIII		*P*		
Measurements	**N**	**Mean ± SD**	**N**	**Mean ± SD**	**N**	**Mean ± SD**	P_{CN}	P_C**III**	P_N**III**
S–Ba	32	44.53 ± 3.19	32	45.68 ± 2.48	24	46.08 ± 5.18	.111	.174	.735
Ba–N	32	100.62 ± 4.57	32	100.38 ± 3.78	24	95.61 ± 7.86	.825	.009∗	.010∗
S–N	32	65.44 ± 3.87	32	64.36 ± 2.60	24	61.47 ± 4.69	.198	.001∗	.010∗
∠NSBa	32	131.70 ± 5.25	32	130.45 ± 6.35	24	125.93 ± 4.80	.394	0.000∗	0.000∗
∠SNA	32	74.15 ± 4.11	32	83.09 ± 2.28	24	76.92 ± 1.83	0.000∗	.001∗	0.000∗
∠SNB	32	77.51 ± 2.63	32	78.12 ± 3.68	24	81.71 ± 3.55	.445	0.000∗	.001∗
MH	32	54.43 ± 2.90	32	54.28 ± 3.55	24	54.52 ± 5.04	.856	.934	.838
MW	32	72.09 ± 6.03	32	75.10 ± 3.23	24	72.43 ± 3.13	.016∗	.803	.003∗
PL	8	42.58 ± 1.71	32	48.45 ± 2.44	24	46.59 ± 6.75	0.000∗	.013∗	.208
M_3W	32	25.94 ± 4.97	32	35.10 ± 3.52	24	33.65 ± 2.43	0.000∗	0.000∗	.091
M_4W	32	34.98 ± 5.47	32	41.71 ± 2.58	24	44.48 ± 3.81	0.000∗	0.000∗	.004∗
M_5W	31	42.44 ± 6.71	32	47.20 ± 2.62	21	49.19 ± 3.08	.001∗	0.000∗	.015∗
$M_{6m}W$	32	49.45 ± 5.85	32	52.52 ± 2.40	24	53.88 ± 4.13	.009∗	.002∗	.159
$M_{6d}W$	32	51.40 ± 5.22	32	54.21 ± 2.17	24	55.78 ± 4.01	.007∗	.001∗	.093
$M_{7m}W$	32	58.90 ± 4.94	32	59.69 ± 3.16	19	60.71 ± 4.10	.449	.185	.323
$M_{7d}W$	32	60.10 ± 4.42	32	60.24 ± 2.53	19	61.58 ± 4.10	.880	.240	.208
P_3W	32	18.82 ± 3.81	32	24.61 ± 2.55	24	22.95 ± 2.59	0.000∗	0.000∗	.020∗
P_4W	32	22.84 ± 4.53	32	27.88 ± 2.64	24	28.90 ± 2.89	0.000∗	0.000∗	.178
P_5W	31	28.59 ± 6.94	32	33.29 ± 3.04	21	34.05 ± 2.87	.001∗	0.000∗	.367
P_6W	32	32.51 ± 3.87	32	36.42 ± 2.55	24	36.42 ± 2.55	.001∗	0.000∗	.114
P_7W	32	39.19 ± 3.79	32	39.23 ± 2.17	19	39.40 ± 1.70	.957	.785	.772
A_1-CP	32	84.09 ± 5.23	32	91.00 ± 5.22	24	82.17 ± 6.06	0.000∗	.209	0.000∗
P_{3M}-CP	32	74.18 ± 4.78	32	79.02 ± 5.53	24	70.41 ± 5.83	0.000∗	.010∗	0.000∗
P_{6M}-CP	32	56.54 ± 4.28	32	58.84 ± 4.61	24	53.11 ± 6.46	.043∗	.020∗	0.000∗
A_1-$P_{3M}\perp$CP	32	9.92 ± 1.69	32	11.98 ± 1.45	24	11.76 ± 2.31	0.000∗	.001∗	.661
P_{3M}-$P_{6M}\perp$CP	32	17.63 ± 1.67	32	20.19 ± 1.84	24	17.30 ± 1.48	0.000∗	.443	0.000∗
A_1-$P_{6M}\perp$CP	32	27.55 ± 2.38	32	32.17 ± 2.15	24	29.06 ± 3.09	0.000∗	.044∗	0.000∗
P_{3M}-CP/A1-CP	32	0.8822 ± 0.0180	32	0.8679 ± 0.0185	24	0.8566 ± 0.0276	.003∗	0.000∗	.092
P_{6M}-CP/A1-CP	32	0.6722 ± 0.0231	32	0.6460 ± 0.0227	24	0.6446 ± 0.0451	0.000∗	.010∗	.889
A_1-$P_{3M}\perp$CP/A1-CP	32	0.1178 ± 0.0180	32	0.1321 ± 0.0185	24	0.1434 ± 0.0276	.003∗	0.000∗	.092
P_{3M}-$P_{6M}\perp$CP/A1-CP	32	0.2099 ± 0.0189	32	0.2218 ± 0.0164	24	0.2120 ± 0.0274	.009∗	.753	.128
A_1-$P_{6M}\perp$CP/A1-CP	32	0.3278 ± 0.0231	32	0.3450 ± 0.0227	24	0.3554 ± 0.0451	0.000∗	.010∗	.889
V_M	32	36794.55 ± 7058.08	32	42583.96 ± 6224.84	24	39265.80 ± 7354.07	.001∗	.208	.073
V_{S1}	32	14256.76 ± 7145.59	32	16558.28 ± 3831.57	24	14546.71 ± 5361.33	.115	.868	.107
V_{S2}	32	14109.19 ± 6152.25	32	15827.22 ± 4306.58	24	17320.66 ± 6580.41	.200	.066	.310
V_T	32	65160.50 ± 15956.70	32	74969.45 ± 9501.87	24	71133.17 ± 11845.20	.004∗	.129	.184

Distance: mm; angle: °; proportion: 100%; volume: mm^3. Independent samples *t* test, significance at $P < 0.05$. *P*∗: statistically significant. P_{CN}: comparison between GC and GN groups; P_CIII: comparison between GC and GIII groups; P_NIII: comparison between GN and GIII groups.

© 2015 Mutaz B. Habal, MD

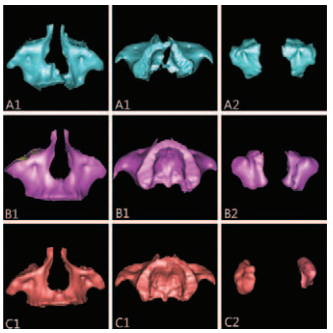

FIGURE 2. The volumetric changes of maxillary body and maxillary sinusin GC, GIII, and GN groups. A1, maxillary body of a patient in GC group, A2, maxillary sinuses of a patient in GC group. B1, maxillary body of a patient in GN group, B2, maxillary sinuses of a patient in GN group. C1, maxillary body of a patient in GIII group, C2, maxillary sinuses of a patient in GIII group.

rotated clockwise and the anterior part collapsed according to the fitting curve of the dental arch; the overall dental arch showed a "V" shape. Ye et al[19] reported a similar conclusion by measuring the dental cast CT. We also found that the UCLP patients have a more constrictive arch width than patients in the GIII group. However, the differences of the maxillary dental widths between the GIII and GN groups were not statistically significant. Although in some reports,[20,21] the mean intermolar and all maxillary alveolar widths of the class III patients were obviously smaller than the control group. Other research has shown that the dental widths of class III patients were larger than that of class I patients.[22] Additionally, anterior, posterior, and overall maxillary length in the GC group was obviously shorter compared with the GN group. We found that the sagittal and transverse sizes of the maxillae in the GC group were both smaller than that of the GN and GIII groups, especially in the anterior part. In this study, the maxillary volume (V_M) and the total volume consisting of maxilla and maxillary sinus (V_T) obviously reduced in the GC group; it may be caused by the inherent hypodevelopment of the maxillary complex, while bone deficiency of the clefts on the palate and aveolar area could be another important reason in point. Although the volume of maxillary sinuses in the GC group was smaller than the other 2 groups, the difference was not significant. Also, in the GC group, A_1-$P_{6M}\perp$CP/$A_1\perp$CP was significantly decreased; in contrast, $P_{6M}\perp$CP/$A_1\perp$CP increased compared with the other 2 groups. We found that the decreased prominence of maxillary complex in the GC group could be mainly caused by the shortened maxillary length; meanwhile, posterior position of the maxillary body may have some influence on maxillary protrusion.

In our study, $A_1\perp$CP, $P_{3M}\perp$CP, and $P_{6M}\perp$CP in the GC group were obviously shorter than those in the GN group; however, $P_{6M}\perp$CP of almost 75% patients were in the normal range (54.22–63.45 mm). It is consistent with the clinical observation that some UCLP patients with severe anterior crossbite and impacted or malaligned anterior teeth have class I molar occlusion. Compared with patients in the GC group, $P_{6M}\perp$CP decreased in the GIII group, while there was no difference in $A_1\perp$CP. Accordingly, in the 2 groups, although the A_1 point retruded in the same degree, the causes may differ. Inherent dysplasia of maxillae leading to the shortened sagittal length in the GC group is more obvious. While in the GIII group, the posterior position of maxillae is more significant compared with the GC group, when compared with the GN group, overall maxillary length (A_1-P_{6M}) and distance from P_{6M} point to coronal plane ($P_{6M}\perp$CP) equally reduced.

In general, patients with severe dento-facial deformities require orthodontic and/or orthognathic treatments. Currently, orthognathic surgery is commonly used with a 3D movement of the jaws including maxillary advancement. LeFort I osteotomy, sometimes combined with mandibular surgery, is the standard procedure for reestablishing facial balance and dental occlusion in patients with cleft lip.[23] Whereas for patients with UCLP, because of scar fibrosis of the lip and palate as well as the pteryomaxilla to be released, performing Le Fort I osteotomy is more difficult. Furthermore, problems, such as dental arch stenosis and severe premaxillary hypogenesis, remain to be solved. Accordingly, for patients with normal molar occlusion, advancement of the intact maxillae sometimes may extremely overcorrect the posterior occlusion relationship. The objective should be to increase the arch length for the affected anterior teeth or for their alignment while maintaining the correct molar relationship. Although previous studies have not reported the exact proportion of patients with normal molar occlusion, the clinicians have paid attention to the problem. For these patients, it is important to fix the maxillary sagittal and transverse deficiency, the anterior maxillary segmental distraction is recommended as an alternative method to the conventional Lefort I osteotomy and rigid external distraction.[24–26] Nevertheless, advancement of intactmaxillary body, such as LeFort I osteotomy, is one of the optimal choices for maxillary retrusion patients without clefts. Our finding will help clinicians diagnose and plan the treatment of malocclusion in UCLP patients.

Many researchers have studied the influences of surgical procedures on the maxillary development of the cleft and lip patients; in this study, to avoid the differences of maxillary development caused by these iatrogenic factors, patients in the GC group all had the same methods of cleft lip and palate repair. However, due to cheiloplasty and palatoplasty surgical procedures were carried out by different surgeons; the bias in our assessments could not be avoided.

CONCLUSION

In summary, for the UCLP patients, the decreased prominence of maxillary complex could be mainly caused by the shortened maxillary length; meanwhile, posterior position of the maxillary body may have some influence on maxillary protrusion. While for the class III patients, maxillary retrusion was resulted from malposition and malmorphology on an equal basis.

REFERENCES

1. Ross RB. Treatment variables affecting facial growth in complete unilateral cleft lip and palate. *Cleft Palate J* 1987;24:5–77
2. Liao YF, Mars M. Long-term effects of clefts on craniofacial morphology in patients with unilateral cleft lip and palate. *Cleft Palate Craniofac J* 2005;42:601–609
3. Diah E, Lo LJ, Huang CS, et al. Maxillary growth of adult patients with unoperated cleft: answers to the debates. *J Plast Reconstr Aesthet Surg* 2007;60:407–413
4. Mars M, Houston WJ. A preliminary study of facial growth and morphology in unoperated male unilateral cleft lip and palate subjects over 13 years of age. *Cleft Palate J* 1990;27:7–10
5. Capelozza JL, Taniguchi SM, Da SJO. Craniofacial morphology of adult unoperated complete unilateral cleft lip and palate patients. *Cleft Palate Craniofac J* 1993;30:376–381
6. Wolford LM, Stevao EL. Correction of jaw deformities in patients with cleft lip and palate. *Proc (Bayl Univ Med Cent)* 2002;15:250–254
7. Figueroa AA, Polley JW. Management of severe cleft maxillary deficiency with distraction osteogenesis: procedure and results. *Am J Orthod Dentofacial Orthop* 1999;115:1–12
8. Vannier MW, Marsh JL, Warren JO. Three dimensional CT reconstruction images for craniofacial surgical planning and evaluation. *Radiology* 1984;150:179–184
9. Park SH, Yu HS, Kim KD, et al. A proposal for a new analysis of craniofacial morphology by 3-dimensional computed tomography. *Am J Orthod Dentofacial Orthop* 2006;129:600–623
10. Li H, Yang Y, Chen Y, et al. Three-dimensional reconstruction of maxillae using spiral computed tomography and its application in postoperative adult patients with unilateral complete cleft lip and palate. *J Oral Maxillofac Surg* 2011;69:e549–e557

© 2015 Mutaz B. Habal, MD

11. Marsh JL, Vannier MW. The "third" dimension in craniofacial surgery. *Plast Reconstr Surg* 1983;71:759–767
12. Kitaura H, Yonetsu K, Kitamori H, et al. Standardization of 3-D CT measurements for length and angles by matrix transformation in the 3-D coordinate system. *Cleft Palate Craniofac J* 2000;37:349–356
13. Cavalcanti MG, Haller JW, Vannier MW. Three-dimensional computed tomography landmark measurement in craniofacial surgical planning: experimental validation in vitro. *J Oral Maxillofac Surg* 1999;57:690–694
14. Hayashi I, Sakuda M, Takimoto K, et al. Craniofacial growth in complete unilateral cleft lip and palate: a roentgeno-cephalometric study. *Cleft Palate J* 1976;13:215–237
15. Smahel Z, Brejcha M, Mullerova Z. Craniofacial morphology in unilateral cleft lip and palate in adults. *Acta Chir Plast* 1991;33:224–241
16. Goyenc YB, Gurel HG, Memili B. Craniofacial morphology in children with operated complete unilateral cleft lip and palate. *J Craniofac Surg* 2008;19:1396–1401
17. A Abuhijleh E, Aydemir H, Toygar-Memikoglu U. Three-dimensional craniofacial morphology in unilateral cleft lip and palate. *J Oral Sci* 2014;56:165–172
18. Liu R, Lu D, Wamalwa P, et al. Craniofacial morphology characteristics of operated unilateral complete cleft lip and palate patients in mixed dentition. *Oral Surg Oral Med Oral Pathol Oral Radiol Endod* 2011;112:e16–e25
19. Ye B, Ruan C, Hu J, et al. A comparative study on dental-arch morphology in adult unoperated and operated cleft palate patients. *J Craniofac Surg* 2010;21:811–815
20. Uysal T, Usumez S, Memili B, et al. Dental and alveolar arch widths in normal occlusion and Class III malocclusion. *Angle Orthod* 2005;75:809–813
21. Kuntz TR, Staley RN, Bigelow HF, et al. Arch widths in adults with Class I crowded and Class III malocclusions compared with normal occlusions. *Angle Orthod* 2008;78:597–603
22. Braun S, Hnat WP, Fender DE, et al. The form of the human dental arch. *Angle Orthod* 1998;68:29–36
23. Bertolini F, De Riu G, Zorzan G, et al. Skeletal relapse of maxillary osteotomies in unilateral cleft lip and palate patients. *Int J Adult Orthodon Orthognath Surg* 2000;15:30–36
24. Wang XX, Wang X, Li ZL, et al. Anterior maxillary segmental distraction for correction of maxillary hypoplasia and dental crowding in cleft palate patients: a preliminary report. *Int J Oral Maxillofac Surg* 2009;38:1237–1243
25. Alkan A, Bas B, Ozer M, et al. Maxillary anterior segmental advancement of hypoplastic maxilla in cleft patients by distraction osteogenesis: report of 2 cases. *J Oral Maxillofac Surg* 2008;66:126–132
26. Dolanmaz D, Karaman AI, Ozyesil AG. Maxillary anterior segmental advancement by using distraction osteogenesis: a case report. *Angle Orthod* 2003;73:201–205

Double-Opposing Unilobar Rotation Flaps in the Reconstruction of Moderate-to-Large Defects of the Scalp

*Rex Moulton-Barrett, FACS***
*and Benjamin Vanderschelden, BSc**

Abstract: Closure of medium-to-large-size defects of the scalp are often associated with unacceptable aesthetic results, wound break down, alopecia, and excessive scarring. The authors present 2 cases of double-opposing unilobar rotation flaps for the reconstruction of large, that is, at least 7 cm diameter, full thickness defects of the scalp. Unlike previously described double flap closures of scalp defects, the double-opposing unilobar rotation flap design are true rotation flaps, which require a Burow triangle excisions and which have a versatility in both width and length of design to accommodate closure of large defects of the scalp. Some of the advantages of this technique are the retention of hair-bearing skin without distortion of the follicle position, an aesthetically pleasing scar, minimal tension at the wound closure site, and the versatility as well as simplicity of the technique.

Key Words: Scalp reconstruction, large defects, rotation flaps, resection closure

In the domain of reconstruction of the scalp with the use of local scalp flaps, there are many techniques to choose from. The issues at hand when deciding on the method of reconstruction are the size of the defect, the location of the defect relative to the midline, the quality of the scalp as a reconstructive donor site, the anticipated degree of disfigurement in context to the lifestyle of the patient, degree of difficulty to avoid undue tension at the suture lines, the resultant orientation of the hair follicles relative to the adjacent scalp and the need for a local flap, skin graft, or regional/free flap, specifically where the scalp is nonhair bearing. The consensus of most authors in terms of defined size of the defect is that small defects are considered <4 cm, medium-size defects are 4 to 6 cm, and large defects are >6 cm in length.[1] Most small defects can be closed primarily and medium-size defects may require local flaps, whereas large-size defects are typically closed with skin grafts, regional flaps, or free tissue transfer.[2] The following 2 case studies describe a novel method.

CLINICAL REPORT 1

A 12-year-old girl presented to our center with a nevus sebaceous of the scalp measuring 5×7 cm (Fig. 1). Because of the risk of malignant transformation, excision was performed. Under general anesthesia, the patient was placed in the semisitting position, which exposed the vertex, anterior, posterior, and lateral scalp. Initially, a shave was performed over the lesion with a 1 cm margin, which exposed a 5×7 cm area of elevated pinkish discolored skin of the nevus sebaceous (Fig. 2). The area was injected with 85 mL of a solution of 0.5% lidocaine mixed equally with 0.5% Marcaine (AstraZeneca Parmaceuticals, Wilmington, DE) and 1 to 200,000 epinephrine solution. The lesion was excised with a 6 mm margin. The hemostasis was achieved with 3 mm needlepoint Colorado. The defect measured 6.5×8 cm. Two opposing unilobar random flaps were designed, incised parallel to hair follicles and elevated in a subgaleal plane. Right posterior and left anterior rotation flaps were elevated parallel to the entire length of the defect and rotated to meet obliquely across the scalp defect itself (Fig. 3). The flaps had a length-to-width ratio of 2 : 1. The galea of each flap was cross-scored at 1 cm intervals and the scalp periphery was undermined 3 cm circumferentially to reduce tension and facilitate primary wound closure. Flaps were then temporarily stapled together to determine the maximal positioning relative to the least skin tension. A Burow triangle excision was performed at the base of each flap to avoid dog ears. A single 10 mm Jackson-Pratt drain (Cardinal Health, Dublin, OH) spanned the scalp and deep 4-0 Vicryl sutures (Ethicon, West

From the *University of California, Berkeley, CA.
Received January 7, 2015.
Accepted for publication June 28, 2015.
Address correspondence and reprint requests to Rex Moulton-Barrett.
E-mail: rex@moulton-barrett.com
The authors report no conflicts of interest.
Copyright © 2015 by Mutaz B. Habal, MD
ISSN: 1049-2275
DOI: 10.1097/SCS.0000000000002029

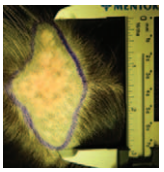

FIGURE 1. Measuring dimensions of lesion.

FIGURE 2. Outline of lesion margins.

FIGURE 3. Flaps meet (picture after complete closure).

Sumerville, NJ) were used to bring the dermis to close apposition. Staples were removed and running interlocking 4-0 chromic catgut sutures were used to close the entire length of the incision. Postoperatively, both flaps had a normal capillary refill and were clean and dry. The duration of procedure was 2 hours and 15 minutes with <100 mL blood loss. Postoperatively, there was no necrosis, no wound break down, and no hair loss. The drains were removed 8 days later. The maximal width of nonhair-bearing postoperative scar was 1 cm 1 year later. Our patient had the option to either tattoo the scar when mature, place hair grafts, or, in this case, as the natural fall of her hair concealed the scar, her choice was no treatment (Fig. 4).

CLINICAL REPORT 2

A 79-year-old lady presented with a 4 × 5 cm ulcerated and biopsy-proven squamous cell carcinoma over the vertex of her scalp. She underwent resection leaving a 7 × 8 cm defect (Fig. 5). Frozen sections of the peripheral margins were negative for tumor. Two opposing unilobar random flaps were designed, similar to Case 1, incised parallel to hair follicles, elevated in a subgaleal plane parallel to the entire length of the defect, and rotated to meet obliquely across the scalp defect itself (Fig. 6). The duration of procedure was 2 hours with <150 mL blood loss. Postoperatively, there was no necrosis, no wound break down, and no hair loss. The drains were removed 8 days later. The maximal width of nonhair-bearing postoperative scar was <1 cm 7 months later (Fig. 7).

FIGURE 4. Results after 1 year, hair parted to show scar.

FIGURE 5. A 5 × 6 cm squamous cell carcinoma resulting in a full thickness 7 × 8 cm defect of scalp vertex.

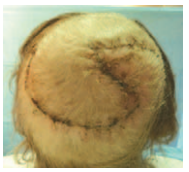

FIGURE 6. Six weeks following double-opposing unilobar rotation flap reconstruction.

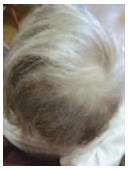

FIGURE 7. Seven months after surgery.

DISCUSSION

Closure of scalp defects requires an individualization of technique based on size, location, hair follicle geography, and the quality of the remaining scalp. Large scalp defects are often better replaced by free tissue transfers or full-thickness skin grafts, especially when the patient has had previous radiation therapy or previous scalp incisions.[1,2] We believe double-opposing unilobar rotation (DOUR) flaps provide a simpler alternative to other techniques used under similar conditions.

One technique for the reconstruction of moderate-sized scalp defects, which is most similar to DOUR flaps, is the Yin-Yang rotation flap.[3] The Yin-Yang flap differs in the overall design, is for a smaller size defect, and the incisions usually invade the parietotemporal scalp. As each component of the Yin-Yang flap is of a shorter length, closure requires an element of transposition, restricting the extent of rotation, increasing the tension on the closure, and limiting the size of the defect able to be reconstructed. The DOUR flap is designed with incisions closer to the defect, which extend parallel to the full length of the defect. The latter requires less involvement of the surrounding parietotemporal tissue, uses a true rotation, and results in scarring, which is less visible. Our design also does not necessitate enough rotation to cause a noticeable change in hair orientation, avoiding another possible unsatisfactory aesthetic result. We have shown this technique can be applied to larger defects and may be considered for those defects up to 4 cm away from the midline of the scalp. The DOUR flap design requires a Burow triangle excision to avoid tension at closure. The design of the width and length of each flap can be modified to provide versatility in the ability to close defects of different sizes (Fig. 8). Striving for simplicity, this would be favorable to using a single large scalp rotational flap and a skin graft to close the donor site.[3–5]

V-Y advancement flaps most often are used to treat scalp defects of small-to-medium size[5–7] and have been used for larger

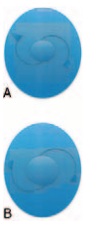

FIGURE 8. Design for A, medium and B, medium-to-large defects of the scalp using double-opposing unilobar rotations flaps.

© 2015 Mutaz B. Habal, MD

defects of the scalp,[5,6] which requires a large amount of surrounding scalp involvement and long incisions, thus creating excess scarring. With larger scalp defects, the V-Y advancement flap must become thinner and longer to distribute the tension over a larger area. We avoid this excess incision and scarring with our flap design.

Dual transposition flaps have also been used to close medium-to-large scalp defects.[4] Pivoting of the base is often associated with distortion of scalp contour and may lead to a larger donor deficit. Swinging almost 90° also disrupts the hair orientation of the surrounding scalp and for larger scalp defects requires a 2-stage closure. Due to the relatively unyielding nature of the scalp, the stretching motion of transposition and advancement flaps are often better replaced by rotation flaps to have maximal tissue movement and minimal tension on wound closure.[8]

The DOUR flap provides an alternative to the approaches mentioned above for closure of medium-to-large defects of the scalp. The advantages include limited involvement of surrounding tissue, simplicity, creating a concealable scar due to retention of hair-bearing skin in an appropriate orientation, and allowing for less tension along the wound closure site. We believe this technique may be considered for medium-to-large-sized defects (10–60 cm^2) up to 4 cm from the midline of the scalp.

The senior author has previously successfully used DOUR flaps for the reconstruction of smaller defects of the scalp, back, extremity, neck, and trunk region.

The limitations of this technique are the same as other local scalp flap designs, namely being less applicable to larger scalp defects in patients with previous radiation therapy or previous scalp incisions.[1,2,8] A limitation specific to this study would be the fact that this is a technique based on 2 case reports for medium-to-large defects of the scalp.

REFERENCES

1. Shonka DC Jr, Potash AE, Jameson MJ, et al. Successful reconstruction of scalp and skull defects: lessons learned from a large series. *Laryngoscope* 2011;121:2305–2312
2. Yap LH, Langstein HN. Reconstruction of the scalp, calvarium, and forehead. In: Thorne CE, Beasley RW, Aston SJ, eds. *Grabb & Smith's Plastic Surgery.* 6th ed. et al, eds. *Grabb & Smith's Plastic Surgery.* 6th ed. Philadelphia, PA: Wolters Kluwer Health/Lippincott Williams & Wilkins; 2007:358–366
3. Iblher N, Ziegler MC, Penna V, et al. An algorithm for oncologic scalp reconstruction. *Plast Reconstr Surg* 2010;126:450–459
4. Fincher EF, Gladstone HB. Dual transposition flaps for the reconstruction of large scalp defects. *J Am Acad Dermatol* 2009;60:985–989
5. Sharma R, Sirohi D, Sinha R, et al. Reconstruction of a large posterior scalp defect using occipital artery based pedicled island V-Y advancement flap: a case report. *J Oral Maxillofac Surg* 2011;10:262–265
6. Bekara F, Yachouh J, Ziade M, et al. Reconstruction of anterior scalp defect with V-Y advancement flap pedicled on the temporal fascia superficialis. *J Craniofac Surg* 2012;23:1434–1435
7. Sowerby LJ, Taylor SM, Moore CC. The double hatchet flap: a workhorse in head and neck local flap reconstruction. *Arch Facial Plast Surg* 2010;12:198–201
8. Seline PC, Siegle RJ. Scalp reconstruction. *Dermatol Clin* 2005;23:13–21

Effect of Restraining Devices on Facial Fractures in Motor Vehicle Collisions

Kun Hwang, MD, PhD and Joo Ho Kim, MD

Abstract: The aim of this systematic review is to summarize and critically evaluate the evidence for or against the effectiveness of restraining devices on facial fractures in motor vehicle collisions (MVCs).

In a PubMed search, the search terms "facial bone fracture and seat belt," "facial bone fracture and air bag," and "facial bone fracture and restraining" were used. The authors abstracted the odds ratio (OR) and 95% confidence intervals (CIs) from each study. Weighted mean differences and 95% CIs were also calculated. The statistical analysis was performed with Review Manager (The Nordic Cochrane Centre).

The authors found 30 potentially relevant articles, of which 6 articles met our inclusion criteria. Five studies were subgrouped, and a meta-analysis of these data suggested beneficial effects of seat belts on decreasing facial fractures in MVCs (n = 15,768,960, OR, 0.46, 95% CI = 0.35–0.60). Three studies were subgrouped, and a meta-analysis of these data suggested that there were beneficial effects of seat belts and air bags on decreasing facial fractures in MVCs (n = 15,768,021, OR, 0.59, 95% CI = 0.47–0.74). Four studies were subgrouped, and a meta-analysis of these data suggested there were no significant effects of an air bag on decreasing facial fracture in MVCs (n = 15,932,259, OR, 1.00, 95% CI = 0.72–1.39).

A seat belt alone (OR, 0.46) or a seat belt and an air bag (OR, 0.59) were effective to decrease facial fractures in MVCs. However, air bags alone had no significant effect (OR, 1.00). In using air bags, seat belt should be applied together to prevent facial fractures in motor vehicle injuries.

Key Words: Air bags, bone, fractures, meta-analysis, motor vehicles, seat belts

Motor vehicle collisions (MVCs) are a serious global health problem and the most common mechanism of injury producing maxillofacial injuries.[1,2] Clinical evidence has suggested these injuries may be modified in both frequencies through the use of active restraining devices.[2] There are injuries that may be decreased by occupant restraining devices such as a seat belt and air bags, yet there is less certainty of their effects on facial trauma.[3] To date, no systematic review of this subject is available. The aim of this systematic review is to summarize and critically evaluate the evidence for or against the effectiveness of restraining devices on facial fractures in MVCs.

METHODS

In a PubMed search, the search terms "facial bone fracture and seat belt," "facial bone fracture and air bag," and "facial bone fracture and restraining" were used. Studies that did not allow an evaluation of the

From the Department of Plastic Surgery, Inha University School of Medicine, Incheon, Korea.
Received May 16, 2014.
Accepted for publication June 28, 2015.
Address correspondence and reprint requests to Kun Hwang, MD, PhD, Department of Plastic Surgery, Inha University School of Medicine, 27 Inhang-ro, Jung-gu, Incheon 400-711, Korea;
E-mail: jokerhg@inha.ac.kr
This work was supported by the grant from INHA University (INHA-Research Grant).
The authors report no conflicts of interest.
Copyright © 2015 by Mutaz B. Habal, MD
ISSN: 1049-2275
DOI: 10.1097/SCS.0000000000002030

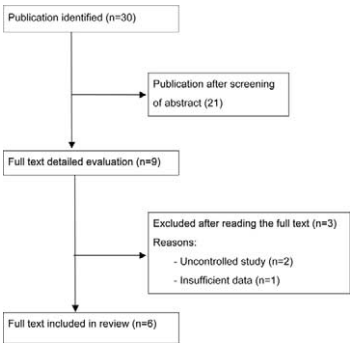

FIGURE 1. Flow chart of the selection process.

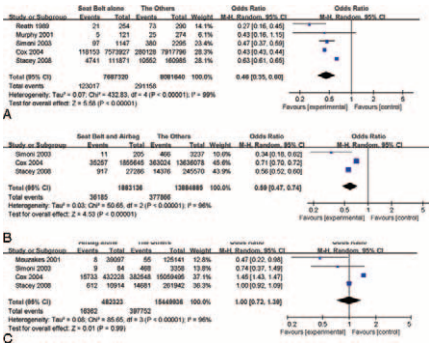

FIGURE 2. Meta-analysis of the restraining devices for decreasing facial fractures in motor vehicle collisions. A, Seat belt alone. B, Seat belt and air bag. C, Air bag alone.

effectiveness of restraining devices (seat belt, air bag) were excluded. No restrictions on language and publication forms were imposed. However, the searched articles were all in English. All articles were read by 2 independent reviewers who extracted data from the articles. To summarize the effectiveness of restraining devices on the facial fractures in MVCs, we abstracted the odds ratio (OR) and 95% confidence intervals (CIs) from each study. Weighted mean differences and 95% CIs were also calculated. The statistical analysis was performed with Review Manager (The Nordic Cochrane Centre).

RESULTS

We found 30 potentially relevant articles (Fig. 1), of which 6 articles met our inclusion criteria (Table 1).[1–6]

Effectiveness of a Seat Belt on Facial Fractures

Five studies were subgrouped, and a meta-analysis of these data suggested there were beneficial effects of seat belts on decreasing facial fractures in MVCs (n = 15,768,960, OR, 0.46, 95% CI = 0.35–0.60, $Z = 5.58$, $P < 0.00001$, heterogeneity: Chi-squared = 432.83, $P < 0.00001$, $I^2 = 99\%$) (Fig. 2A).

Effectiveness of a Seat Belt and an Air Bag on Facial Fractures

Three studies were subgrouped, and a meta-analysis of these data suggested there were beneficial effects of a seat belt and an air bag on decreasing facial fractures in MVCs (n = 15,768,021, OR, 0.59, 95% CI = 0.47–0.74, $Z = 4.53$, $P < 0.00001$, heterogeneity: Chi-squared = 50.65, $P < 0.00001$, $I^2 = 96\%$) (Fig. 2B).

Effectiveness of an Air Bag on Facial Fractures

Four studies were subgrouped, and a meta-analysis of these data suggested there were no significant effects of an air bag on decreasing facial fractures in MVCs (n = 15,932,259, OR, 1.00, 95% CI = 0.72–1.39, $Z = 0.01$, $P < 0.00001$, heterogeneity: Chi-squared = 85.65, $P < 0.00001$, $I^2 = 96\%$) (Fig. 2C).

DISCUSSION

All the studies analyzed were retrospective database studies because no randomized controlled study was available for the safety devices. We used a random effect model because heterogeneities were high (Higgins I^2 were above 90%). Our meta-analysis implies that a seat belt alone (OR, 0.46) or a seat belt and an air bag (OR, 0.59) have beneficial effects on decreasing facial fractures in MVCs. However, no significant effect of an air bag was demonstrated (OR, 1.00).

The reasons for no significant effects of an air bag could be that air bags still inflate at a high velocity despite the air bag designers having decreased the original velocity of inflating air bags.[4] In addition, air bags inflate toward the weakest parts of the facial skeleton—the nose and zygomatic complex. Air bags could decrease the impact in frontal crashes; however, it could not do so in lateral crashes without a seat belt.

TABLE 1. Summary of Retrospective Database Studies Included

			Facial Bone Fracture		Without Facial Bone Fracture		
	Author (Year)	Total Group Size (n)	Intervention Group (n)	Control Group (n)	Intervention Group (n)	Control Group (n)	Results (OR [CI])
Seat belt alone	Reath et al (1989)	544	21	73	233	217	0.27 [0.16, 0.45]
	Murphy et al (2001)	395	5	25	116	249	0.43 [0.16, 1.15]
	Simoni et al (2003)	3442	97	380	1050	1915	0.47 [0.37, 0.59]
	Cox et al (2004)	15,491,723	118,153	280,128	7,455,774	7,637,668	0.43 [0.43, 0.44]
	Stacey et al (2008)	272,856	4741	10,552	107,130	150,433	0.63 [0.61, 0.65]
Seat belt and air bag	Simoni et al (2003)	3442	11	466	194	2771	0.34 [0.18, 0.62]
	Cox et al (2004)	15,491,723	35,257	363,024	1,820,388	13,273,054	0.71 [0.70, 0.72]
	Stacey et al (2008)	272,856	917	14,376	26,369	231,194	0.56 [0.52, 0.60]
Air bag alone	Mouzakes et al (2001)	164,238	8	55	39,089	125,086	0.47 [0.22, 0.98]
	Simoni et al (2003)	3442	9	468	75	2890	0.74 [0.37, 1.49]
	Cox et al (2004)	15,491,723	15,733	382,548	416,495	14,676,947	1.45 [1.43, 1.47]
	Stacey et al (2008)	272,856	612	14,681	10,302	247,261	1.00 [0.92, 1.09]

CI, confidence interval; OR, odds ratio.

© 2015 Mutaz B. Habal, MD

Loo suggested that frontal air bags must address frontal crash, lower extremity injuries induced by the steering wheel, the instrument panel, and the toepan passenger compartment structure intrusions, and lateral crash injuries may be incurred from side air bag supplemental restraint protection.

Rivara et al[7] stated seat belts alone could reduce the risk of death and serious injury. Sutyak et al[8] wrote that air bags have not been proven to be as effective in preventing injury when used alone. He insisted air bags should be used with supplement seat belts as additional protection to prevent head and upper body injuries that result from an occupant striking the vehicle's interior. Results of our systematic review correspond well with the above previous studies.

There have been reports of air bags causing facial trauma. Huff et al[9] stated that injuries have occurred when seat belts and shoulder harnesses were not used properly in conjunction with air bags. In our review, an air bag alone had no significant effect to the risk of facial fracture (OR, 1.00, CI = 0.72–1.39).

In conclusion, a seat belt alone (OR, 0.46) or a seat belt and an air bag (OR, 0.59) were effective to decrease facial fractures in MVCs. However, an air bag alone had no significant effect (OR, 1.00). In using air bags, seat belts should be applied together to prevent facial fractures in motor vehicle injuries.

REFERENCES

1. Murphy RX Jr, Birmingham KL, Okunski WJ, et al. Influence of restraining devices on patterns of pediatric facial trauma in motor vehicle collisions. *Plast Reconstr Surg* 2001;107:34–37
2. Reath DB, Kirby J, Lynch M, et al. Patterns of maxillofacial injuries in restrained and unrestrained motor vehicle crash victims. *J Trauma* 1989;29:806–809
3. Stacey DH, Doyle JF, Gutowski KA. Safety device use affects the incidence patterns of facial trauma in motor vehicle collisions: an analysis of the National Trauma Database from 2000 to 2004. *Plast Reconstr Surg* 2008;121:2057–2064
4. Simoni P, Ostendorf R, Cox AJ 3rd. Effect of air bags and restraining devices on the pattern of facial fractures in motor vehicle crashes. *Arch Facial Plast Surg* 2003;5:113–115
5. Mouzakes J, Koltai PJ, Kuhar S, et al. The impact of airbags and seat belts on the incidence and severity of maxillofacial injuries in automobile accidents in New York State. *Arch Otolaryngol Head Neck Surg* 2001;127:1189–1193
6. Cox D, Vincent DG, McGwin G, et al. Effect of restraint systems on maxillofacial injury in frontal motor vehicle collisions. *J Oral Maxillofac Surg* 2004;62:571–575
7. Rivara FP, Koepsell TD, Grossman DC, et al. Effectiveness of automatic shoulder belt systems in motor vehicle crashes. *JAMA* 2000;283:2826–2828
8. Sutyak JP, Passi V, Hammond JS. Air bags alone compared with the combination of mechanical restraints and air bags: implications for the emergency evaluation of crash victims. *South Med J* 1997;90:915–919
9. Huff GF, Bagwell SP, Bachman D. Airbag injuries in infants and children: a case report and review of the literature. *Pediatrics* 1998;102:e2

Pedicled Supraclavicular Artery Island Flap Versus Free Radial Forearm Flap for Tongue Reconstruction Following Hemiglossectomy

Senlin Zhang, MD, Wei Chen, MD, Gang Cao, MD, and Zhen Dong, MD

Abstract: This study investigated the tongue function and donor-site morbidity of patients with malignant tumors who had undergone immediate flap reconstruction surgery. Twenty-seven patients who had undergone immediate reconstruction after hemiglossectomy were observed. Twelve patients were reconstructed using the pedicled supraclavicular artery island flap (PSAIF) and 15 patients using the free radial forearm flap (FRFF). Flap survival, speech and swallowing function, and donor-site morbidity at the 6-month follow-up were evaluated. All the flaps were successfully transferred. No obvious complications were found in either the transferred flaps or donor regions. Age, sex, defect extent, speech and swallowing function were comparable between the 2 groups. Donor-site complications were less frequent with PSAIF reconstruction than FRFF reconstruction. The PSAIF is reliable and well suited for hemiglossectomy defect. It has few significant complications, and allows preservation of oral function.

Key Words: Free radial forearm flap, hemiglossectomy, pedicled supraclavicular artery island flap, reconstruction, tongue cancer

Options for reconstructing the tongue after cancer resection vary from primary closure to free tissue transfer. Choice of reconstruction methods depends on the size and location of a defect, with the main goal of reconstruction being the ability for the patient to maintain speech and swallowing function. For small defects, primary closure or healing by secondary intention may be sufficient. For larger defects, free tissue transfer has traditionally been used. The free radial forearm flap (FRFF) is considered as the major choice for soft tissue reconstruction of oral cavity defects as it confers good tongue mobility, resulting in acceptable long-term articulation and swallowing ability.[1] However, it requires microvascular surgery and the accompanying requisites, often resulting in a long operative duration, prolonged hospital stay, and possible donor-site morbidity.

The supraclavicular flap was first described by Lamberty[2] in 1979 as an axial pattern fasciocutaneous flap. Pallua et al[3] used the supraclavicular flap as an island flap for the release of a mental scar contracture. In a recent anatomic and clinical study by the same author, the supraclavicular artery, the arterial part of the pedicle of this flap, was confirmed to be a constant branch of the transverse cervical artery.[4] The vascular territory of this flap extends from the supraclavicular region to the shoulder cap. The area of this angiosome ranges from 10 to 16 cm in width and 22 to 30 cm in length. Usually, the donor site of this flap can be closed primarily by extensive undermining, thus avoiding the need for additional skin

From the Department of Stomatology, Jinling Hospital, School of Medicine, Nanjing University, Nanjing, Jiangsu, China.
Received April 8, 2015.
Accepted for publication June 28, 2015.
Address correspondence and reprint requests to Senlin Zhang, MD, Department of Stomatology, Jinling Hospital, School of Medicine, Nanjing University, 305 East Zhongshan Road, 210002 Nanjing, Jiangsu, China; E-mail: doczhangsl@gmail.com
SZ and WC contributed equally to this work, and are joint first authors.
This study was supported by grants from the National Natural Science Foundation of China (Grant No. 81102051), the Natural Science Foundation of Jiangsu Province (Grant No. BK2011659), and the Nanjing University Fundamental Research Funds for the Central Universities (Grant No. 021414340210).
The authors report no conflicts of interest.
Copyright © 2015 by Mutaz B. Habal, MD
ISSN: 1049-2275
DOI: 10.1097/SCS.0000000000002031

grafting. To improve the vascularity of the flap, Di Benedetto et al[5] advised using a fascial pedicle. Since its clinical use, the flap has been controversial because of the reported incidence of distal flap necrosis.[6] Beginning in the 1990s, Pallua et al "rediscovered" this flap and popularized its use by performing detailed anatomic studies examining the vascularity of what is known today as the supraclavicular artery island flap (SAIF).[3,4,7]

The use of SAIF in head and neck reconstruction has been described, and it has been shown to be well suited for defects of tongue, floor of the mouth, buccal mucosa, oropharynx, palate, lower gingiva, parotid, and neck.[8,9] Particularly when used for intraoral reconstruction, the SAIF possesses many advantages of the FRFF because it is thin and pliable, and allows a large surface area to be harvested. Although the SAIF can be harvested for free tissue transfer, its main advantage for intraoral reconstruction is that it can be used as a pedicled flap and tunneled into the defects. Accordingly, one might expect shorter operative time with the pedicled supraclavicular artery island flap (PSAIF) than is seen with free flap alternatives. Without the need for microvascular anastomosis, it requires less intensive postoperative flap monitoring and may also demonstrate shorter hospital stay. The PSAIF is believed to offer good functional results, although there have been no reports to date comparing it with other reconstructive options.

The purpose of this study was to evaluate tongue function as well as donor-site morbidity in patients with tongue cancer surgically treated and reconstructed with the PSAIF or the FRFF.

METHODS

Patients

In total, 27 patients with anterior lateral tongue carcinoma who underwent surgical resection of the tumors and reconstructed of the resultant defects with the PSAIF or FRFF at the Department of Stomatology, Jinling Hospital, Nanjing, China, between July 2008 and December 2013 were included in the current study. All tumors were squamous cell carcinomas and none of the tumors involved the mandible. The patients who underwent preoperative radiation <5 years were excluded.

Reconstruction was performed immediately after tumor resection by a single surgeon (Senlin Zhang), and tongue resection and neck dissection were carried out by an oral and maxillofacial team. All patients in the study underwent subtotal glossectomy, with at least 50% of the anterior tongue resected and laryngeal preservation. Fourteen patients were reconstructed using FRFF (Fig. 1A–C) and the remaining patients with PSAIF (Fig. 2A–F). Technical details regarding harvesting the FRFF and PSAIF were well described previously.[10,11] The tip of the reconstructed tongue was left as mobile as possible.

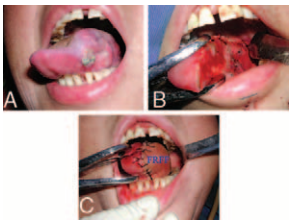

FIGURE 1. A 51-year-old male with squamous cell carcinoma in the left tongue that was reconstructed by a free radial forearm flap (FRFF) following cancer ablation. A, Preoperative presentation with squamous cell carcinoma in the left tongue. B, The tongue defect after cancer ablation. C, The tongue defect was reconstructed by an FRFF.

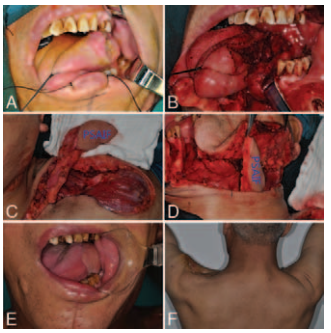

FIGURE 2. A 64-year-old male with squamous cell carcinoma in the left tongue reconstructed by a pedicled supraclavicular artery island flap (PSAIF) following cancer ablation. A, Preoperative presentation with squamous cell carcinoma in the left tongue. B, The tongue defect after cancer ablation. C, Intraoperative view of the PSAIF. D, The PSAIF was passed through a left neck subcutaneous tunnel. E, Postoperative intraoral view at 6 months. F, Postoperative view of the donor site and fully raised-up arms of the patient.

Data Collection

Patients were identified and their medical records were reviewed and relevant data extracted using a data extraction form. Demographic information (age and sex) was obtained. Operative notes were reviewed for information on the extent of resection and choice of flap. The overall operation time and hospital stay of both flaps were recorded and compared. Medical record was reviewed for complications, including flap complication, recipient site complication, and donor-site complication. Patients were followed up postoperatively to determine the functional outcome of speech and swallowing. Functional results were subjectively assessed by 2 independent surgeons (Wei Chen and Gang Cao). If the 2 surgeons have different judgment, the final decision was made by the corresponding author (Senlin Zhang). Swallowing function was stratified into the full diet, soft diet, and liquid diet. Speech intelligibility was categorized as excellent (>80% intelligibility), good (50%–80% intelligibility), and poor (<50% intelligibility). All the subjects were evaluated at the 6-month follow-up visit.

Statistical Analysis

The study cohort was grouped according to choice of flap: FRFF and PSAIF. Data were analyzed by Student's *t*-test, Chi-squared test, and 2-tailed Mann-Whitney test. Statistical analysis was performed using the SPSS, version 16 (SPSS Inc, Chicago, IL). The significance level was set to $P < 0.05$.

RESULTS

Patient characteristics, defect extent, and operation time are shown in Table 1. The average operation time (minutes) of FRFF group was 81 ± 8, and it was 55 ± 7 minutes of PSAIF group. The average hospital stay (days) of FRFF group was 17 ± 2.5, and it was 12 ± 1.7 days of PSAIF group. Patients in the FRFF and PSAIF group were comparable in age, sex, and defect extent. The average operation time of the FRFF and PSAIF group were also comparable, whereas average hospital stay of the PSAIF group were significantly shortened compared with the FRFF group.

Speech and swallowing function were graded and tabulated for both groups (Table 2). Speech results were excellent in most patients regardless of reconstruction method, with 12 patients receiving FRFF (80.0%) and 11 patients receiving PSAIF (91.7%) achieving an excellent outcome in speech function. Three patients in the FRFF group and 1 patient in PSAIF group had a good outcome in speech function. Swallowing function was largely

© 2015 Mutaz B. Habal, MD

TABLE 1. Patient Demographic and Baseline Characteristics by FRFF and PSAIF

Variable	FRFF	PSAIF	P
Number	15	12	
Age, y			1.00
<50	3	2	
≥50	12	10	
Sex			0.69
Male	10	9	
Female	5	3	
Defect area			0.70
Tongue	7	7	
Tongue/floor of mouth	8	5	
Average operation time (min)	81 ± 8	55 ± 7	>0.05
Average hospital stay (d)	17 ± 2.5	12 ± 1.7	<0.05

FRFF, free radial forearm flap; PSAIF, pedicled supraclavicular artery island flap.

TABLE 2. Speech and Swallowing Function Following Flap Reconstruction

Variable	FRFF	PSAIF	P
Number	15	12	
Speech			0.62
Excellent	12	11	
Good	3	1	
Poor	0	0	
Swallowing			1.00
Full diet	13	10	
Soft diet	2	2	
Liquid diet	0	0	

FRFF, free radial forearm flap; PSAIF, pedicled supraclavicular artery island flap.

normal in the majority of the patients, with 13 patients receiving FRFF (86.7%) and 10 patients receiving PSAIF (83.3%) on full oral diet. Two patients each receiving FRFF or PSAIF were on the soft diet. Differences in speech and swallowing function were not significantly different between the 2 groups.

Data on surgical complications are shown in Table 3. One patient had complete flap loss in the FRFF group (6.7%, 1/15) and no partial flap loss was reported. Conversely, partial flap loss was reported in 2 patients in the PSAIF group (16.7%, 2/12), whereas no patients experienced complete flap loss. Furthermore, no patients in both groups developed recipient site complications

TABLE 3. Complications of FRFF and PSAIF

Variable	FRFF	PSAIF	P
Number	15	12	
Flap complications	1	2	0.19
Flap failure	1	0	
Partial flap necrosis	0	2	
Donor-site complications	29	7	<0.05
Partial loss of skin graft	4	NA	
Wound dehiscence	1	0	
Hypertrophic scarring	12	2	
Numbness	9	4	
Function impairment	3	0	

FRFF, free radial forearm flap; NA, not applicable; PSAIF, pedicled supraclavicular artery island flap.

such as wound dehiscence and orocutaneous fistula. Donor-site complications were more prevalent with FRFF reconstruction: 4 patients had partial loss of skin grafts, 1 patient had wound dehiscence, 12 patients had hypertrophic scarring, 9 patients had numbness, and 3 patients had function impairment. Conversely, there were only 7 patients with donor-site complications: 1 patient had wound dehiscence, 2 patients had hypertrophic scarring, and 4 patients had numbness.

DISCUSSION

The qualities of the ideal soft tissue free flap for head and neck reconstruction may be defined as versatility in design, adequate tissue stock, superior texture, minimal donor-site morbidity, availability of diverse tissue types on 1 pedicle, potential for reinnervation, large and long pedicle, feasibility of a 2-team approach, and consistent anatomy for easy and safe flap harvesting.[12] Both FRFF and PSAIF fulfill many of these qualities, providing thin and pliable skin to replace tongue defect after resection, which not only acts as a spacer, but also allows the remaining tongue a certain degree of movement.[9] In addition, both these flaps contain cutaneous nerves and can be used as sensate flaps. In this study, differences in functional outcomes between both flaps were not statistically significant. The skin and subcutaneous tissue of both flap types are thin, which is suitable for wounds not requiring bulk grafting. Elevation of either FRFF or PSAIF is technically easy. However, donor-site morbidity was higher in FRFF than in PSAIF.

The PSAIF was used for a variety of head and neck oncologic patients in whom traditional musculocutaneous and free flap techniques would normally be used for reconstruction.[8] Regional flaps remain the preferred technique in more difficult patients such as those with advanced age, poor nutrition, or multiple medical issues as they are not always acceptable surgical candidates for potentially prolonged microsurgery. The PSAIF has been harvested successfully in patients with various comorbidities, including obesity, poor nutrition, diabetes, and smoking history. Flap survival is no different from that for any traditional flap. Contraindications have been limited to patients who have previous ipsilateral neck dissections and/or radiated necks. Today when the level V lymph nodes not to be involved in cancer, a radical neck dissection is rarely performed in this area, therefore, the thyrocervical trunk can usually be preserved on the ipsilateral side.

The PSAIF is a thin, pliable, vascularized, regional, axially based flap. It is also a fasciocutaneous flap with minimal shoulder donor-site morbidity. Functional impairment of upper limb movement has not been observed.

Donor-site closure is performed after flap insertion. Wide undermining, both anteriorly and posteriorly, is usually required. Any flap that is wider than 8 cm may be difficult to close, and skin grafting should be performed without hesitation. Although a scar may be noticeable when the patient is shirtless or wearing a tank top, compromised shoulder function was not observed in this series.

The PSAIF offers a regional flap alternative with comparable functional outcomes and minimal donor-site morbidity, and provides an excellent flap option for patients who are poor candidates for microvascular surgery. This thin flap is easily and quickly harvested, has a reliable pedicle, and gives the reconstructive surgeon the opportunity to close large defects in the tongue in 1 operation, without the need for microsurgical skills. The reliability of the distal part of the flap can be improved by using a fascial pedicle.[5]

In brief, the PSAIF is a suitable pedicled flap for the reconstruction of hemiglossectomy defects following tumor ablation. It may offer advantages of reduced complications while maintaining acceptable speech and swallowing function compared with the FRFF.

© 2015 Mutaz B. Habal, MD

REFERENCES

1. Nakatsuka T, Harii K, Asato H, et al. Analytic review of 2372 free flap transfers for head and neck reconstruction following cancer resection. *J Reconstr Microsurg* 2003;19:363–369
2. Lamberty BG. The supra-clavicular axial patterned flap. *Br J Plast Surg* 1979;32:207–212
3. Pallua N, Machens HG, Rennekampff O, et al. The fasciocutaneous supraclavicular artery island flap for releasing postburn mentosternal contractures. *Plast Reconstr Surg* 1997;99:1878–1884
4. Pallua N, Magnus NE. The tunneled supraclavicular island flap: an optimized technique for head and neck reconstruction. *Plast Reconstr Surg* 2000;105:842–851
5. Di Benedetto G, Aquinati A, Pierangeli M, et al. From the 'charretera' to the supraclavicular fascial island flap: revisitation and further evolution of a controversial flap. *Plast Reconstr Surg* 2005;115:70–76
6. Blevins PK, Luce EA. Limitations of the cervicohumeral flap in head and neck reconstruction. *Plast Reconstr Surg* 1980;66:220–224
7. Pallua N, Demir E. Postburn head and neck reconstruction in children with the fasciocutaneous supraclavicular artery island flap. *Ann Plast Surg* 2008;60:276–282
8. Chiu ES, Liu PH, Friedlander PL. Supraclavicular artery island flap for head and neck oncologic reconstruction: indications, complications, and outcomes. *Plast Reconstr Surg* 2009;124:115–123
9. Chen WL, Zhang DM, Yang ZH, et al. Extended supraclavicular fasciocutaneous island flap based on the transverse cervical artery for head and neck reconstruction after cancer ablation. *J Oral Maxillofac Surg* 2010;68:2422–2430
10. Takato T, Harii K, Ebihara S. Oral and pharyngeal reconstruction using the free forearm flap. *Arch Otolaryngol Head Neck Surg* 1987;113: 873–879
11. Telang P, Jagannathan M, Devale M. A study of the use of the supraclavicular artery flap for resurfacing of head, neck, and upper torso defects. *Indian J Plast Surg* 2009;42:4–12
12. Hayden RE. Microvascular free flaps for soft-tissue defects. *Otolaryngol Clin N Am* 1991;24:1343–1366

Temporomandibular-External Auditory Canal Fistulas Treatment: Patient With Air Into the Synovial Compartment

Piero Cascone, MD, PhD, Valerio Ramieri, MD,* Valentino Vellone, MD,* Diletta Angeletti, MD,* Giannicola Iannella, MD,† and Giuseppe Magliulo, MD†*

Fistulas of the temporomandibular joint-external auditory canal (TMJ-EAC) are permanently epithelialized communications extending between the temporomandibular joint (TMJ) and the external auditory canal.[1,2]

From the *Maxillofacial Surgery Department; and †'Organi di Senso' Department, ENT, Sapienza' Università di Roma, Rome, Italy.
Received September 19, 2014.
Accepted for publication June 28, 2015.
Address correspondence and reprint requests to Valentino Vellone, MD, Maxillo-Facial Surgery Department, Sapienza Università di Roma, Rome, Italy; E-mail: valentino.vellone@gmail.com
The authors report no conflicts of interest.
Copyright © 2015 by Mutaz B. Habal, MD
ISSN: 1049-2275
DOI: 10.1097/SCS.0000000000002032

A TMJ-EAC fistula may be secondary to otitis externa, radiotherapy of the head and neck, fractures of the mandibular condyles or otologic, and TMJ surgery.[2,3]

Spontaneous fistula is a very rare entity.[1,4] A defect of the antero-inferior part of the tympanic bone, better known as foramen of Huschke, could be the cause of this rare condition.[1–4]

The authors describe the unusual case of a patient with a congenital Huschke foramen who developed a TMJ-EAC fistula secondary to radiation therapy, allowing the entry of air into the synovial compartment during jaw movements.

In the literature, very few studies have described TMJ-EAC fistulae[1–6]: only 1 patient of TMJ air because of EAC communication has been described so far.[7]

At the time of this writing, there is no consensus on how to manage TMJ-EAC fistulas, particularly those in which previous radiotherapy was performed. We propose closure of the fistula through a temporalis muscle rotation flap.[2,5,6]

CLINCAL REPORT

A 55-year-old woman came to our department presenting left external auditory canal secretions, aural pain, and an unusual TMJ noise at each jaw movement.

The patient's clinical history was notable for ovarian carcinoma, which had been treated 7 years earlier with surgery and subsequent chemotherapy. Radiotherapy, at a total dose of 35 Gy in 14 fractions of 2.5 Gy/day was performed 2 years after the first operation because of the occurrence of brain metastases.

Medical history was negative for facial trauma, condylar fractures, external otitis, otologic procedures, or TMJ dysfunction. Moreover, no evidence of cancer recurrence was evident.

Physical examination revealed an unusual audible noise like a "squelch" during jaw movement when the patient opened her mouth. Left TMJ was slightly tender but no subcutaneous emphysema could be palpated. Otoscopic examination showed a normal tympanic membrane: erythema of the proximal anterior canal wall and a fluid leak in the anterior wall of the EAC were visible without a clear TMJ herniation. At oropharyngeal examination no pathologic aspect could be seen.

A high-resolution computed tomography scan of the TMJ and external auditory canal revealed the presence of a dehiscence in the anterior wall of the tympanic bones identified as the foramen of Huschke, with a visible communication between the TMJ and the EAC. Note the presence of air that filled the synovial space of the TMJ and extended through the joint capsule into the adjacent tissue planes. No cholesteatoma or other middle ear disease could be seen (Fig. 1).

Magnetic resonance imaging showed increased vascularity of the masseter and pterygoid muscles, the ramus and condyle of the mandible, and of the parotid gland, with apparently preserved anatomy (Fig. 2).

FIGURE 1. Computed tomography scan of the temporomandibular joint in coronal view. Note the presence of air filling synovial space and extended through the joint capsule into the adjacent tissue planes.

© 2015 Mutaz B. Habal, MD

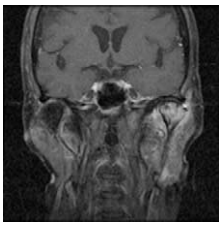

FIGURE 2. Magnetic resonance imaging showed increased vascularity of the masseter and pterygoid muscles, the ramus, and condyle of the mandible and of the parotid gland.

We opted for a surgical strategy to evaluate the nature of the fistula and to close it. A preauricular pretragal incision was made, the auriculotemporal nerve was identified, and preserved. Subsequently, tissue blunt dissection below the zygomatic arch, adjacent to the external auditory cartilage was performed.

The posterior portion of the glenoid fossa of the temporal bone was subperiosteally exposed and dissection was carried downwards to the tympanic plate, where a bony dehiscence was evident. No necrotic bone was observed. A superior TMJ compartment arthrocentesis followed by arthroscopy was performed with injection of ringer fluid, and ringer leakage from the EAC was immediately observed. Subsequently, the initial tract of the fistula in the posterior recess of the TMJ capsule was identified and sutured.

The temporalis muscle rotation flap was raised directly superior to the location of the fistula. The flap was elevated over the zygomatic arch, interposed between the glenoid cavity of the joint capsule, and finally sutured to the soft tissues adjacent to the fistula with 4-0 Vicryl suture.

Postoperatively, there was no change in her mouth occlusion and no TMJ symptoms appeared after 6 months follow-up.

DISCUSSION

A permanent communication between the TMJ and the EAC is a very rare condition. In 1988, Hawke et al[4] first reported a fistula between the TMJ and EAC, which developed through a congenital dehiscence in the anterior wall of the tympanic bone, previously identified as a Huschke foramen.[8]

A Huschke foramen usually closes at 5 year old. A persistent communication, however, was found in a recent retrospective review in 12% of men and in 20% of women ($P < 0.0001$).[9]

Anatomically, the EAC and the TMJ are separated by the tympanic plate of the temporal bone. Because of its thinness, however, the tympanic plate is susceptible to fractures when a posterior displacement of condyle occurs. Radiation therapy or chronic otitis externa may often play a role in fistula formation. Moreover, iatrogenic damage to the tympanic plate, after otologic or TMJ surgery, has been reported in the literature.[1–3]

The etiology of the fistula in our patient appears to be related to congenital dehiscence and subsequent radiation therapy that compromised the local tissue.

Defects of the anterior wall of the EAC can result in clicking, tinnitus, conductive hearing loss, otalgia, and otorrhea, although often no symptoms are reported.

Few reports published in the literature have described patients of fistula between the TMJ and the EAC.[1–6] The only patient of a permanent communication with air present in the synovial space was reported by Schwartz et al,[7] who defined this condition with the name of pneumarthrosis of the TMJ.

Occasionally, it is possible for a TMJ-EAC fistula to be confused with a TMJ herniation into the external auditory meatus or with salivary fistula between the parotid gland and the EAC. Such conditions, more frequently because of the persistence of a Huschke foramen, were absent in the current patient.[10,11]

At the time of this writing, there is no common consensus on how to manage TMJ-EAC fistulas. Spontaneous closure of a small communication sometimes occurs in early age. Conservative procedures, which require the patient to wear a mandibular advancement splint have been previously described.[1,2,6,7]

Crombie et al[2] proposed a conservative management with aural toilet and mandibular advancement splint as first line treatment. They postulated that a mandibular advancement splint allows healing by moving the condylar head forward, thus relieving the pressure on the posterior aspect of the glenoid fossa.

In selected patients, surgical management, however, may be required. Sinn et al[6] were the first to propose surgical correction of the fistula using a vascularized temporalis flap, whereas, Schwartz et al[7] used a nonvascularized fascial graft from the fascia lata of the thigh.

In our patient, because of the history of radiotherapy, conservative management was excluded and the authors opted for a surgical correction of the fistula through a temporalis muscle rotation flap as first line treatment.

The advantages of a temporalis rotation flap have been well documented.[5,6] The flap is usually well vascularized and easy to fashion and use: morbidity and aesthetic outcomes were more favorable using this surgical technique. The main goal of the surgery was closure of the fistula and restoration of the physiological movement of the TMJ, without causing any aural pathology. The size of the temporalis flap has to be decided during surgery, after the exposure of the fistula, because the flap should be at least 5 cm in length to reach the glenoid fossa without tension.[2,5–7] The use of nonvascularized tissue or synthetic grafts is unadvisable in previously irradiated patients for the potential negative radiotherapic effects on the regional vessels.

In conclusion, in patients with a persisting Huschke foramen subsequently submitted to radiation treatment, the creation of a communication between the TMJ, and the EAC with air entering inside the joint capsule is feasible.

The temporalis rotation muscle flap is a safe and effective surgical technique in which ensures fistula closure, while reducing possible complications or fistula recurrence.[2,5,6]

Nevertheless, a greater number of patients with this pathology should be evaluated to define the fistula etiology and identify the treatment of choice.

REFERENCES

1. Adjuk J, Ries M, Vagic D, et al. Temporomandibular joint fistula into the external ear canal. *J Laryngol Otol* 2012;126:837–839
2. Crombie AK, Batstone MD, Voltz M, et al. LynhamAJ. Management of temporomandibular-external auditory canal fistulas: a report of 3 cases. *Am J Otolaryngol* 2010;31:59–60
3. Dingle AF. Fistula between the external auditory canal and the temporomandibular joint: a rare complication of otitis externa. *J Laryngol Otol* 1992;106:994–995
4. Hawke M, Kwok P, Shankar L, et al. Spontaneous temporomandibular joint fistula into the external auditory canal. *J Otolaryngol* 1988;17:29–31
5. Edwards SP, Feinberg SE. The temporalis muscle flap in contemporary oral and maxillofacial surgery. *Oral Maxillofac Surg Clin North Am* 2003;15:513–535
6. Sinn DP, Tharanon W, Culbertson MC, et al. Surgical correction of an aural-temporomandibular joint fistula with a temporalis flap. *J Oral Maxillofac Surg* 1994;52:197–200
7. Schwartz HC, Sedhom A. Pneumarthrosis of the temporomandibular joint: report of case. *J Oral Maxillofac Surg* 1997;55:287–289
8. Hawke M, Kwok P, Mehta M, et al. Bilateral spontaneous temporomandibular joint herniation into the external auditory canal. *J Otolaryngol* 1987;16:387–389
9. Hashimoto T, Ojiri H, Kawai Y. The foramen of Huschke: age and gender specific features after childhood. *Int J Oral Maxillofac Surg* 2011;40:743–746

© 2015 Mutaz B. Habal, MD

10. Park YH, Kim HJ, Park MH. Temporomandibular joint herniation into the external auditory canal. *Laryngoscope* 2010;120:2284–2288
11. Tozoglu U, Caglayan F, Harorli A. Foramen tympanicum or foramen of Huschke: anatomical cone beam CT study. *Dentomaxillofac Radiol* 2012;41:294–297

Use of Pedicled Trapezius Myocutaneous Flap for Posterior Skull Reconstruction

Mansher Singh, MD, Arturo J. Rios Diaz, MD,† Ryan Cauley, MD,* Timothy R. Smith, MD, PhD,‡ and E.J. Caterson, MD, PhD**

Background: Soft-tissue defects in posterior skull can be challenging for reconstruction. If related to tumor resection, these wound beds are generally irradiated and can be difficult from a recipient-vessel perspective for a free tissue transfer. Locoregional flaps might prove to be important reconstructive option in such patients. There is a very limited data on the usage of pedicled trapezius myocutaneous flaps for such defects.

Methods: The authors reviewed existing study for usage of trapezius flap for posterior skull repair and used pedicled trapezius myocutaneous flaps based on the descending branch of superficial cervical artery (SCA) for reconstruction of posterior skull soft-tissue defect in an irradiated and infected wound.

Results: Two patients were operated for trapezius myocutaneous flap for posterior skull defects complicated by cerebrospinal fluid (CSF) leakage and epidural abscess. There was no recipient or donor-site complication at a mean follow-up of 12.5 months. Neither of the 2 patients had any functional deficits for the entire duration of the follow-up. Although this flap was able to help in controlling the CSF leakage in the first patient, it successfully healed the cavity generated from epidural abscess drainage in the second patient.

Conclusion: The large angle of rotation coupled with the ability to complete the procedure without repositioning the patients makes trapezius myocutaneous flap an attractive option for posterior skull reconstruction. In our limited experience, the pedicled trapezius flaps are a reliable alternative as they are well vascularized and able to obliterate the soft-tissue defect completely. The recipient site healed completely in infected as well as irradiated wound beds. In addition, the donor site can be primarily closed with minimal donor-associated complication.

From the *Division of Plastic Surgery, Department of Surgery, Brigham and Women's Hospital; †Center for Surgery and Public Health, Department of Surgery, Brigham and Women's Hospital; and ‡Department of Neurosurgery, Brigham and Women's Hospital, Boston MA.

Received March 5, 2015.
Accepted for publication June 28, 2015.

Address correspondence and reprint requests to Edward J. Caterson, MD, PhD, Division of Plastic Surgery, Brigham and Women's Hospital, Harvard Medical School, 75 Francis Street, Boston, MA 02115; E-mail: ecaterson@partners.org

The authors report no conflicts of interest.

Copyright © 2015 by Mutaz B. Habal, MD

ISSN: 1049-2275
DOI: 10.1097/SCS.0000000000002033

Key Words: CSF leak, posterior skull reconstrcution, trapezius myocutaneous flap

Soft-tissue defects in posterior skull can be challenging for reconstruction. If related to tumor resection, these wound beds are generally irradiated increasing the risk of cerebrospinal fluid (CSF) leak.[1] In addition, CSF leaks are relatively common in posterior fossa surgery because of difficulty in achieving water tight dural closure.[2] A CSF leak into such dead space can result into pseudomeningocele. In addition, accumulation of CSF or hematoma in a dead space can result in secondary infections that have a potential to develop into epidural abscess.[3] Such situations may develop into life-threatening intracranial complications. A myocutaneous flap can obliterate this cavity and resist CSF leak or hematoma formation. Free tissue transfer has emerged as a reliable choice for complex head and neck repair.[4] However, locoregional flaps have better matched skin color and texture, which makes them aesthetically more appealing for reconstruction involving skin defects.[4–6] Moreover, most of the patients with posterior skull tumors have significant comorbidities and have generally been treated with radiation therapy, which increases the risks of postoperative complications with free tissue transfer. Based on these observations, there has been renewed interest in the usage of locoregional flaps.

The pectoralis major myocutaneous flap is considered the "workhorse" flap for head and neck reconstruction.[7] Lattisimus dorsi myocutaneous flap is also used for posterior neck and skull reconstruction.[8] However, use of these flaps for posterior skull reconstruction requires extensive mobilization. Trapezius muscle mycocutaneous flap provides another alternative for reconstruction. Different types of myocutaneous trapezius flaps described in the study include the superior, the lateral island, the vertical, and the lower island flap.[9–12] This flap is easy to harvest, has a large arc of rotation, is well vascularized, and is more pliable than both lattisimus dorsi and pectoralis major flap. In addition, it can provide bulk to the soft-tissue defect and can be extended with the use of a tissue expander.[13]

We present a set of 2 patients with posterior skull soft-tissue defects who were successfully treated with trapezius myocutaneous flap. Through this series, we aim to establish trapezius myocutaneous flap as an alternative option for posterior skull soft-tissue defects. It can be successfully used in a setting of radiation, infection, and other conditions which impact wound healing.

METHODS

Two patients with soft-tissue defect in the posterior skull underwent trapezius myocutaneous flap placement. The hospital records of both the patients were reviewed, and patient characteristics, operative details, and follow-up data were recorded.

Trapezius Muscle and Surgical Technique

The anatomy of the trapezius muscle has been extensively described in the study.[14,15] It originates from the medial third of the superior nuchal line of the occipital bone, the external occipital protuberance, the ligamentum nuchae, the spinous process of the seventh cervical vertebrae, and all the thoracic vertebrae and inserts into the lateral third of the clavicle, the medial border of the acromion, and the entire length of the scapular spine. It is a triangular shaped thin and large muscle, which assists in raising and rotating the shoulder. The nerve supply to this muscle comes from accessory nerve.

The main blood supply of the trapezius muscle and the overlying skin is from the superficial and deep branches of the transverse cervical artery (TCA), which is generally a branch of the

 © 2015 Mutaz B. Habal, MD

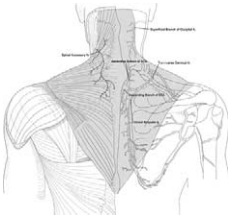

FIGURE 1. Anatomy and vascular supply of trapezius muscle. The flap in our series was raised on the descending branch of the superficial cervical artery.

thyrocervical trunk (Fig. 1). Most of the myocutaneous trapezius flap are raised on these 2 dominant flaps: the superficial branch of TCA (SCA) and the deep branch of TCA (DSA)[16] The SCA gives rise to an ascending and a descending branch, which can be individually used to raise the trapezius flap. The minor pedicles, such as the occipital artery and the intercostals perforators, are uncommonly used for trapezius flap elevation.[14]

We decided to use the descending branch of the superficial cervical artery for our myocutaneous trapezius flap. As the accessory nerve mainly traverses through the upper trapezius muscle, there is minimal to no risk of nerve injury with this technique as it raises the lower half of the trapezius muscle. In addition, the whole procedure can be done in a prone position so that there is no need for repositioning the patient for posterior skull reconstruction. The skin island is outlined after localizing the vascular pedicle with a Doppler (Fig. 2A). The course of SCA is followed under the anterior border of the trapezius muscle. Once the descending branch is identified, the pedicle is freed completely and the vertical skin island is elevated (Fig. 2B). The myocutaneous trapezius flap is then elevated (Fig. 2C) and the donor site is closed primarily (Fig. 2D).

RESULTS

Two patients underwent the abovementioned procedure for soft-tissue defect in the posterior skull. In both the patients, the flap healed completely and was able to effectively obliterate the soft-tissue defect. There was no flap-related or donor-site complication in either of the patients at a mean follow-up of 12.5 months. Neither of the 2 patients had any functional deficits for the entire duration of the follow-up.

Patient 1

The patient was a 57-year-old male with a history of brainstem heamngioblastoma who was operated for subtotal suboccipital craniectomy and C1 laminectomy in 2007 followed by radiation for residual tumor and VP shunt placement. Unfortunately, his clinical course was complicated by meningitis, which required shunt removal. In 2012, he developed new neurologic symptoms in the form of upper extremity numbness and was found to have tumor recurrence for which he required reresection of his hemangioma and complex watertight dural closure using alloderm patch. Postoperatively, the patient reported spontaneous copious amount of clear fluid drainage from the inferior aspect of his wound, which was consistent with pseudomeningocele on CT scan. He was taken back to the operating room for decompression of his pseudomenigocele and was found to have 3 points of clear leakage from the allograft, which was sutured with 4-0 Nurulon. His pseudomeningocele persisted postoperatively despite lumbar drainage and was therefore operated for a VP shunt placement. However, within next few weeks, he was readmitted with reports of fluid "gushing" from his suboccipital craniotomy incision. Given his continued wound leakage, it was decided to take him back to the operating room for wound exploration and definitive closure. A large amount of CSF was evacuated from his pseudomeningocele. The prior alloderm patch had thinned out with a number of openings resulting in CSF leakage. It was replaced with a new alloderm patch, and a watertight closure was confirmed with valsalva maneuver. The plastic surgery team was consulted to help with closure of his wound. As the patient had a longstanding cavity in a radiated field, it was decided to use a myocutananeous trapezius flap to obliterate the cavity. The skin paddle, which was 6 cm × 14 cm, was marked preoperatively, and a trapezius flap was raised based upon the descending branch of superficial cervical artery. A large portion on the distal flap was de-epithelialized and was tucked against the skull base and posterior cervical spine to bolster the alloderm repair resulting in a transposition flap for wound closure. Postoperatively, the patient reaccumulated a 6 cm × 6 cm CSF collection necessitating another trip to the operating room. No definite leak was observed in the dural alloderm patch after multiple valsalva maneuvers, and it was determined that the patient has an occult CSF leakage. It was decided to separate the cutaneous portion of the flap from the trapezius muscle flap and use this as a 2-layered closure. The muscle portion of the trapezius flap was inset by parachuting it down into the skull base along the paraspinal muscles. A Blake drain was placed inferior to the trapezius flap, and a lumbar drain was also placed in the pseudomeningocele. Two weeks postoperatively, the patient presented to the clinic with leakage of CSF around the Blake drain. Given the known occult CSF leak and continued CSF leakage, it was decided to internalize the lumbar drain, and a lumbar peritoneal shunt was placed for definitive management of his CSF leakage. His trapezius flap was completely intact during this time without any concern for wound dehiscence. On his 6-week follow-up appointment, his trapezius flap and the donor sites had healed completely without any bogginess associated with recurrent CSF leak (Fig. 3A). It was determined that that the trapezius flap was doing an effective job at blocking any further built up of CSF. The patient's remainder clinical course was unremarkable from reconstructive standpoint, but his magnetic resonance imaging (MRI) showed an increase in the size of his tumor around 6 months after the flap procedure. As he was an extremely poor surgical candidate, alternative options were sought and he was started on Pazopanib therapy with plans for restaging MRI. However, his tumor continued to progress slowly on this therapy and the patient was placed under hospice care. During his last clinical visit, he was

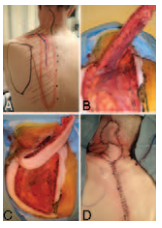

FIGURE 2. Trapezius flap: A, outline of skin island after localization of the vascular pedicle with a Doppler; B, isolation of vascular pedicle and elevating the skin island; C, elevation of myocutaneous trapezius flap; and D, primary closure of the donor site.

FIGURE 3. Completely healed donor and recipient site in patient 1 (A) and in Patient 2 (B).

© 2015 Mutaz B. Habal, MD

23 months out from his trapezius flap procedure without any complications.

Patient 2

The patient was a 60-year-old male who was diagnosed with a nonfunctioning pituitary adenoma in 2001 and underwent a transsphenoidal resection. During his work-up, he was found to have a left cerebellar epidermoid mass that was followed over several years with serial imaging. Owing to an increase in the size of the epidermoid tumor, which was essentially filling the entire left posterior fossa and compressing the cerebellum, a left suboccipital craniectomy with titanium plate was performed in 2008. In December 2012, he started noticing drainage on his pillowcases, mostly at the nighttime while lying down. The drainage from the scalp was not concerning for CSF leak based in its appearance. The patient also noticed left ear tinnitus, fullness, and decreased left-sided hearing since his epidermoid tumor resection. A brain MRI in June 2013 demonstrated a large nonenhancing mass in the left posterior fossa that seemed to track extracranially through the titanium mesh with areas of small puckered sites in the scalp at the site drainage. The findings were thought to represent either a recurrence of epidermoid mass or a chronic infection in the epidural space. The pituitary area appeared unremarkable without any evidence of recurrence. It was determined that the caustic contents of the epidermoid cyst might be responsible for poor healing along the site of titanium mesh attached to the scalp and could also result in scalp wound dehiscence resulting in drainage. As the patient did not have any concern for rhinorrhea or CSF leak and was nontoxic in appearance, it was decided to perform a wound exploration in an elective fashion. He was followed conservatively for over a year with malodorous yellowish drainage from 2 spots on his scalp along the suboccipital craniotomy incision. He also reported further decrease in his left-sided hearing along with increased tinnitus and fullness during this time period. A follow-up MRI demonstrated interval development of epidural air in the resection cavity and development of 2 fistulous tracks extending from the epidermoid tumor to the scalp. In addition, the imaging showed hair within the extradural cavity suggesting communication with the mastoid air cells. On examination, the patient had 2 areas along his left suboccipital incision with dried and crusted fluid. Based on these findings, the patient was planned for wound exploration and closure with a trapezius rotational flap. The previous incision was reopened, and the fistulous tracts were excised along with 4 cm $\times$ 2 cm section of flap that had 2 areas of hypergranulation tissue where the chronic infection had indurated through the scalp itself. The skin flap was carefully undermined revealing the cranial defect and the titanium plate, which was covered with exuberant granulomatous tissue beneath which was obvious pus. The plate was removed and pus was cultured. The pus was odiferous and was quite extensive in its range through the suboccipital region. It was thoroughly removed, and the bone edges of the previous craniectomy were freshened. The mastoid areas were exposed and there was no open mastoid air cell, but several air cells were exposed with their mucous membranes evident. With all of the pus removed and careful irrigation of the wound cavity, it was decided to obliterate this dead space with the fascial and muscle extensions of the trapezius flap. The fashioned flap extended distal to the insertion of the muscle to have a fasciocutaneous tongue that would be depepithelialized and tucked down into the mastoid air spaces. The flap was then raised on its vascular pedicle, turned 180° and inset to effectively obliterate the dead space. Postoperatively, the patient had uncomplicated recovery, and his flap and the donor site have completely healed (Fig. 3B). The trapezius flap has effectively prevented any wound leakage secondary to fistulous tracks from chronic infection.

DISCUSSION

The purpose of this study was to establish the trapezius myocutaneous flap as a reconstructive option for soft-tissue defect in posterior skull area. Such defects are generally secondary to tumor resection, which generally requires radiation. Irradiated wound bed and other coorbidities, generally present in these patients, would increase the postoperative complication rates of free tissue transfer. In addition, distant tissue transfer would not have similar skin color and texture as the locoregional flaps.[6] Free tissue transfer would require extended operative time exposing the patients to the complications of general anesthesia. Among locoregional flaps, pectoralis major and lattisimus dorsi-based myocutaneous flaps are considered "workhorse" flaps for head and neck reconstruction.[7,8] Pectoralis major-based flap is the first choice regional flap in head and neck surgery as it is easy to harvest and does not require repositioning for anterior reconstruction. However, use of pectoralis major flap might require repositioning of the patient for posterior skull reconstruction. In addition, it would be aesthetically unpleasing in women, and the amount of skin may be limited due to mobility of the breast on the underlying pectoralis musculature.[17] There is also a possibility of secondary contracture of the pedicle or gravitational displacement with time.[7] Lattisimus dorsi muscle flap will require extensive mobilization to reach the posterior skull, and function preservation might not be possible in some cases.

Trapezius myocutaneous flap has a large arc of rotation and is more pliable than both lattisimus dorsi and pectoralis major flaps.[18] As the upper portion of the muscle contains the spinal accessory nerve, which provides innervation to the entire muscle, the well-vascularized lower portion of the trapezius muscle is considered a dispensable unit. Use of the highly vascularized lower portion of the muscle serves to prevent the motor function of the muscle while providing an excellent reconstructive option. Trapezius muscle flap enables posterior skull reconstruction in prone position without the need to reposition the patient. The donor site can be primarily closed, and there is minimal donor-site-associated morbidities with this flap.

Trapezius flap has been described in the study for head and neck reconstruction,[16–24] but there are only few reports of its usage for posterior skull reconstruction.[25–27] The complication rate varies from 0% to 57% in the study with most of the studies showing a complication rate $<$20%.[16–24] A recently published study by Can et al[17] demonstrated 35% complication rates in a series of 43 consecutive patients operated for myocutaneous trapezius flap. Nine patients (21%) had recipient-site-related complications, but only 1 patient had a complete flap failure. Only 1 out of the 43 patients required flap for posterior skull reconstruction. In our series, there was no donor or recipient-site complication at a mean follow-up of 12.5 months.

Our study shows that the trapezius flaps can be effectively used for reconstruction of CSF leakage in the posterior skull. Among pedicled myocutaneous flap, pectoralis major has been described in 1 case report for CSF leakage,[28] but there has been no report of trapezius flap being used for this indication. Our second patient demonstrated complete healing of myocutnaeous flap in a patient with epidural abscess. There is another case report of 2 patients with epidural abscess who had complete recovery after debridement of the abscess cavity and obliterating the dead space with trapezius myocutaneous flap.[27]

Trapezius myocutaneous flap is a very safe and reliable option for posterior skull reconstruction, especially in a setting of hostile host environment such as infection or radiation. There is limited data related to reconstruction with this technique. With this study, we hope to establish trapezius myocutaneous flap as an alternative option for posterior skull reconstruction.

© 2015 Mutaz B. Habal, MD

CONCLUSION

The large angle of rotation coupled with the ability to complete the procedure without repositioning the patients makes trapezius myocutaneous flap an attractive option for posterior skull reconstruction. In our limited experience, the pedicled trapezius flaps are a reliable alternative as they are well vascularized and they are able to completely obliterate the soft-tissue defect. The evidence provided shows that the recipient site can heal completely despite an infected and irradiated wound bed. In addition, the donor site can be primarily closed with minimal complication. Finally, using our technique the accessory nerve and the motor function of the muscle can be preserved by using the highly vascularized lower portion of the muscle.

REFERENCES

1. Thorp BD, Sreenath SB, Ebert CS, et al. Endoscopic skull base reconstruction: a review and clinical case series of 152 vascularized flaps used for surgical skull base defects in the setting of intraoperative cerebrospinal fluid leak. *Neurosurg Focus* 2014;37:E4
2. Magliulo G, Sepe C, Varacalli S, et al. Cerebrospinal fluid leak management following cerebellopontine angle surgery. *J Otolaryngol* 1998;27:258–262
3. Sait M, Rahmathulla G, Chen TL, et al. Rare case of intracranial *Salmonella* enteritidis abscess following glioblastoma resection: case report and review of the literature. *Surg Neurol Int* 2011;2:149
4. Krijgh DD, Mureau MA. Reconstructive options in patients with late complications after surgery and radiotherapy for head and neck cancer: remember the deltopectoral flap. *Ann Plast Surg* 2013;71:181–185
5. Hofer SO, Mureau MA. Pedicled perforator flaps in the head and neck. *Clin Plast Surg* 2010;37:627–640
6. Mureau MA, Posch NA, Meeuwis CA, et al. Anterolateral thigh flap reconstruction of large external facial skin defects: a follow-up study on functional and aesthetic recipient- and donor-site outcome. *Plast Reconstr Surg* 2005;115:1077–1086
7. Van Rossen ME, Verduijn PV, Mureau MA. Survival of pedicled pectoralis major flap after secondary myectomy of muscle pedicle including transection of thoracoacromial vessels: does the flap remain dependent on its dominant pedicle? *J Plast Reconstr Aesthet Surg* 2011;64:323–328
8. Maves MD, Panje WR, Shagets FW. Extended latissimus dorsi myocutaneous flap reconstruction of major head and neck defects. *Otolaryngol Head Neck Surg* 1984;92:551–558
9. Demergasso F, Piazza MV. Trapezius myocutaneous flap in reconstructive surgery for head and neck cancer: an original technique. *Am J Surg* 1979;138:533–536
10. Baek SM, Biller HF, Krespi YP, et al. The lower trapezius island myocutaneous flap. *Ann Plast Surg* 1980;5:108–114
11. Tan KC, Tan BK. Extended lower trapezius island myocutaneous flap: a fasciomyocutaneous flap based on the dorsal scapular artery. *Plast Reconstr Surg* 2000;105:1758–1763
12. Mathes SJ, Nahai F. Classification of the vascular anatomy of muscles: experimental and clinical correlation. *Plast Reconstr Surg* 1981;67: 177–187
13. Ulrich D, Fuchs P, Pallua N. Preexpanded vertical trapezius musculocutaneous flap for reconstruction of a severe neck contracture after burn injury. *J Burn Care Res* 2008;29:386–389
14. Haas F, Weiglein AH. Trapezius flap. In: Wei FC, Mardini S, eds. *Flaps and reconstructive surgery.* Philadelphia: Saunders; 2009:249–269
15. Yang D, Morris SF. Trapezius muscle: anatomic basis for flap design. *Ann Plast Surgl* 1998;41:52–57
16. Can A, Orgill DP, Dietmar Ulrich JO, et al. The myocutaneous trapezius flap revisited: a treatment algorithm for optimal surgical outcomes based on 43 flap reconstructions. *J Plast Reconstr Aesthet Surg* 2014;67:1669–1679
17. Dinner MI, Guyuron B, Labandter HP. The lower trapezius myocutaneous flap for head and neck reconstruction. *Head Neck Surg* 1983;6:613–617
18. Uğurlu K, Ozçelik D, Hüthüt I, et al. Extended vertical trapezius myocutaneous flap in head and neck reconstruction as a salvage procedure. *Plast Reconstr Surg* 2004;114:339–350
19. Aviv JE, Urken ML, Lawson W, et al. The superior trapezius myocutaneous flap in head and neck reconstruction. *Arch Otolaryngol Head Neck Surg* 1992;118:702–706
20. Netterville JL, Panje WR, Maves MD. The trapezius myocutaneous flap. Dependability and limitations. *Arch Otolaryngol Head Neck Surg* 1987;113:271–281
21. Cummings CW, Eisele DW, Coltrera MD. Lower trapezius myocutaneous island flap. *Arch Otolaryngol Head Neck Surg* 1989;115:1181–1185
22. Chen WL, Zhang B, Wang JG, et al. Reconstruction of large defects of the neck using an extended vertical lower trapezius island myocutaneous flap following salvage surgery for neck recurrence of oral carcinoma. *J Plast Reconstr Aesthet Surg* 2011;64:319–322
23. Chen WL, Li J, Yang Z, et al. Extended vertical lower trapezius island myocutaneous flap in reconstruction of oral and maxillofacial defects after salvage surgeryfor recurrent oral carcinoma. *J Oral Maxillofac Surg* 2007;65:205–211
24. Chen WL, Deng YF, Peng GG, et al. Extended vertical lower trapezius island myocutaneous flap for reconstruction of cranio-maxillofacial defects. *Int J Oral Maxillofac Surg* 2007;36:165–170
25. Mathes SJ, Stevenson TR. Reconstruction of posterior neck and skull with vertical trapezius musculocutaneous flap. *Am J Surg* 1988;156:248–251
26. Lynch JR, Hansen JE, Chaffoo R, et al. The lower trapezius musculocutaneous flap revisited: versatile coverage for complicated wounds to the posterior cervical and occipital regions based on the deep branch of the transverse cervical artery. *Plast Reconstr Surg* 2002;109:444–450
27. Kiyokawa K, Tai Y, Inoue Y, et al. Surgical treatment for epidural abscess in the posterior cranial fossa using trapezius muscle or musculocutaneous flap. *Skull Base Surg* 2000;10:173–177
28. Suzuki S, Tanaka H, Koshima I. Reconstruction of cerebrospinal fluid leakage on the occipital region of the head with the pedicled pectoralis major myocutaneous flap. *Plast Reconstr Surg* 2011;128:17e–18e

Accurate Evaluation of Cone-Beam Computed Tomography to Volumetrically Assess Bone Grafting in Alveolar Cleft Patients

Wei-na Zhou, MD,[*†] *Yan-bin Xu, MD,*[*‡] *Hong-bing Jiang, PhD,*[*§] *Linzhong Wan, MD,*[*§] *and Yi-fei Du, MD*[*§]

From the [*]Jiangsu Key Laboratory of Oral Diseases; [†]Orofacial Pain and TMD Research Unit, Institute of Stomatology, Affiliated Hospital of Stomatology; [‡]The Research Institute of Stomatology, The Second Clinical Department, School of Stomatology; and [§]The Research Institute of Stomatology, Department of Oral and Maxillofacial Surgery, School of Stomatology, Nanjing Medical University, Nanjing, China.

Received February 9, 2015.

Accepted for publication June 28, 2015.

Address correspondence and reprint requests to Yi-fei Du, MD, The Research Institute of Stomatology, Department of Oral and Maxillofacial Surgery, School of Stomatology, Nanjing Medical University, 136 Hanzhong Road, Nanjing 210029, China;
E-mail: danxiangren2006@163.com

The authors report no conflicts of interest.

Copyright © 2015 by Mutaz B. Habal, MD

ISSN: 1049-2275

DOI: 10.1097/SCS.0000000000002034

Objective: The aim of this study was to investigate the accuracy of cone-beam computed tomography (CBCT) to assess the volume of bone graft in alveolar cleft patients.

Materials and Methods: Twelve patients of unilateral alveolar cleft were included in this study. All patients were taken CBCT preoperative and 1 week postoperative. The digital imaging and communications in medicine (DICOM) files were imported into Simplant software and three-dimensional (3D) reconstruction of the alveolar defect was achieved. With 3D volumetric measurements module, the volume of alveolar cleft was calculated preoperatively. During operation, the syringe compression method was adopted to calculate the actual amount of bone graft. One week postoperative, CBCT scan was performed again to measure the bone volume grafted to the defect. The volumetric ratio of the syringe compression method to preoperative CBCT assessment and the volume difference between syringe compression method and postoperative CBCT assessment were analyzed to evaluate the accuracy of CBCT measurement.

Results: The 3D structure of the alveolar cleft and the boundary of bone graft was clear from CBCT images. The estimated volume of alveolar cleft by preoperative CBCT scans was $1.06 \pm 0.09\,cm^3$, and the actual amount of bone graft determined by the syringe compression method was $1.51 \pm 0.12\,cm^3$. The ratio between the latter to the former was 1.43 ± 0.07. The calculated volume of bone graft by 1-week postoperative CBCT scans was $1.53 \pm 0.11\,cm^3$, with no significant difference compared with the actual amount of bone graft ($P > 0.05$).

Conclusions: CBCT was an accurate measurement to calculate the volume of alveolar defect and bone graft in alveolar cleft patients. Preoperative scans could aid in quantitatively determining the bone amount needed to adequately fill the bone defect, and the postoperative scans give accurate follow-up evaluation after surgery.

Key Words: Alveolar cleft, bone graft, CBCT, measurement accuracy

Alveolar cleft is a congenital disease caused by fusion obstacles between globular and maxillary processes in embryonic development. Patients of alveolar cleft are often accompanied with cleft lip and palate (CLP), resulting in varying degrees of physiological and psychological impact. These patients commonly need to undergo secondary alveolar bone graft (SABG) for reconstruction of the maxillary arch and to improve nasolabial basal collapse.[1] Preoperative assessment about the volume and the anatomical morphology of alveolar defect is essential to provide a successful surgery with a good outcome. Furthermore, postoperative radiographic follow-up to grasp the information of bone graft survival is vital to subsequent treatments such as orthodontics and dental implant.

Maxillary periapical and occlusal radiographs or panoramic films are the common clinical methods but with shortcomings to interpret because of the overlapping of complex osseous structure in two-dimensional (2D) radiographic images.[2,3] The development of computed tomography (CT) enables three-dimensional (3D) assessment of craniofacial structures and becomes a widely available means for head and neck diagnosis [4,5] and various oral surgical procedures.[6] However, CT is not the ideal diagnostic tool for the particular dental leision like alveolar cleft, and excessive radiation exposure with increased cost impedes the routine use of this technology for dental applications. Cone-beam computed tomography (CBCT) is an advanced imaging technology based on CT, especially in the application of craniofacial bone imaging. Compared with multislice CT (MSCT), CBCT has its unique advantages including low dose of radiation and high spatial resolution of bone tissue.[7–9] Over the past decade, CBCT has been widely used in dentomaxillofacial diseases including alveolar cleft. Recently, some scholars reported the use of CBCT on SABG surgery, mainly in a variety of risk factors on the survival of postoperative bone resorption.[10–15] There are fewer studies on accuracy of quantitative evaluation to alveolar cleft and bone graft, while it is important to SABG results.

The purpose of this study was to investigate the reliability of CBCT to estimate the volume of bone graft needed to adequately fill the alveolar cleft in patients with unilateral CLP and to evaluate the accuracy of volumetric measurements of bone graft after SABG surgery.

METHODS

The study was performed on 12 selected patients with unilateral alveolar cleft hospitalized in the Department of Oral and Maxillofacial Surgery of Stomatological Hospital affiliated to Nanjing Medical University from September 2011 to September 2012. Seven patients were male and 5 patients were female, aging from 8 to 12 years with the average of 10.2 years. All patients underwent SABG surgery with iliac cancellous bone graft by 1 surgeon and pre- and postoperative CBCT imaging (NewTom VGi, Quantitative Radiology Corporation, Verona, Italy) was taken for data analysis. CBCT radiation parameters were set 110 kV, 5 mA, with 3.6-s exposure and 0.2-mm scanning layer thickness.

The digital imaging and communications in medicine (DICOM) files were imported into Simplant software (11.04) and 3D reconstruction of the alveolar defect was achieved. 3D measurements were performed from coronal, sagittal, and horizontal levels (Fig. 1). With 3D volumetric measurement module, the volume of the alveolar cleft for each patient was calculated preoperatively. One week postoperative, CBCT scan was performed again to measure the bone volume grafted to the defect with the same protocol to preoperative. Pre- and postoperative imaging was marked with different colors.

According to preoperative CBCT prediction, the amount of iliac cancellous bone was determined during operation. Considering bone resorption, the bone mass during operation was appropriately increased about 50%.[16] To verify the accuracy of preoperative CBCT prediction, the actual amount of bone graft was calculated by the syringe compression method during operation (Fig. 2).

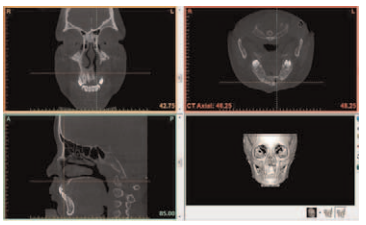

FIGURE 1. Three-dimensional and reconstructive images of cone beam computed tomography in alveolar cleft preoperative.

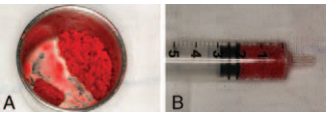

FIGURE 2. Iliac cancellous bone harvesting (A) and bone amount assessment by syringe compression method (B) during operation.

© 2015 Mutaz B. Habal, MD

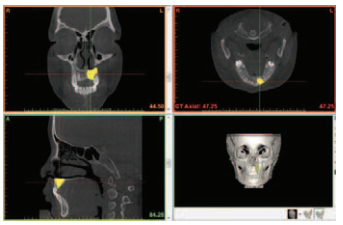

FIGURE 3. Three-dimensional drawing images of cone beam computed tomography preoperative.

The data were presented as means ± SD. The difference between the actual amount bone graft and postoperative CBCT estimate was analyzed with pair T-test. Statistical significance was set at $P < 0.05$.

RESULTS

The defect of alveolar cleft preoperative was marked with yellow color from coronal, sagittal, and horizontal levels of CBCT for each patient. The data of 3D measurements were collected to calculate the volume of the defect with Simplant software (Fig. 3). The boundary between grafted iliac cancellous bone and alveolar bone was clear from postoperative CBCT images (Fig. 4). The grafted bone was marked with green color and the volume was calculated (Fig. 5).

The data of alveolar cleft volume of each patient are shown in Table 1. The mean volume of alveolar defect by preoperative CBCT scans was $1.06 \pm 0.09\ cm^3$ and the mean actual bone amount by the syringe compression method was $1.51 \pm 0.12\ cm^3$. The average rate of actual amount during operation to volume of preoperative CBCT assessment was 1.43 ± 0.07. The mean volume of bone graft 1 week after operation was $1.53 \pm 0.11\ cm^3$ by postoperative CBCT scans. There was no significant difference between postoperative CBCT measurements of grafted bone volume and actual amount of bone graft (Fig. 6).

DISCUSSION

The radiographic scanning and reconstruction of the alveolar cleft lesions could provide characteristic details of anatomical structures, which directly influence the outcomes of SABG surgery and orthodontic intervention. Results from previous studies showed

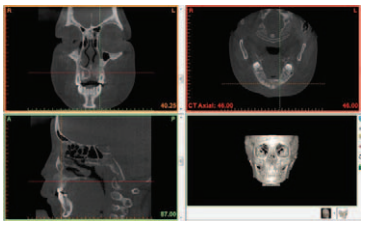

FIGURE 4. Three-dimensional images of cone beam computed tomography postoperative.

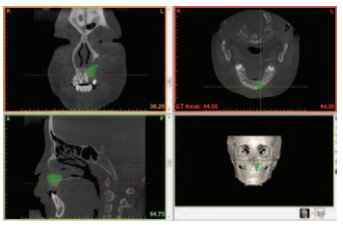

FIGURE 5. Three-dimensional drawing images of cone beam computed tomography postoperative.

TABLE 1. The Volume of Alveolar Cleft With CBCT and Syringe Compression Method Assessments

Case Number	Volume of Preoperative CBCT Assessment (cm^3)	Actual Amount With Syringe Compression Method (cm^3)	Volume of Postoperative CBCT Assessment (cm^3)
1	1.07	1.60	1.58
2	0.99	1.50	1.54
3	0.92	1.40	1.43
4	1.24	1.70	1.75
5	1.08	1.50	1.54
6	1.13	1.60	1.60
7	0.95	1.30	1.38
8	1.11	1.50	1.53
9	1.06	1.50	1.52
10	1.13	1.60	1.57
11	0.96	1.30	1.32
12	1.05	1.60	1.50

CBCT, cone-beam computed tomography.

that CBCT image quality was comparable and even superior in depicting delicate structures to that of MSCT.[9,17] The purpose of the current study was to assess the accuracy of CBCT scans on volumetric measurement in CLP patients. Our results showed that the average volume of bone defect in unilateral alveolar cleft was about $1\ cm^3$. This is clinically significant since it provided information to surgeons for harvesting iliac cancellous bone. Autologous iliac cancellous bone graft was first reported by Boyne and Sands in 1972 to repair alveolar cleft and was regarded as gold standard for SABG surgery.[1] Patients who underwent SABG surgery were usually at the age of 8–10 years, which was the key stage of growth and development. Although some authors reported low incidence of morbidity from harvesting cancellous bone from the anterior iliac crest in CLP patients,[18] less surgical trauma and short operation time were benefit to recovery from SABG surgery.[19,20] In this study, the volume of the alveolar defect area could be calculated preoperatively which could accurately predict bone mass for filling the defect before surgery. Therefore, it could reduce the unnecessary injury and also shorten the operation time by taking needful amount of iliac cancellous bone. Furthermore, the data showed that the average volume ratio of actual bone amount by the syringe compression method to preoperative CBCT prediction was 1.43 ± 0.07, indicating that grafted bone mass was on average 43% more than the preoperative prediction. This result basically met the requirements of appropriate increase of about 50% in bone mass in case of graft bone resorption postoperative.[16]

The visual assessment of 3D reconstruction of alveolar cleft made the performer have a better understanding of bony structure in contrast with clinical examination. It was clarified that the use of intraoral radiographs was inadequate in assessing the bone graft

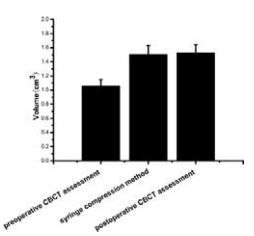

FIGURE 6. The average volume of alveolar cleft and bone graft.

© 2015 Mutaz B. Habal, MD

results and could underestimate the level of bone support of teeth.[2,3,21] CT scan, with high radiation dose, went beyond the maximum risk threshold for the medical radiation exposure, particularly to a pediatric patient. CBCT offered an alternative approach with short scanning time and reduced radiation dose up to 15 times lower than multislice CT scans (MSCT).[7] Many studies were reported to evaluate the clinical outcome of patients undergoing SABG surgery. Oberoi et al[12] found after SABG surgery, most canines on both the cleft and noncleft sides moved incisally, facially, and mesially. In patients with BCLP in the mixed dentition, Garib et al[14] identified teeth adjacent to the alveolar cleft were covered by a thin alveolar bone plate, although the level of alveolar bone crest around these teeth seemed to be normal with no bone dehiscence. From comparing the CBCT images before and 6 months after SABG surgery, Suomalainen et al revealed that the resorption of the bone graft was observed mostly in the apical and palatal areas of the defect.[15] For enabling quantitative assessment, Quereshy et al[20] used CBCT to calculate the estimated volume of the alveolar cleft by measuring facial width, facial height, and facial–palate length of defect. By 3D reconstruction of the bone grafts with limited CBCT scans, Zhang et al[13] proposed a protocol to obtain a valuable objective assessment of the graft volume. These studies showed CBCT was a promising method for the evaluation of the alveolar bone grafts. However, few studies concerned about the accuracy of CBCT for volumetric measurements. Kasaven et al[22] first studied the validity of CBCT for calculating volume and found 3D volumetric measurement using i-CAT CBCT scans was similar to the volumes determined by micro-CT in a simulated maxillary alveolar bone defect model. The complexity of 3D structures in patients with CLP was challenging for assessing the volumetric measurement of bone defect. In this study, we calculated the actual amount of bone graft by the syringe compression method during SABG surgery. One week after the surgery, before bone resorption occurs, the CBCT was performed again and the volume of bone graft was estimated using 3D volumetric measurements with Simplant software. The data showed no statistical difference between these 2 volumetric results. On this basis, our study confirmed the accuracy of CBCT for quantitative volumetric analysis in patients with alveolar cleft.

Sufficient bony bridge in patients with CLP was essential to attain orthodontic repositioning and alignment of maxillary teeth. Occasionally, the teeth laterally adjacent to alveolar cleft could loose and even fall off in orthodontic treatment due to bone resorption of the reconstructive alveolus after SABG surgery.[23] Therefore, the precisely postoperative evaluation of bone survival amount was vital to the process of subsequent treatment. Feichtinger et al reported about 51% bone loss over a period of 1 year after bone graft based on CT scans.[16] Zhang et al used limited CBCT apparatus in 1- and 6-month postoperative and separated patients into 2 groups (with or without eruption of the cleft-adjacent teeth into the graft) for analysis. In patients who had eruption of the cleft-adjacent teeth into the graft, the resorption rate was 10.4%, significantly lower than 36.6% in patients who did not.[13] In the current study, CBCT could clearly display the boundaries of the graft bone around alveolar cleft but the data of the bone resorption were not obtained because of follow-up reasons. It was the shortcoming of this preliminary study and needed to make up in further investigations.

In conclusion, CBCT imaging could be used to accurately calculate the volume of alveolar clefts and grafted bone. This could be of great benefit to SABG surgery by quantitatively predicting the amount of bone necessary to repair the void. Preoperative CBCT imaging analysis would decrease morbidity by allowing clinicians to have more information about the morphology of the defect in complex cases of alveolar clefts. Postoperative CBCT imaging analysis could aid in subsequent orthodontic treatment, making a better overall outcome.

REFERENCES

1. Boyne PJ, Sands NR. Secondary bone grafting of residual alveolar and palatal clefts. *J Oral Surg* 1972;30:87–92
2. Liang X, Jacobs R, Lambrichts I. Appearance, location, course and morphology of the superior and inferior genial spinal foramina and their bony canals: an assessment on spiral CT scan. *Surg Radiol Anat* 2006;28:98–104
3. Pohlenz P, Blessmann M, Blake F, et al. Major mandibular surgical procedures as an indication for intraoperative imaging. *J Oral Maxillofac Surg* 2008;66:324–329
4. Fuchs T, Kachelriess M, Kalender WA. Technical advances in multi-slice spiral CT. *Rev Eur J Radiol* 2000;36:69–73
5. Bou Serhal C, Jacobs R, Flygare L, et al. Perioperative validation of localisation of the mental foramen. *Dentomaxillofac Radiol* 2002;31:39–43
6. Sarment DP, Sukovic P, Clinthorne N. Accuracy of implant placement with astereolithographic surgical guide. *Int J Oral Maxillofac Implants* 2003;18:571–577
7. Scarfe WC, Farman AG, Sukovic P. Clinical applications of cone-beam computed tomography in dental practice. *J Can Dent Assoc* 2006;72:75–80
8. De Vos W, Casselman J, Swennen GR. Cone-beam computed tomography (CBCT) imaging of the oral and maxillofacial region: a systematic review of the literature. *Int J Oral Maxillofac Surg* 2009;38:609–625
9. Liang X, Jacobs R, Hassan B, et al. A comparative evaluation of cone beam computed tomography (CBCT) and multi-slice CT (MSCT) Part I. On subjective image quality. *Eur J Radiol* 2010;75:265–269
10. Hamada Y, Kondoh T, Noguchi K, et al. Application of limited cone beam computed tomography to clinical assessment of alveolar bone grafting: a preliminary report. *Cleft Palate Craniofac J* 2005;42:128–137
11. Oberoi S, Chigurupati R, Gill P, et al. Volumetric assessment of secondary alveolar bone grafting using cone beam computed tomography. *Cleft Palate Craniofac J* 2009;46:503–511
12. Oberoi S, Gill P, Chigurupati R, et al. Three-dimensional assessment of the eruption path of the canine in individuals with bone-grafted alveolar clefts using cone beam computed tomography. *Cleft Palate Craniofac J* 2010;47:507–512
13. Zhang W, Shen G, Wang X, et al. Evaluation of alveolar bone grafting using limited cone beam computed tomography. *Oral Surg Oral Med Oral Pathol Oral Radiol* 2012;113:542–548
14. Garib DG, Yatabe MS, Ozawa TO, et al. Alveolar bone morphology in patients with bilateral complete cleft lip and palate in the mixed dentition: cone beam computed tomography evaluation. *Cleft Palate Craniofac J* 2012;49:208–214
15. Suomalainen A, Aberg T, Rautio J, et al. Cone beam computed tomography in the assessment of alveolar bone grafting in children with unilateral cleft lip and palate. *Eur J Orthod* 2014;36:603–611
16. Feichtinger M, Zemann W, Mossböck R, et al. Three dimensional evaluation of secondary alveolar bone grafting using a 3D-navigation system based on computed tomography: a two-year follow-up. *Br J Oral Maxillofac Surg* 2008;46:278–282
17. Ito K, Gomi Y, Sato S, et al. Clinical application of a new compact CT system to assess 3-D images for the preoperative treatment planning of implants in the posterior mandible A case report. *Clin Oral Implants Res* 2001;12:539–542
18. Baqain ZH, Anabtawi M, Karaky AA, et al. Morbidity from anterior iliac crest bone harvesting for secondary alveolar bone grafting: an outcome assessment study. *J Oral Maxillofac Surg* 2009;67:570–575
19. Cho-Lee GY, García-Díez EM, Nunes RA, et al. Review of secondary alveolar cleft repair. *Ann Maxillofac Surg* 2013;3:46–50
20. Quereshy FA, Barnum G, Demko C, et al. Use of cone beam computed tomography to volumetrically assess alveolar cleft defects-preliminary results. *J Oral Maxillofac Surg* 2012;70:188–191
21. Zybutz M, Rapoport D, Laurell L, et al. Comparisons of clinical and radiographic measurements of inter-proximal vertical defects before and 1 year after surgical treatments. *J Clin Periodontol* 2000;27:179–186

© 2015 Mutaz B. Habal, MD

22. Kasaven CP, Ivekovic S, McIntyre GT, et al. Validation of the volumetric measurement of a simulated maxillary alveolar bone defect using cone-beam computed tomography. *Cleft Palate Craniofac J* 2013;50:e115–e120
23. Toscano D, Baciliero U, Gracco A, et al. Long-term stability of alveolar bone grafts in cleft palate patients. *Am J Orthod Dentofacial Orthop* 2012;142:289–299

Mandibular Reconstruction Based on the Concept of Double Arc Reconstruction

Shunji Sarukawa, MD, Tadahide Noguchi, DDS,† Hideaki Kamochi, MD, DDS,* Ataru Sunaga, MD,* Hirokazu Uda, MD,* Hiroshi Nishino, MD,‡ and Yasushi Sugawara, MD**

Abstract: The natural mandible has 2 arcs, the marginal arc and the occlusal arc. The marginal arc is situated along the lower margin of the mandible and affects the contour of the lower third of the face. The occlusal arc is situated along the dental arc and affects the stability of prosthodontics. The gap between these 2 arcs widens in the molar area. Our developed concept of ''double arc reconstruction'' involves making these 2 arcs for the reconstructed mandible. For the double-barrel fibula reconstruction, 2 bone segments are used to make both arcs. For reconstructions using the iliac crest, the double arc is made by inclination of the top of the bone graft toward the lingual side. Ten patients underwent double arc reconstruction: 2 underwent reconstruction with the double-barrel fibula, and 8 underwent reconstruction with the iliac crest. Four patients had a removable denture prosthesis, 1 had an osseointegrated dental implant, and 5 did not require further prosthodontic treatment. The shape of the reconstructed mandible after double arc reconstruction resembles the native mandible, and masticatory function is good with the use of a dental implant or removable denture prosthesis, or even without prosthodontics.

Key Words: Mandible, mouth neoplasm, reconstructive surgical procedures, tissue transplantation

Occlusal rehabilitation is one of the most important goals of mandibular reconstruction. Advances in rehabilitation have been made with the combined use of the vascularized bone-containing free flap (VBCFF) and osseointegrated dental implant.[1] Many recent reports, however, describe only the implantation of the osseointegrated dental implant, and the shape and lining of the reconstructed mandible has not been discussed sufficiently, despite its importance for the stability of prosthodontics.

The principles that relate to the bony shape of the reconstructed mandible are bridging, contour, and alveolar height.[2] If we do not consider the three-dimensional relationship of these 3 elements, the reconstructed mandible cannot function as a good foundation for stable prosthodontics. In this article, we describe a new concept for reconstructing the bony shape of the mandible, namely, ''double arc reconstruction.''

METHODS

Surgical Procedure

The natural mandible has 2 horizontal arcs, the marginal arc and the occlusal arc (Fig. 1). The marginal arc is situated along the lower margin of the mandible and affects the contour of the lower third of the face—it can be said to represent the "aesthetic arc." The occlusal arc follows the dental arc and affects the stability of prosthodontics—it can represent the "functional arc." These 2 arcs are separated widely in the molar area.

Many reports describe reconstruction of the marginal arc only, but reconstruction of the occlusal arc that fits the dental arc of the maxilla is necessary for stable prosthodontics, especially in the case of L or H defects of the HCL classification[3] that include the molar area. The concept of double arc reconstruction involves surgical procedures that reconstruct these 2 arcs.

There are 2 surgical procedures that can achieve double arc reconstruction. One is the double-barreled fibula[4] approach (Fig. 2). Two bony segments are used to make each arch: the lower segment is positioned conventionally along the marginal arc and the upper segment is positioned along the occlusal arc. The posterior stump of the upper segment is positioned toward the lingual side, so it does not make contact with the stump of the mandibular ramus. Thus, it cannot function as a bridging segment in cases of a molar area defect with preservation of the posterior margin of the mandibular ramus.

The second surgical procedure is the iliac crest[5] approach (Fig. 3). The upper stump of the bone graft is inclined toward the lingual side: the lower margin of the graft corresponds to the marginal arc and the upper margin corresponds to the occlusal arc. Accordingly, the plane of the posterior stump of the graft does not fit the lateral plane of the mandibular ramus.

FIGURE 1. Double arc of the natural mandible. Blue line indicates the "marginal (aesthetic) arc" that is situated along the lower margin of the mandible. Yellow line indicates the "occlusal (functional) arc" that is situated along the dental arc.

FIGURE 2. Double arc reconstruction with the double-barrel fibula. The posterior stump of the upper segment is positioned toward the lingual side, so it does not make contact with the stump of the mandibular ramus.

From the *Department of Plastic Surgery; †Department of Dentistry, Oral and Maxillofacial Surgery; and ‡Department of Otolaryngology, Head and Neck Surgery, Jichi Medical University, Yakushiji, Shimotsuke, Tochigi, Japan.
Received February 20, 2015.
Accepted for publication June 28, 2015.
Address correspondence and reprint requests to Shunji Sarukawa, MD, Department of Plastic Surgery, Jichi Medical University, 3311-1 Yakushiji, Shimotsuke, Tochigi 329-0434, Japan;
E-mail: fwkc8662@nifty.com
The authors report no conflicts of interest.
Copyright © 2015 by Mutaz B. Habal, MD
ISSN: 1049-2275
DOI: 10.1097/SCS.0000000000002035

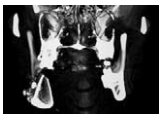

FIGURE 3. Double arc reconstruction with the iliac crest. The plane of the posterior stump of the graft does not match the lateral plane of the mandibular ramus.

Other major bone grafts such as the single fibula[6] and scapular flap[7] approaches cannot create a sufficiently high alveolus for double arc reconstruction.

Patients

Of the 27 patients who underwent segmental mandibulectomy and reconstructive surgery between May 2011 and March 2013, 10 underwent double arc reconstruction and were followed for 1 year postoperatively (Table 1). The details of the other 17 patients are as follows: 5 patients died within 1 year postoperatively, 7 had reconstruction with a single fibula, 1 underwent reconstruction with the scapula, 1 underwent reconstruction with soft tissue only, 1 had graft loss, 1 did not have a defect that included the molar area, so the double arc reconstruction was not needed, and 1 had a condyle defect so reconstruction of the condyle took priority and an occlusal arc could not be made.

The mandibular defects of the 10 patients who underwent double arc reconstruction consisted of 9 L defects and 1 H defect as determined by the HCL classification. Eight patients underwent immediate reconstruction after malignant tumor extirpation and the remaining 2 had experienced osteoradionecrosis. The grafts were 2 double-barreled fibulas and 8 iliac crests. The covering procedures of the reconstructed alveolus involved 4 direct closures, 4 skin paddles, and 2 bare bone grafts.[8] No patient became completely edentulous just after reconstruction.

RESULTS

There were no patients of graft loss or major complications. Occlusal rehabilitation at 1 year postoperatively was as follows: 4 patients had a removable denture prosthesis, 1 had an osseointegrated dental implant, and 5 did not require further prosthodontic treatment as they did not have any functional disturbance of mastication and no aesthetic problems. The occlusal contacts on the healthy side in all the patients who did not require prosthodontics were completely preserved, enabling them to masticate without any dietary restrictions.

PATIENT PRESENTATIONS

Patient 2

An 80-year-old patient was diagnosed with squamous cell carcinoma of the left lower alveolus (T4aN1) and underwent immediate mandibular reconstruction with a vascularized fibula osteocutaneous flap following left segmental mandibulectomy and ipsilateral supraomohyoid neck dissection. The mandible was reconstructed with double-barreled fibula bone, and the oral lining was covered by a skin paddle. The upper segment of the fibula graft was positioned toward the lingual side along the occlusal arc (Fig. 4). The postoperative course was uneventful and no adjuvant therapy was given. Secondary alveoloplasty with thinning of the skin paddle covering the reconstructed alveolus was performed under local anesthesia 6 months after reconstructive surgery, and a removable denture prosthesis was applied 3 months after revision surgery (Fig. 5). As of 2 years after the initial surgery, there has been no tumor recurrence and the patient maintains an unrestricted diet because of the presence of a complete maxillary denture.

Patient 3

A 63-year-old patient was diagnosed with squamous cell carcinoma of the left lower alveolus (T2N2b) and underwent immediate mandibular reconstruction with a vascularized iliac crest osteocutaneous flapas a bare bone graft following left segmental mandibulectomy and left type II modified radial neck dissection. The skin paddle was de-epithelialized and used for soft tissue augmentation of the submandibular space and the lateral neck. The double arc was reconstructed with inclination of the upper stump of the bone graft toward the lingual side along the occlusal arc (Fig. 6). The intraoral defect underwent healing by secondary intention within 3 months of surgery. A removable partial denture prosthesis was fitted 1 month after surgery without the need for revision surgery (Fig. 7). As of 1 year after the initial surgery, the patient can eat almost any foods.

DISCUSSION

Recent advances in the VBCFF technique have enabled reconstructive surgeons to make various bony shapes, even for mandibular

TABLE 1. Patient Characteristics and Results

Patient	Age	Cause of Mandibular Defect	Graft	Oral Lining	HCL Classification	Length of Defect (mm)	Adjuvant Therapy	Prosthodontics	No. of remaining mandibular teeth	Follow-up period (months)
1	79	Malignancy	Double-barreled fibula	Secondary intention	L	55	–	Denture	9	25
2	80	Malignancy	Double-barreled fibula	Skin paddle	L	55	–	Denture	4	24
3	63	Malignancy	Iliac crest	Secondary intention	L	90	–	Denture	6	18
4	64	Malignancy	Iliac crest	Secondary intention	L	50	–	Denture	9	10
5	66	Malignancy	Iliac crest	Direct closure	L	55	RT 60 Gy	Not required	9	24
6	61	Osteoradionecrosis	Iliac crest	Direct closure	H	70	–	Not required	11	19
7	51	Malignancy	Iliac crest	Direct closure	L	55	–	Implant	10	12
8	78	Malignancy	Iliac crest	Skin paddle	L	60	RT 60 Gy	Not required	10	18
9	50	Osteoradionecrosis	Iliac crest	Skin paddle	L	50	–	Not required	10	18
10	76	Malignancy	Iliac crest	Skin paddle	L	90	–	Not required	5	18

RT, radiotherapy; Gy, gray.

© 2015 Mutaz B. Habal, MD

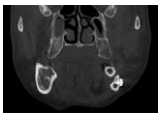

FIGURE 4. Coronal computed tomography image 3 months after surgery (patient 2).

FIGURE 5. One year after surgery (patient 2). Intraoral view after fitting is movable denture prosthesis.

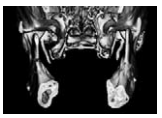

FIGURE 6. Three-dimensional computed tomography image 6 months after surgery (patient 3).

FIGURE 7. One year after surgery (patient 3). Intraoral view after fitting is movable denture prosthesis.

FIGURE 8. Coronal computed tomography image of a patient with mandible reconstruction using the double-barrel fibula, which did not follow the double arc reconstruction concept.

reconstruction. In particular, use of the vascularized iliac crest, which has sufficient bone quantity, results in a reconstructed mandible that is almost the same as the natural mandible, albeit dentulous. The concept of double arc reconstruction can be used to guide the reconstructive procedure to create a more functional and aesthetic mandibular shape.

The principles of mandibular reconstruction are bridging, which is needed to stabilize the jaw position while maintaining mobility, contour, which is required for the aesthetics of the lower third of the face, and alveolar height, which is required to keep the prosthodontics stable. If the double-barreled fibula or iliac crest is used to achieve alveolar height without employing double arc reconstruction, the graft may be positioned along the plane of the mandibular ramus, the top of the graft may not fit the maxillary dental arch and may be buried in the buccal mucosa (Fig. 8), and functional prosthodontics may be very difficult or impossible to achieve.[9,10] To reconstruct an effective high alveolus, application of the double arc reconstruction concept is required.

Double arc reconstruction using either the double-barrel fibula or iliac crest has 2 disadvantages compared with the single fibula, which is probably the most popular VBCFF for mandibular reconstruction. These disadvantages restrict the surgical indication. The first consideration is the length of the vascular pedicle. The vascular pedicle of both the double-barrel fibula and iliac crest is about 6 cm in many patients, so recipient vessels that can reach the pedicle in the ipsilateral upper neck are needed in patients without vascular interposition. The second consideration is the size of the graft. The length of the defect for reconstruction is limited to 10 cm when the double-barrel fibula is used and 12 cm when the iliac crest is used.

Two requirements for double-arc reconstruction are the existence of usable recipient vessels in the ipsilateral upper neck and a defect that is smaller than 10 cm when the double-barrel fibula is used or smaller than 12 cm when the iliac crest is used. In patients in whom double arc reconstruction is not indicated, we use a single fibula and make only the marginal arc with aesthetics as a priority, although Smolka[11] reported a procedure that created only the occlusal arc with a single fibula.

In addition to the bony shape, the condition of the oral lining affects the stability and reliability of prosthodontics. A tight covering such as the natural gingival mucosa is appropriate, whereas a bulky skin paddle with thick subcutaneous adipose tissue is not. For the intraoral covering, we perform 3 procedures: direct closure of the preserved mucosa; a bare bone graft (healing of the naked bone graft by secondary intention); and a skin paddle. The reconstructed alveolus after direct closure in many patients following extirpation of a malignant lesion is covered by the buccal mucosa and floor of the mouth mucosa (both mobile mucosa), so direct closure is not suitable for prosthodontics. In contrast, the reconstructed alveolus following a bare bone graft has a tight mucosa-like covering that is suitable for prosthodontics. Almost all of our patients could be fitted with a removable denture prosthesis without revision surgery after a bare bone graft. However, this procedure cannot be adapted for patients who are scheduled for adjuvant radiotherapy because complete wound healing might take more than 3 months in some patients.[8] For this reason, we perform direct closure or use a skin paddle covering for some alveolar defects. In such patients, we recommend secondary vestibuloplasty with/without defatting and a split-thickness skin graft, although few patients accept the revision surgery because they are unwilling to undergo additional surgery after the initial invasive surgery for their malignancy.

Half of our patients with double arc reconstruction did not require prosthodontics. Prosthodontics contributes to masticatory function and aesthetics, and the lack of teeth in the ipsilateral molar area does not markedly affect function and aesthetics. Following double arc reconstruction, the high alveolus influences masticatory function by dividing the intraoral space into the tongue space and buccal space. If the reconstructed alveolus in the molar area is low, a bolus cannot be held in the tongue space and masticatory function is therefore poor.

The osseointegrated dental implant produces good results for patients after mandibular reconstruction. Again, not many patients accept osseointegration surgery, so we have to consider a removable denture prosthesis or no prosthodontics. Reconstruction of the mandible with a natural shape remains one of the solutions.

REFERENCES

1. Anne-Gaelle B, Samuel S, Julie B, et al. Dental implant placement after mandibular reconstruction by microvascular free fibula flap: current knowledge and remaining questions. *Oral Oncol* 2011;47:1099–1104
2. Urken ML. Composite free flaps in oromandibular reconstruction. *Arch Otolaryngol Head neck Surg* 1991;117:724–732
3. Boyd JB, Gullane PJ, Rostein LE, et al. Classification of mandibular defects. *Plast Reconstr Surg* 1993;92:1266–1275
4. Jones NF, Swarz WM, Mears DC, et al. The "double barrel" free vascularized fibular bone graft. *Plast Reconstr Surg* 1988;81:378–385
5. Taylor GI, Townsend P, Corlett R. Superiority of the deep circumflex iliac vessels as the supply for free groin flaps. *Plast Reconstr Surg* 1979;64:745–759
6. Hidalgo DA. Fibula free flap: a new method of mandible reconstruction. *Plast Reconstr Surg* 1989;84:71–79

© 2015 Mutaz B. Habal, MD

7. Swarz WM, Banis JC, Newton ED, et al. The osteocutaneous scapular flap for mandibular and maxillary reconstruction. *Plast Reconstr Surg* 1986;77:530–545
8. Sarukawa S, Noguchi T, Oh-iwa I, et al. Bare bone graft with vascularized iliac crest for mandibular reconstruction. *J Craniomaxillofac Surg* 2012;40:61–66
9. Ch'ng S, Ashford BG, Clark JR. Alignment of the double barreled fibula free flap for better cosmesis and bone height for osseointegrated dental implants. *Plast Reconstr Surg* 2013;132:e688–e689
10. Ohyama T, Toyama H, Nagai E, et al. Effectiveness of surgical template for dental implants placed in bone graft. *J Prosthodont Res* 2009;53:146–149
11. Smolka K, Kraehenbuehl M, Eggensperger N, et al. Fibula free flap reconstruction of the mandible in cancer patients: evaluation of a combined surgical and prosthodontics treatment concept. *Oral Oncol* 2008;44:571–581

Association of a Subperiosteal Hematoma With Minor Injury

Yukinori Akiyama, MD, PhD,† Masafumi Ohtaki, MD,† Sangnyon Kim, MD,† Yuusuke Kimura, MD,† and Nobuhiro Mikuni, MD**

Abstract: An intraorbitalsubperiosteal hematoma is a rare clinical entity that is usually caused by head trauma. The authors experienced a patient involving an intraorbital hemorrhage that was associated with minor injury in the forehead and that required surgical decompression. The authors describe this rare case involving an intraorbitalsubperiosteal hematoma that occurred in a conscious young boy who had no remarkable head injury and who had sudden onset of proptosis. Three-dimensional computed tomography, which was conducted with a volume-rendering method, was very useful, and the transorbital approach that was used to remove the hematoma was very effective. The patient showed good recovery. The pathogenesis of the intraorbitalsubperiosteal hemorrhage could not be fully explained, and, thus, the authors suggest that a possible pathogenesis involved the migration of the hemorrhage from the forehead into the intraorbital region.

Key Words: Intraorbital, minor trauma, subperiosteal hematoma

CLINICAL PRESENTATION

A 1-year-old boy was admitted to our hospital with a 3-day history of deteriorating frontal subcutaneous effusion with right-eyelid swelling, disturbances in his right-eye movement, and a lower deviation of his right-eye position. The right eye was grossly proptotic with inferolateral dystopia, eyelid swelling, and an afferent papillary defect. Visual acuity could not be examined because of the patient's age. His right-eye pupil was sluggishly reactive to light.

There was no major head or orbital injury. The patient's mother did not recognize any definite trauma involving her son. The patient's mother noticed his abnormal face appearance 3 days before admission. The facial swelling had been slowly growing for 3 days. A pediatrician investigated patient's mother in detail if there was abuse or not. The pediatrician concluded there was no abuse at this time. The patient had grown normally on the growth curve, except for his verbal or mental growth. The patient could not complain of anything because of his verbal growth abnormality.

A computed tomography (CT) scan demonstrated an abnormal area of high density from the forehead to the intraorbital space. The density of the hematoma in the forehead and orbit was comparatively low, and high, respectively. The abnormally dense area did not cross over the coronal suture. A skull X-ray showed no remarkable fractures or any bone abnormalities. The patient seemed not to experience pain during a touch test to the forehead. The author felt fluid collection in the skull, but when compression was done, the fluid collection did not disappear. This ruled out a sinus pericranium. The sagittal view of an MRI scan showed a right subperiosteal hematoma in the orbit and forehead. Thus, a right orbital hyperdense fluid collection was pushing on the eyeball inferiorly.

Operation: an operation was conducted on the patient because his eyeball and optic nerve were compressed and deviated by the hematoma in the orbit. A 5-mm straight incision was performed on the right eyebrow. The hematoma was evacuated, and the eyeball was decompressed. A property of the hematoma in the forehead and the orbit was comparatively liquid and solid, respectively. The tension of the skin decreased immediately after the evacuation. The pressure of the hematoma in the orbit was much higher than that of the hematoma in the forehead.

Postoperative course: after the operation, the proptosis improved. The patient's ocular movements continued to improve within the following 3 days. On the 7th postoperative day, ocular movements were greatly improved, and the proptosis and papilledema had disappeared (Fig. 1). He was discharged on the 14th day after admission.

DISCUSSION

An intraorbitalsubperiosteal hematoma is a rare clinical entity that is usually caused by head trauma.[1,2] Magnetic resonance imaging (MRI) and CT scans have revealed subperiorbital hematomas that originated from the frontal skull bone. Intraorbital hematomas without any definite causes have been reported.[3,4] In those studies, surgical removal of the hematomas was performed, and histopathological examinations revealed organized hematomas without any evidence of tumor or vascular anomalies. Intraorbitalsubperiorbital hematomas that are associated with minortrauma are extremely rare, with only a few patients reported in the literature. Most intraorbital hemorrhage patients require surgical or endoscopic decompression because of a persistent mass effect in spite of medical treatment that does not relieve the clinical symptoms. In this patient, it was necessary to decompress by open surgery because the hematoma was slowly growing and the property of the hematoma was solid which could absorb very slowly and it was hard to evacuate by only a needle.

The causes of hemorrhages in the orbit may be divided into the following 3 main groups: spontaneous, traumatic, and congestive, which are due to thoracic trauma with resulting increased venous

From the *Department of Neurosurgery, Sapporo Medical University School of Medicine, Sapporo; and †Department of Neurosurgery, Obihiro Kosei Hospital, Obihiro, Japan.
Received February 25, 2015.
Accepted for publication June 28, 2015.
Address correspondence and reprint requests to Yukinori Akiyama, MD, PhD, Department of Neurosurgery, Sapporo Medical University School of Medicine, S1 W16 Chuo-ku Sapporo, Hokkaido 060-8543, Japan; E-mail: akiyuki@sapmed.ac.jp
The author reports no conflicts of interest.
Copyright © 2015 by Mutaz B. Habal, MD
ISSN: 1049-2275
DOI: 10.1097/SCS.0000000000002036

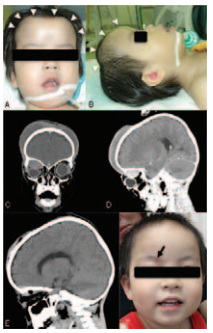

FIGURE 1. Photograph showing frontal and eyelid swelling (arrowheads) with the deviation of the right-eye position (A and B). A reconstructed view of the coronal and sagittal computed tomography (CT) scans show subperiosteal effusion on the skull bone and that the hematoma invaded the subperiorbital space. The superior rectus muscle was compressed toward the eyeball, and the eyeball was indirectly compressed by the hematoma (C and D). Postoperative sagittal CT scan showing the decreased size of the hematoma in the frontal and intraorbital regions (E). A photograph shows the improved face appearance 1 month after the operation. An arrow demonstrates the surgical skin incision that was made on the eyebrow (F). The patient's symptoms gradually improved, and the hematoma disappeared.

pressure in the jugular vein.[5] In this patient, there was no definite history of head or orbital injury, but we believe that the patient might have received unrecognized trauma to his forehead. Intraorbital hematomas following minor head trauma with no evidence of bone fracture have rarely been reported. Kuban et al[6] described a subgaleal hematoma that developed between 1 and 8 days following minor head trauma in 4 children and in 2 infants. Although the patient experienced no remarkable strong injury, the skin might have been abraded, and arterial bleeding could have occurred. At younger ages, the connection between bone and the pericranium is very weak, and it might be easy for it to be abraded. On the other hand, a trauma in the forehead might cause an orbital bone strain or distortion, which occur an intraorbitalbleeding instead of subgalealhematom in the forehead. We found that the tension of the skin on the forehead was low. However, the tension in the hemorrhagic fluid in the orbit was high during the operation. We suggest that, somehow, there was a backwater valve between the subperiosteum in the forehead and the orbit, possible due to a sharp angle between the forehead and the orbital roof. In other words, the reason why the tension in the intraorbital hematoma was high was that the hematoma migrated into the orbit unidirectionally. Although the angle between the frontal cranium and the orbital roof is sharp, it can be abraded and the hematoma can migrate from one to another. It was also suggested by CT density and hematoma tension that intraorbital hematoma occurred first and migrate to the forehead, following the 2 hematomas were divided somehow because of sharp angle between the forehead and orbital roof. In addition, the hematoma in the orbit continued to grow continuously, which cause high tension of the hematoma in the orbit.

We would like to emphasize that it is important to be careful in the treatment of injuries of frontal pericranial hematomas, especially in patients of younger ages or with mental retardation because the patients might not be able to complain about his or her symptoms, such as diplopia or pain.

Surgical treatment was performed on the patient, and his symptoms improved. Only a small incision was needed during the surgery to evacuate both the intraorbital and forehead hematomas.

We have described in this report a patient involving an intraorbital hematoma. CT and MRI scans of the brain supported the finding that the lesion was a hematoma in the orbit. However, any definite causes were not found in our patient, and the hematoma in his forehead suggested that there might have been a minor injury to his forehead. The increased intraorbital pressure might have obstructed venous drainage, which deteriorated the increasing intraorbital pressure, resulting in a vicious circle.

Some authors have reported subperiorbital hematomas that were related to head injuries, and invasive surgical treatments were performed to treat these patients. However, is it necessary to treat young patients with invasive surgical treatments, such as bifrontal incisions and very large exposure of the skull? We believe that the hematoma in the orbit came from the frontal bone, and even the optic nerve was compressed and deviated by the hematoma. Only a small skin incision and evacuation of the hematoma was necessary without any treatment of the hemorrhage origin because the compression was effective to stop the bleeding from the frontal bone easily.

CONCLUSION

This article illustrated an unusual presentation of a subperiosteal hematoma in the orbit, which was possibly related to a minor injury. In this patients, only a small incision was needed during the surgery to evacuate both the intraorbital and forehead hematomas. The results were satisfactory.

REFERENCES

1. Sharma AK, Diyora BD, Shah SG, et al. Orbital subperiosteal hematoma associated with subfrontal extradural hematoma. *J Trauma* 2007;62: 523–525
2. Umansky F, Pomeranz S. Epidural haematoma and unilateral exophthalmos: a review. *ActaNeurochir (Wein)* 1989;99:145–147
3. Martinez Devesa P. Spontaneous orbital haematoma. *J Laryngol Otol* 2002;116:960–961
4. Tsutsumi S, Higo T, Kondo A, et al. Orbital pseudotumor associated with retrobulbar hematoma: case report. *Neurol Med Chir (Tokyo)* 2007;47:265–268
5. Pasaoglu A, Orhon C, Akdemir H, et al. Subperiostealintraorbital-haematoma following minor head trauma. Case report. *ActaNeurochir(Wien)* 1989;97:83–85
6. Kuban K, Winston K, Bresnan M. Childhood subgaleal hematoma following minor head trauma. *Am J Dis Child* 1983;137:637–640

Recurrent Lymphoepithelial Carcinoma of the Parotid Gland

Ozan Gökdoğan, MD and Ahmet Koybasioglu, MD**

Background: Lymphoepithelial carcinomas (LECs) are rare tumors of parotid gland. Although few cases were reported in literature, there is no reported recurrent case.

Method: The authors report a case of recurrent LEC after 8 months of primary surgery. Total parotidectomy and selective neck dissection surgery were performed. Radiation therapy after surgery

From the *Department of Otorhinolaryngology, Ankara Memorial Hospital, Balgat, Ankara, Turkey.

Received March 9, 2015.
Accepted for publication June 28, 2015.

Address correspondence and reprint requests to Dr Ozan Gökdoğan, MD, Ankara Memorial Hospital, 06250 Balgat, Ankara, Turkey; E-mail: ozangokdogan@gmail.com

The authors report no conflicts of interest.

Copyright © 2015 by Mutaz B. Habal, MD

ISSN: 1049-2275
DOI: 10.1097/SCS.0000000000002037

was planned. Patient had partial facial weakness in the early postoperative period that was getting better with follow-up.

Conclusions: In the diagnosis of LECs of parotid region, nasopharyngeal carcinomas must be excluded. If LECs are not treated properly, recurrences may occur.

Key Words: Lymphoepithelial carcinomas, parotid tumors, recurrent tumors

Salivary gland tumors (SGTs) are rare and constitute <3% of all head and neck tumors.[1] Lymphoepithelial carcinoma (LEC) constitutes approximately 0.4% of malign SGTs and is mostly seen in Alaskan Eskimos/Inuits and in southeastern Asian populations.[2]

Lymphoepithelial carcinoma is accepted as a subtype of undifferentiated salivary gland carcinoma. Many risk factors have been accused in the development of SGTs such as low-dose radiation, ultraviolet radiation, wood and wood dust, alcohol, hair dyes in women, and Epstein-Barr virus (EBV).[3] Although there are many risk factors related with LECs, an EBV oncogene latent membrane protein 1 accused in the carcinogenic pathway in salivary gland LECs such as latent membrane protein 1 effect in the carcinogenesis process of nasopharyngeal carcinoma (NPC).[2]

CLINICAL PRESENTATION

A 45-year-old man presented with a slow-growing mass in the left parotid area. The mass has appeared 3 months ago and the patient had a slow-growing painless right parotid mass. He had the history of left superficial parotidectomy 8 months ago. The pathology of the operation was LEC of the left parotid gland. The tumor size was 1.5×2.1 cm. There were 2 reactive lymph nodes and there were not any perineural, neural, or lymphovascular invasion, and there was not any tumoral tissue in the margins of parotidectomy material. Endomysial and pancytokeratin antibodies were found strongly positive, whereas it was found negative for S-100 antibody staining in immunohistochemical examination.

Patient had routine follow-up and no further treatment had been recommended. There was not any problem until 3 months ago when a mass appeared in left parotid gland region. Patient had no pain with slow-growing mass and his facial nerve functions were normal. The computed tomography (CT) scan showed a 1.5 cm tumor with defined borders, affecting both superficial and deep lobule. Magnetic resonance imaging documented involvement of the deep parotid lobule as well as deep muscles and lymph nodes. Positron emission tomography (PET) CT evaluation showed high glucose uptake in deep parotid region (SUVmax:6.5) (Fig. 1)

Patient was diagnosed as recurrent disease and total parotidectomy and right selective neck dissection including zone 1, 2, and 3 were planned to the patient.

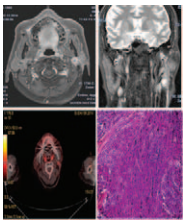

FIGURE 1. A, Axial image of tumor in the left parotid region before second surgery. B, Coronal image of tumor in the left parotid region before second surgery. C, FDG Positron emission tomography-computed tomography image that shows high glucose uptake in left parotid area (SUVmax:6). D, Pathologic examination of tumor shows neoplastic epithelial cells which form syncytial series with mature lymphoid cells.

Facial root and all branches were identified and preserved during surgery. After completing total parotidectomy, selective neck zone 1, 2, and 3 dissections were performed. A complete neck dissection was not performed because there were not any suspected metastatic lymph nodes both in the preoperative evaluation and in the operative examination. There was a right facial weakness (House-Brackman grade 4) in the early postoperative period, which was getting better with time (House-Brackman grade 3 in postoperative first month).

Pathology result was LEC in the parotidectomy material without involvement of any lymph nodes in the neck dissection material. The tumor size was 1.3 cm. There were not any neural/perineural or lymphoepithelial invasion, and the borders of parotidectomy and neck dissection material were tumor-free. All the lymph nodes in the neck had negative test result for tumoral infiltration. Epstein-Barr virus was not found positive in the mass. Ki-67 proliferation index was also found high. After radiation therapy, patient did not have any sign of recurrence in 6 months follow-up.

DISCUSSION

Lymphoepithelial carcinoma mostly affects women in the fifth decade.[4] Lymphoepithelial carcinoma is reported especially in Eskimo and Asiatic populations in literature; however, cases all over the world have been published.[5] Lymphoepithelial carcinoma is commonly found in nasopharynx and in the parotid gland but rarely in the lung, thymus, stomach, larynx, trachea, soft palate, and skin.

Major histopathologic finding is the combination of varying amount of nonneoplastic lymphocytic infiltration with a differently sized infiltrative growth epithelioid neoplastic proliferation. Most of the patients have >40% Ki-67 score.[6] We also found high Ki-67 scores in our patient. The parotid LEC tumors may present as multinodular mass or infiltrative pattern. In histologic examination, irregular islands of neoplastic malignant epithelial cells composed with nonmalignant small lymphocytes were found.

Metastasis of extraglandular cancer, especially the metastasis of NPC or lowly differentiated extraglandular carcinoma must be excluded before the diagnosis of LEC of the parotid gland.

Epstein-Barr virus is known to be associated with NPC and also associated with LEC. Approximately 100% in endemic areas and in high degree in nonendemic areas, LEC patients have a positive serology test for EBV. Lymphoepithelial carcinomas' origin still remains unknown but EBV has been found in the neoplastic cells.[5] Latent infection with a type II pattern was recognized in the epithelial neoplastic cells in LECs of salivary glands.

Lymphoepithelial carcinoma may be rarely associated with lymphoepithelial lesions of salivary glands such as Sjögren syndrome. There are few cases reported LEC is associated with lymphoepithelial lesions of salivary glands and is called secondary LEC. Secondary LEC of salivary glands has some differences such as bilateral involvement, multiple lesions, low Ki-67 values, and negative serology of EBV.[7]

Approximately 80% of salivary gland LEC cases are seen in major salivary glands.[4] Most of the patients have unilateral disease; however, sudden growth, pain, or facial weakness may indicate a malignant process. Lymphoepithelial carcinoma is mostly seen as a slow-growing parotid mass. As a malignant tumor, involvement of adjacent structures and distal metastases such as lung, liver, bone, and brain may be seen in clinical progress.

Facial paralysis may be seen in 20% of LEC patients and 10% to 40% of LEC patients have enlarged cervical lymph nodes.[4,7] Most of the disease is present as solitary intraglandular lesion on radiologic evaluation.[7]

© 2015 Mutaz B. Habal, MD

After a LEC tumor in the parotid region is identified, firstly NPC must be excluded. Radiologic evaluation such as fluoro 2 deoxy D glucose (FDG) PET-CT is very useful in the evaluation of LEC of salivary gland, which has been widely used in the identification of origin or extension of tumors. We also performed FDG PET-CT scan before revision surgery and found that tumor is located in only parotid region.

Presence of disease in parotid gland and positive serology for EBV was accepted as risk factors, although the origin of patient was not from an endemic area. Our case was a recurrent case that had both pathologic LEC diagnosis. Although there is not a recurrent case of parotid LEC in English literature, inappropriate treatment strategies may result in recurrences in all tumor types. Facial functions were normal in both primary and secondary surgery. Although facial nerve was preserved with the use of facial nerve monitor, the patient had facial weakness (House-Brackmann grade 4) in the early postoperative period. Facial functions got better with time (House-Brackmann grade 3 in postoperative fist months). The tumor size was 1.3 cm in the revision surgery and there were 47 reactive lymph nodes. Poor prognostic findings of tumor such as perineural invasion and positive margins were not found positive.

Surgery, radiation therapy, chemotherapy, and its combinations are used for the treatment of malignant parotid tumors as well as LECs. Five-year survival rates range between 50% and 87%.[8] Inappropriate treatment strategies may result in treatment failures or recurrences. There are few recurrent diseases reported in literature we think that this linked to very infrequency of this tumor rather than good response to the treatment strategies.

In conclusion, LEC should be considered in patients with the suspicion of malignant parotid tumors. Main treatment option is surgery followed by radiation therapy. Inappropriate treatment modalities may result in treatment failure and recurrences.

CONCLUSIONS

Lymphoepithelial carcinoma should be considered in patients with the suspicion of malignant parotid tumors. In the diagnosis of LECs of parotid region, NPCs must be excluded. Main treatment option is surgery followed by radiation therapy. Inappropriate treatment modalities may result in treatment failure and recurrences.

REFERENCES

1. Ito FA, Ito K, Vargas PA, et al. Salivary gland tumors in a Brazilian population: a retrospective study of 496 cases. *Int J Oral Maxillofac Surg* 2005;34:533–536
2. Jen KY, Higuchi M, Cheng J, et al. Nucleotide sequences and functions of the Epstein-Barr virus latent membrane protein 1 genes isolated from salivary gland lymphoepithelial carcinomas. *Virus Genes* 2005;30:223–235
3. Al-Khateeb TH, Ababneh KT. Salivary tumors in North Jordanians: a descriptive study. *Oral Surg Oral Med Oral Pathol Oral Radiol Endod* 2007;103:e53–e59
4. Schneider M, Rizzardi C. Lymphoepithelial carcinoma of the parotid glands and its relationship with benign lymphoepithelial lesions. *Arch Pathol Lab Med* 2008;132:278–282
5. Manganaris A, Patakiouta F, Xirou P, et al. Lymphoepithelial carcinoma of the parotid gland: is an association with Epstein-Barr virus possible in non-endemic areas? *Int J Oral Maxillofac Surg* 2007;36:556–559
6. Zhang G, Tang J, Pan Y, et al. CT features and pathologic characteristics of lymphoepithelial carcinoma of salivary glands. *Int J Clin Exp Pathol* 2014;7:1004–1011
7. Ellis GL. Lymphoid lesions of salivary glands: malignant and benign. *Med Oral Patol Oral Cir Bucal* 2007;12:E479–E485
8. Gupta S, Loh KS, Petersson F. Lymphoepithelial carcinoma of the parotid gland arising in an intraglandular lymph node: report of a rare case mimicking metastasis. *Ann Diagn Pathol* 2012;16:416–421

Nasal Vestibular Furunculosis Presenting as the Rudolph Sign

Muhammed Sedat Sakat, MD, Korhan Kilic, MD,† and Harun Ucuncu, MD**

Abstract: Nasal furunculosis is a deep infection of hair follicle within the nasal vestibule. In this report, the authors presented a 49-year-old woman with 4-day history of focal red area and tender swelling on the tip of her nose. On physical examination, together with a swelling at nasal vestibulum, erythema, and edema on the skin of nasal tip were observed, which is called the Rudolph Sign. The patient was treated with intranasal topical mupirocin and oral sodium fusidate. Because nasal furunculosis may lead to serious complications such as ophthalmic vein thrombosis and cavernous sinus thrombosis, early diagnosis and effective treatment is essential.

Key Words: Folliculitis, furunculosis, Rudolph Sign

Folliculitis, an inflammation of hair follicle, may occur from superficial or deep portion of the hair follicle. It can be infectious or noninfectious. Nasal furunculosis is a deep infection of hair follicle within the nasal vestibule.[1] In this infection, the tip of the nose becomes red and very painful, which is called "The Rudolph Sign". In this report, we presented a rare patient of nasal furunculosis leading to Rudolph Sign.

CLINICAL REPORT

A 49-year-old woman presented with 4-day history of focal red area and tender swelling on the tip of her nose. She indicated that after picking off a scab, her nose became painful and tender to touch. Soon afterward, because swelling inside her nose occurred, she referred to our clinic. On physical examination, together with a swelling at nasal vestibulum, erythema, and edema on the skin of nasal tip were observed which is called the Rudolph Sign (as in Rudolph, The Red Nosed Reindeer) (Fig. 1A). The diagnosis was nasal vestibular furunculosis presenting with the Rudolph Sign. The swelling at the nasal vestibulum was drainaged surgically (Fig. 1B). The microbiologic examination of the pus revealed *Staphylococcus aureus*. The patient was treated with intranasal topical mupirocin and oral sodium fusidate. After 7 days of treatment, the patient was discharged with complete healing (Fig. 1C).

DISCUSSION

Nasal vestibular furunculosis is an uncommon disease of otorhinolaryngology clinic. The usual cause is infection of *S. aureus* and generally caused by nose picking or plucking nose hair with tweezers. Furunculosis is very uncommon in young children but

From the *Department of Otorhinolaryngology, Faculty of Medicine, Ataturk University; and †Palandoken State Hospital, Otorhinolaryngology Clinics, Erzurum, Turkey.

Received March 10, 2015.
Accepted for publication June 28, 2015.

Address correspondence and reprint requests to Harun Ucuncu, MD, Department of Otorhinolaryngology, Faculty of Medicine, Atatürk University, Erzurum 25240, Turkey; E-mail: hucuncu61@gmail.com

The authors report no conflicts of interest.

Copyright © 2015 by Mutaz B. Habal, MD

ISSN: 1049-2275
DOI: 10.1097/SCS.0000000000002038

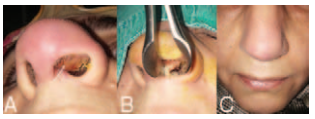

FIGURE 1. A, The erythema and edema at the nasal tip (the Rudolph Sign) of the patient with swelling at the nasal vestibulum (arrow). B, Surgical drainage of nasal vestibular furunculosis. C, The appearance of the patient after 7 days of treatment.

it occurs more frequently after puberty. The incidence and prevalence of nasal vestibular furunculosis is still unclear.[2]

The first symptom of the disease is focal pain in the tissue overlying nasal vestibule. When this area is palpated, it is found to be tender. Later, the area becomes reddened. Soon afterwards pustule at nasal vestibular area may be observed.

The treatment of the disease is systemic and topical antibiotherapy. Mupirocin is the most effective choice for topical treatment. The pain and erythema start to improve within 12 hours after topical therapy.[3] When the symptoms seem to be resistant to topical therapy, surgical drainage of the abscess must be considered. In our patients as the pain at the nose was resistant to topical treatment, surgical drainage was performed. After drainage the symptoms improved rapidly.

The danger triangle zone of the face has a venous system that is interconnected and valveless, which results in open communication between orbit, nasal cavity, sinuses, skin of the nose, and cavernous sinus.[4] This means in a patient with an infection on the vestibular region of the nose, these communications may lead the infections to spread through these venous channels through the facial vein to the inferior or superior ophthalmic vein and cavernous sinus.

Nasal furunculosis seems to be a local and simple infection but if left untreated, it may cause serious life-threatening complications such as ophthalmic vein thrombosis and cavernous sinus thrombosis.

REFERENCES

1. Laureano AC, Schwartz RA, Cohen PJ. Facial bacterial infections: folliculitis. *Clin Dermatol* 2014;32:711–714
2. Dahle KW, Sontheimer RD. The Rudolph sign of nasal vestibular furunculosis: questions raised by this common but under-recognized nasal mucocutaneous disorder. *Dermatol Online J* 2012;18:6
3. Conners GP. Index of suspicion. Case 1. Nasal furuncle. *Pediatr Rev* 1996;17:405–406
4. Van Dissel JT, de Keizer RJ. Bacterial infections of the orbit. *Orbit* 1998;17:227–235

Surgical Enucleation of the Mucocele on the Inferior Orbit Using Transantral Approach

Seunggon Jung, DDS, MSD,[*] Hee-Kyun Oh, DDS, PhD,[†] Hong-Ju Park, DDS, PhD,[†] and Min-Suk Kook, DDS, PhD[†]

Abstract: The mucocele on the inferior orbit is infrequent. When there is occurrence on the inferior orbit, the infraorbital approach, such as transantral, subciliary approach is used commonly. But because of some side effects, the authors use transantral approach intraorally. A 26-year-old woman visited our department with complaint of palpable mass. Computed tomography (CT) disclosed cystic lesion on the left inferior orbit. Surgical approach to the lesion was established with bony window opening on the anterior maxillary wall intralorally. Medpor sheet was placed on orbital floor after the removal of the lesion. Histopathologically, the lesion was diagnosed as mucocele. Orbital volume was kept well after the operation and no ocular sequela was observed.

Key Words: Mucocele, orbit, transantral approach

Mucocele from paranasal sinus can invade into the orbit as mucous accumulates. Of the orbital mucocele, frontoethmoidal lesion is most common, followed by ethmoidal and sphenoidal lesions. Orbital mucocele from maxillary sinus is rare.[1,2] Mucocele is resulted from obstruction or chronic inflammation of paranasal sinus, caused by chronic sinusitis, sinus polyps, tumors involving sinus, previous surgery of orbit or sinus, fractures involving the nasofrontal duct.[1,3] Treatment of orbital mucocele is surgical enucleation, reestablishment of drainage or obliteration of the sinus.[2,4] Surgical approaches for enucleation of mucocele vary by location and origin of the mucocele. Transcaruncular incision, transconjunctival incision, and Lynch incision are usually hired.[1,2] Here we report a patient of mucocele in inferior orbit, treated using another approach.

CLINICAL REPORT

A 26-year-old woman was referred from the Department of Ophthalmology for surgical treatment of cystic lesion in inferior orbit. Presenting complaint of this patient was palpable mass lesion without pain. Cystic lesion was identified in the left inferior orbit and the inferior orbital wall showed thinning and protruding into the left maxillary sinus in facial computer tomography (CT) (Fig. 1A). Surgical enucleation using transantral approach was planned. General anesthesia via nasotracheal intubation was induced. Vestibular incision was placed on buccal of the #22 to 26. For transantral approach to the inferior orbital wall, a bony window in square-shape was made on the anterior wall of the left maxilla after the mucoperiosteal elevation (Fig. 2A). Bony wall of the lesion was identified and ground with round bur after which cystic lesion was dissected and enucleated carefully (Fig. 2B-C). Medpor sheet (Stryker Co, MI) was inserted in orbit and placed to cover the bone defect of the inferior orbital wall and to prevent the herniation of the orbital content (Fig. 2D). Size of Medpor sheet was slightly larger than the bone defect for reconstruction because the sheet needs to be supported by the inferior orbital wall margin. Bone fragment was repositioned on the bony window of the anterior wall of the left maxilla with fibrin sealant (Tisseel, Baxter, IL). Then submucosal and mucosal suture was done. Histopathologic diagnosis was mucocele. Position of the globe and the inferior margin of the orbit were symmetric in the postoperative CT (Fig. 1B). No sequela from inferior orbital wall defect, such as limitation of global movement, diplopia, was observed during the follow-up.

From the [*]Department of Oral and Maxillofacial Surgery, Chonnam National University Hwasun Hospital; and [†]Department of Oral and Maxillofacial Surgery, School of Dentistry, Dental Science Research Institute, Chonnam National University, Gwangju, South Korea.

Received March 16, 2015.
Accepted for publication June 28, 2015.

Address correspondence and reprint requests to Min-Suk Kook, DDS, PhD, Department of Oral and Maxillofacial Surgery, School of Dentistry, Dental Science Research Institute, Chonnam National University 77, Yongbongro, Buk-Gu, Gwangju, 500-757, South Korea;
E-mail: mskook2@gmail.com

This study was supported by the National Research Foundation of Korea (NRF) grant funded by the Korea government (MSIP 2011-0030121).
The authors report no conflicts of interest.

Copyright © 2015 by Mutaz B. Habal, MD

ISSN: 1049-2275
DOI: 10.1097/SCS.0000000000002039

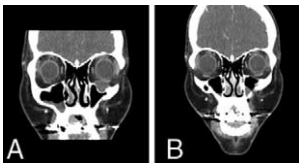

FIGURE 1. Facial CT scan. A, Before the operation. A 1.9 cm well-defined cystic lesion with rim enhancement in left inferior extraconal orbit and widening of infraorbital foramen are observed. B, Evidence of surgical excision of cystic lesion is observed and orbital contents are kept in orbit after the operation. CT, computed tomography.

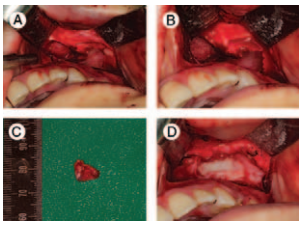

FIGURE 2. Intraoperative photographs. A, Transantral approach via left maxillary anterior wall. B, Reconstruction of left inferior orbital wall after enucleation using Medpor. C, Closure of left maxillary anterior wall with Tisseel. D, Surgical specimen after enucleation.

DISCUSSION

Mucoceles of orbit usually occur in adults with a history of chronic sinusitis and show progressive proptosis or globe displacement.[5] They present chronic headache and visual disturbance less commonly. Maxillary sinus lesions usually lead to upward displacement of the globe but have been reported to cause enophthalmos.[2]

Infraorbital nerve and vessels are important anatomic structure during the performing transantral approach, which are vertical limit of the maxillary window. It is recommended to avoid invading nasal buttress and zygomaticomaxillary buttress. The bone fragment from maxillary window can be fixed with microplate or sutures. In this case we made the bone fragment in its position using the fibrin glue. The bone fragment kept its position where we placed intraoperatively during the follow-up period and there was no sign of infection or necrosis of the fragment.

Infraorbital canal is located midline to the orbit.[6] In this patient, the mucocele was placed on just medial to the infraorbital canal. The mucocele was removed with caution to avoid damage to infraorbital canal. Removal of the mucocele left a defect with size of approximately 1 cm^2 on orbital floor. It is generally accepted that an orbital floor defect size of more than 1 cm^2 is indicated to repair in orbital fractures.[7] Advantages of transantral approach are the absence of lower eyelid scar formation without risk of ectropion and the possibility of immediate surgery before resolution of orbital swelling in orbit wall reconstruction.[6] We applied this transantral approach to remove the mucocele of the orbital floor. With the advantages described previously, the transantral approach provided wideness of the access to lesion. The wideness of access to lesion can be limited in transconjunctival approach because of the globe.

In conclusion, the transantral approach has a certain advantages of following compared with transorbital approaches, which are transconjunctival approach or subciliary approach: absence of visible scar, no risk of ectropion or entropion, wider access to remove the lesion of the floor.

REFERENCES

1. Kersten RC. Mucocele. In: Roy FH, Fraunfelder Jr F, Fraunfelder FT, eds. *Roy and Fraunfelder's Current Ocular Therapy.* 6th ed. Elsevier Health Sciences; 2008
2. Wang TJ, Liao SL, Jou JR, et al. Clinical manifestations and management of orbital mucoceles: the role of ophthalmologists. *Jpn J Ophthalmol* 2005;49:239–245
3. Evans C. Aetiology and treatment of fronto-ethmoidal mucocele. *J Laryngol Otol* 1981;95:361–375
4. Lai PC, Liao SL, Jou JR, et al. Transcaruncular approach for the management of frontoethmoid mucoceles. *Br J Ophthalmol* 2003;87:699–703
5. Feldman M, Lowry LD, Rao VM, et al. Mucoceles of the paranasal sinuses. *Trans Pa Acad Ophthalmol Otolaryngol* 1987;39: 614–617
6. Polligkeit J, Grimm M, Peters JP, et al. Assessment of indications and clinical outcome for the endoscopy-assisted combined subciliary/ transantral approach in treatment of complex orbital floor fractures. *J Craniomaxillofac Surg* 2013;41:797–802
7. Burnstine MA. Clinical recommendations for repair of isolated orbital floor fractures: an evidence-based analysis. *Ophthalmology* 2002;109: 1207–1210

Head Spear Gun Injury: An Atypical Suicide Attempt

David Bakhos, MD, PhD,[*] Alexandre Villeneuve, MD,[*] Soo Kim, MD,[*] Helene Lebrun, MD,[†] and Xavier Dufour, MD[†]

Abstract: Weapon injuries with spear gun are rare. The aim of this case report is to report the emergency and surgical management when this event occurs. A 35-year-old man attempted suicide with a spear gun. The entry of the shaft was localized through the submental area without an obvious exit point. The projectile passed through the tongue and palatal bone. A tracheotomy was performed. Preoperative cranial computed tomography (CT) showed the harpoon was gone upward through the submental area, the oral cavity, the ethmoid paranasal sinus, the cribriform plate, and the frontal region without vessel damages. Under general anesthesia, the harpoon was pulled out in order to extract the shaft tip and the articulated wishbone. Osteo-meningeal defect of the ethmoid roof was closed using a middle turbinate flap. There were no neurologic deficit and no cerebro-spinal rhinorrhea at his 3-year follow-up visit. The trajectory of the shaft is different between attempted suicide and accident. Cranial CT scan is helpful to show the trajectory of the shaft. Angiogram can be helpful to see the relations between the tip shaft and the vessels. The knowledge of the shaft tip and the imagery findings are important to decide the best surgical approach.

From the [*]Department of Head and Neck Surgery, Tours Hospital, University François-Rabelais de Tours, Tours; and [†]Department of Head and Neck Surgery, Poitiers Hospital, University of Poitiers, Poitiers, France.

Received March 16, 2015.
Accepted for publication June 28, 2015.

Address correspondence and reprint requests to Alexandre Villeneuve, MD, Department of Head and Neck Surgery Tours Hospital, Boulevard Tonnellé 37000, Tours, France; E-mail: avilleneuve1986@gmail.com

The authors report no conflicts of interest.

Copyright © 2015 by Mutaz B. Habal, MD

ISSN: 1049-2275
DOI: 10.1097/SCS.0000000000002040

Key Words: Craniofacial injury, osteo-meningeal defect, skull base, spear gun

Weapon injuries with spear gun are extremely rare and only few patients of craniofacial injuries have been reported in the literature.[1–7] We present the case of a 35-year-old man with an unusual craniofacial injury after a spear gun shot and discuss the radiologic management and surgical characteristics of this unusual case.

CLINICAL REPORT

A 35-year-old man was admitted to the intensive care after he attempted suicide with a spear gun. He had a history of depression without treatment. Her sister found him with a shaft penetrating the submental area. A tracheotomy was performed in an outside institution because the trajectory of the harpoon impeded the intubation maneuver. Then, the patient was referred to our hospital in the intensive care unit (ICU). The Glasgow coma scale score was 15/15.

The entry of the shaft was localized through the midline of the submental area. X-ray of the face showed the localization of the harpoon. The preoperative CT scan of the head and neck, showed the entry point and extent of penetration of the spear gun shaft (Fig. 1 A-C). The harpoon was gone through upwards the submental area, the buccal cavity, the ethmoid paranasal sinus, the cribriform plate, and the frontal region.

Under general anesthesia, the harpoon was removed with success. It was pulled out to extract the shaft tip and the articulated wishbone (Fig. 2). During this procedure the patient presented a preoperative rhinorrhea. After an endoscopic endonasal examination, a skull base defect was identified at the left ethmoid roof and evaluated to be almost 1 cm^2. The ENT specialist and neurosurgeon decided operating strategy conjointly. We performed an endoscopic endonasal approach and a middle turbinate flap was used for closure the osteo-meningeal defect of the left ethmoid roof. This flap was placed endonasally (overlay). Then, laceration tongue was sutured. For the laceration of the hard palate and the skin of the submental area, a controlled healing was preferred.

A postoperative cerebral CT scan was performed and revealed bleeding at the frontal region. Prophylactic antibiotics were used for a total of 2 weeks: 10 days with intravenous (IV) antibiotics (ceftriaxone 4 g × 2/day and ornidazole 500 × 2 IV/day for 5 days then amoxicillin 1.5 g × 6 and ornidazole 1 g IV/day for 5 days) and 5 days with oral antibiotics (amoxicillin 3 g × 3 /day and metronidazole 500 × 2/day).

Decannulation was performed 13 days postoperative. Complete healing of the submental area and hard palate occurred within 3 weeks.

After a follow-up of 3 years, the patient had no rhinorrhea and the endonasal endoscopic examination showed no defect at the ethmoid roof. The patient had no neurologic deficit.

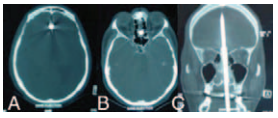

FIGURE 1. A-C, Computed tomography scan of head and neck. A, Axial CT scan showed the shaft in the frontal area. B, Axial CT scan, the shaft had penetrated the cribriform plate. C, Coronal CT scan, showed the trajectory of the harpoon. CT, computed tomography.

FIGURE 2. The harpoon with the articulated wishbone.

DISCUSSION

Craniofacial penetrating injuries related to a spear gun injury are extremely rare and can be life-threatening. Only a few patients have been described in the literature and generally they occurred underwater during diving.[2–7] To our knowledge, we found only 1 more report about an attempt of suicide, as in our patient, with spear gun in the literature.[1] The entry point was in the mouth. The main difference between underwater weapon injury and suicide cases is the course of the weapon. In fact, in our patient and Ban's case report,[1] the course was vertical, with a point entry in the mouth or in the submental area. And, in the underwater weapon injuries, the course was anteroposterior.[2,3]

In such situations, it is important to determine the position of the vessels and the object by an angiogram[1] before and after removing the harpoon. If there is no injury of important anatomic structures, removal of the spear can be attempted without surgical exploration. To decide the best surgical approach, in cases of injury with a harpoon, it will be important to know the type of shaft tip involved.[3] In ourpatient, we performed an endonasal endoscopic procedure because the articulated wishbone had not completely penetrating the cribriform plate. In case we failed to remove the harpoon, we had to drill the cribriform plate and/or the hard palate and a flap had to be used to close the defect of the hard palate. For the meningeal defect, even if a drilling had to be necessary, the closure of the meningeal defect will be the same procedure as used. Some authors[1] removed the shaft in an anterograde direction during a neurosurgical procedure because of an articulated wishbone. Bleeding and infection can occur during the postoperative period and CT scan of the head and neck is important to reveal bleeding or cerebral abscess along the trajectory of the shaft.

In summary, craniofacial spear gun injuries are very rare. The trajectory of the shaft is different between attempted suicide and accident. Computed tomographic scan is helpful to show the trajectory of the shaft. Angiogram can be helpful to see the relations between the tip shaft and the vessels. The knowledge of the shaft tip is important to decide the best surgical approach.

REFERENCES

1. Ban LH, Leone M, Visintini P, et al. Craniocerebral penetrating injury caused by a spear gun though the mouth: case report. *J Neurosurg* 2008;108:1021–1023
2. Fernandez-Melo R, Moran AF, Lopez-Flores G, et al. Penetrating head injury from harpoon. Case report. *Neurocirugia (Astur)* 2002;21:397–400
3. Hefer T, Joachims HZ, Loberman Z, et al. Craniofacial spear gun injury. *Otolaryngol Head Neck Surg* 1996;115:553–555
4. Alper M, Totan S, Cankayali R, et al. Maxillofacial spear gun accident: report of two cases. *J Oral Maxillofac Surg* 1997;55:94–97
5. Gutierrez A, Gil L, Sahuguillo J, et al. Unusual penetrating craniocerebral injury. *Surg Neurol* 1983;19:541–543
6. Lopez F, Martinez-Lage JF, Herrera A, et al. Penetrating craniocerebral injury from an underwater fishing harpoon. *Child Nerv Syst* 2000;16:117–119
7. Rocca A, Casu G, Sechi CS. Penetrating craniocerebral injuries. Report of two unusual cases. *J Neurosurg Sci* 1987:19–21

© 2015 Mutaz B. Habal, MD